UNIVERSITÉ PARIS SUD

Comprendre le monde, construire l'avenir®

École doctorale 142 de mathématiques de la région Paris-Sud

Spécialité : Mathématiques

Processus auto-interagissants et grandes déviations

Laure DUMAZ

Directeurs de thèse :

M. Bálint Tóth : Professeur à l'université BME (Budapest)
M. Wendelin Werner : Professeur à l'université Paris-Sud

Rapporteurs :

M. Pierre Tarrès : Rapporteur
M. Jonathan Warren : Rapporteur

Soutenue le 7 Décembre 2012 devant le jury composé de :

M. Jean-François Le Gall : Examinateur, Président du jury
M. Pierre Tarrès : Rapporteur
M. Bálint Tóth : Directeur de thèse
M. Jonathan Warren : Rapporteur
M. Wendelin Werner : Directeur de thèse

À mes parents, À Romain

Remerciements/Acknowledgements

En premier lieu, je tiens à remercier mes deux directeurs de thèse Bálint Tóth et Wendelin Werner. Cette cotutelle a été très enrichissante d'un point de vue mathématique et personnel et j'ai eu l'immense chance de bénéficier de deux excellents encadrements. Je remercie Bálint Tóth pour son enthousiasme, son dynamisme, sa convivialité et ses explications mathématiques détaillées toujours très claires, ainsi que pour l'accueil très agréable à chacune de mes visites à Budapest. Wendelin Werner s'est toujours montré incroyablement disponible malgré ses nombreuses obligations, et tout ceux qui l'ont eu en M2 savent à quel point les mathématiques sont intuitives et passionnantes avec lui. Je le remercie vivement pour tout ce qu'il m'a appris au cours de cette thèse, pour son exigence mathématique, ses conseils pertinents et ses explications patientes.

Je suis extrêmement reconnaissante envers Pierre Tarrès et Jonathan Warren d'avoir accepté d'être les rapporteurs de ma thèse et d'être présents à ma soutenance.

C'est un grand honneur d'avoir Jean-François Le Gall dans mon jury de thèse et je le remercie d'avoir accepté d'en faire partie. Ce sont notamment ses cours exceptionnels qui m'ont décidée à choisir la voie des probabilités.

My M2 internship in Toronto has been the opportunity to enter into the research world. I am very grateful to Bálint Virág for his careful guidance and help during my stay. Learning from and working with him was a great experience. I discovered what research is, with its pitfalls (Balint compared our problem to the hydra !), but above all its convivial moments (we finished the writing of our article in a tea house in Budapest) and its resolutions.

Thanks to my "cotutelle", I had many opportunities to visit the university BME of Budapest. It is an understatement to write that during all my stays, I was warmly welcomed by the probability department of BME. I was also very impressed by the scientific skills and the kindness of the Hungarian I met. In particular, Köszönöm szépen to Balázs, Bálint (Vető), Gabor, Marton, Peter, Tomi (Koi and Vajk) and especially to Juli, who became a great friend. Thanks to them, I felt at home in a city in which I do not understand the language !

Je remercie le département de mathématiques de l'école Normale Supérieure dans lequel j'ai passé la majeure partie de ma thèse et mes nombreux "cobureaux" et collègues du passage vert, Thibaut, Vincent, Augusto, Cécile, Oriane, Nicolas, Igor ainsi que les occupants du bureau des doctorants avec qui j'ai passé de très bons moments. Merci aussi aux équipes administratives d'Orsay et de l'ENS, je pense bien sûr à Zaïna, Bénédicte, Laurence et Valérie Lavigne, qui ont toujours facilité mes démarches dans la bonne humeur et avec efficacité.

Durant les trois derniers mois de ma thèse, j'ai été accueillie par le département de mathématiques de l'université ETH de Zurich. L'ambiance chaleureuse et studieuse de ce laboratoire m'a beaucoup plue et je remercie en particulier Blanka, Danijel, David, Erich, Pierre, Pierre-François pour leur accueil. Et surtout, un grand merci à Hao, ma colocataire et cobureau durant cette période.

De nombreux professeurs m'ont fait découvrir la beauté des mathématiques et partager leur passion, je pense à Mme Broust (au collège, pour $\sqrt{2}$ irrationnel), M. Tholozan (au lycée, pour la définition de la continuité), M. Dakhli en sup et M. Tosel en spé (pour tant de choses !), et bien sûr à tous les professeurs dont j'ai eu la chance de suivre les cours à l'école Normale et à l'université d'Orsay.

Ces remerciements sont l'occasion de s'égarer un peu : une pensée pour mes amis, le fameux club athlé de l'ENS, nos soirées au "gymnase" et nos défis sportifs, ainsi qu'à l'ensemble vocal du COGE, j'ai d'excellents souvenirs avec vous en dehors de mon bureau ! J'espère que ce travail retient un peu de votre force et de votre enthousiasme.

Je remercie ma famille, et tout particulièrement mes parents, mes grands-parents, Suzanne et mes soeurs Cécile et Clara. Je dois beaucoup à mon père qui m'a donné toute petite le goût des sciences et dont j'admire la curiosité scientifique. Ma mère a toujours été présente pour moi et m'a soutenue et aidée. Mes deux soeurs ont écouté patiemment mes tentatives d'explications sur "ce que je fais" : je suis fière que Clara connaisse parfaitement la définition de l'uniform spanning tree et mes découpages avant de savoir résoudre une équation du second degré !

Enfin, je remercie Romain pour sa patience et son soutien indéfectible, ainsi que pour tout ce que je ne peux écrire ici.

Résumé

Cette thèse porte sur divers aspects de lois et de processus non-gaussiens qui partagent des propriétés de changement d'échelle où intervient l'exposant 2/3. Les deux principaux objets probabilistes que nous allons présenter sont :

- *La loi de Tracy-Widom* : C'est la loi limite de la plus grande valeur propre de matrices aléatoires appartenant aux β-ensembles lorsque leur dimension tend vers l'infini. Dans un travail en commun avec Bálint Virág [19], nous avons établi le comportement asymptotique de la queue droite de cette loi pour tout $\beta > 0$, en utilisant des outils d'analyse de diffusions du type Girsanov. C'est l'objet du chapitre II de l'introduction et du chapitre VI.
- *Le "vrai" processus auto-répulsif ("true self repelling motion") TSRM* : C'est un processus auto-interagissant qui a été introduit par Bálint Tóth et Wendelin Werner dans [59]. Nous nous sommes intéressés à des propriétés de cet objet liées à ses trajectoires (grandes déviations, lois du logarithme itéré) [16] et à des calculs explicites de lois marginales (travail en collaboration avec Bálint Tóth [18]). Cette étude nous a aussi amenés à aborder des questions liées à la théorie des jeux [17]. Nous présentons ce modèle et divers objets associés dans le chapitre I de l'introduction. Nos articles sur ce thème se trouvent dans les chapitres III, IV et V.

Abstract

This thesis focuses on various aspects of non-Gaussian distributions and processes sharing scaling properties where the exponent 2/3 appears. The two probabilistic objects that we will introduce are :

- *Tracy-Widom distribution* : This is the large dimensional limit of the top eigenvalue of random matrices in β-ensembles. In a joint work with Bálint Virág [19], we studied the asymptotic behavior of its right tail for all $\beta > 0$, using tools coming from diffusion analysis, such as the Girsanov formula. It is the subject of chapter II of the introduction and of chapter VI.
- *The "true self repelling motion" (TSRM)* : This is a self-interacting process which was introduced by Bálint Tóth and Wendelin Werner in [59]. We have been interested in properties related to trajectories of this motion (large deviations, law of the iterated logarithm) [16] and explicit distribution computations (joint work with Bálint Tóth [18]). During this study, we have also dealt with questions related to game theory [17]. We introduce this model and various related objects in chapter I of the introduction. Our articles about this subject can be found in chapters III, IV and V.

Table des matières

Introduction

CHAPITRE I

Le “vrai” processus auto-répulsif (TSRM)

Ce chapitre introduit le “vrai” processus auto-répulsif (“true” self-repelling motion, TSRM) et les résultats que nous avons obtenus sur ce processus. La partie I.1 décrit deux modèles discrets à l'origine de la construction du TSRM. Ces modèles font apparaître une structure de marches aléatoires coalescentes dont la limite continue est la toile brownienne (brownian web, BW), sujet de la partie I.2. Cette structure est au cœur de la construction du TSRM (partie I.3, §I.3.2). Dans I.3, nous donnons quelques éléments pour comprendre cette construction et les principales propriétés du TSRM. Nous décrivons dans une dernière partie I.4 les résultats des articles [16, 18, 17].

I.1 Marches aléatoires auto-répulsives

Pour comprendre l'origine de la construction du TSRM, il est utile de se pencher sur les modèles discrets dont le TSRM est issu. Notons cependant pour le lecteur pressé que ces modèles, s'ils aident à la compréhension et donnent un aperçu historique, ne sont pas indispensables pour définir le modèle continu, voir directement les paragraphes I.2, I.3 et I.4 pour le continu.

Nous nous intéressons à des marches aléatoires auto-répulsives : le marcheur aura tendance à préférer les endroits qu'il a le moins visités (on peut penser à un touriste qui aime découvrir de nouveaux lieux, ou à une bactérie laissant des déchets derrière elle). La principale difficulté dans l'étude de ce modèle est la perte de la propriété de Markov : la marche a une longue mémoire et connaître ses derniers pas ne permet pas de prédire son comportement futur. Ainsi l'application de méthodes efficaces pour la marche aléatoire simple se révèle-t-elle infructueuse. Pour définir

rigoureusement un tel modèle, nous avons besoin d'introduire ce que nous appelons les "temps locaux". Pour les modèles discrets, nous entendons simplement le temps passé en chaque point (ou arête) du domaine que l'on visite.

Le modèle discret le plus naturel de marche aléatoire auto-répulsive sur $\mathbb{Z}^d$ ($d \in \mathbb{N}^*$) a été introduit par D. Amit, G. Parisi et L. Peliti dans [3] et est appelé "vraie" marche aléatoire auto-répulsive ("true" self-repelling walk, TSRW), le terme "vraie" provenant du fait que c'est une vraie marche, c'est à dire que l'on peut construire le chemin de longueur $n+1$ à partir du chemin de longueur n, contrairement par exemple à la marche auto-évitante ou plus généralement à des modèles de polymères.

Plusieurs questions naturelles se posent :

- Quel est l'ordre de grandeur du déplacement pour des temps très grands ?
- Existe-t-il une limite d'échelle et est-elle différente du mouvement brownien ?

Il a été prédit par les auteurs de [3], en s'appuyant sur des arguments non rigoureux de groupe de renormalisation que pour des dimensions supérieures à trois, la TSRW se comporte de façon diffusive de manière similaire à la marche aléatoire simple, et que pour la dimension deux, des corrections logarithmiques apparaissent. En dimension 1, il était attendu que la marche soit super diffusive. Dans le papier [46], L. Peliti et L. Pietronero ont conjecturé que l'ordre de grandeur typique du déplacement lorsque $d = 1$ pour un temps $t \gg 1$ est de $t^{2/3}$, sans précision sur une limite d'échelle éventuelle. La réponse à ces questions et une description plus précise de ce modèle *en dimension* 1 forment la sous partie I.1.1.

Nous introduisons également un autre modèle de marche aléatoire auto-répulsive (en dimension 1), moins naturel et plus combinatoire, que nous appelons "modèle jouet" car ses règles sont très simples et il suffit d'une pièce non biaisée pour y jouer. Ce modèle a le mérite de faire apparaître une famille de marche aléatoires simples coalescentes qui est l'analogue discret de la toile brownienne étudiée partie I.2 et il nous aide à mieux comprendre le lien entre ces deux objets (BW et TSRM). Par ailleurs, cette marche aléatoire a été utilisée dans notre article [17] pour déduire des résultats sur la loi conditionnelle de la position au temps n connaissant le temps local passé en chacun des points à cet instant.

I.1.1 La "vraie" marche aléatoire auto-répulsive en dimension 1 (TSRW)

Pour plus de clarté, nous parlons seulement de la marche aléatoire auto-répulsive repoussée par le temps passé sur les *arêtes*, pour laquelle des résultats mathématiques rigoureux sont connus. En fait, la définition de [3] fait intervenir les sites plutôt que les arêtes, mais intuitivement, ces deux modèles devraient se comporter de la même façon. Des travaux récents allant dans ce sens ont été effectués par B. Tóth et B.

Vető, voir [58].

Soit $S(n)$ une marche aléatoire sur $\mathbb{Z}$ qui commence en $S(0) = 0$ et qui saute uniquement sur ses plus proches voisins. Nous identifions les arêtes de $\mathbb{Z}$ à des éléments de $\mathbb{Z} + 1/2$ (l'arête $\{x, x+1\}$ correspond à $x + 1/2$). Les temps locaux (nombre de sauts effectués) de cette marche sur les arêtes $e \in \mathbb{Z} + 1/2$ à l'instant n sont notés $l(n, e) := \#\{k \in \{0, \cdots, n-1\} : \{S(k), S(k+1)\} = \{e - 1/2, e + 1/2\}\}$. Son évolution est donnée par les règles suivantes :

$$\begin{aligned}\mathbb{P}\left(S(n+1) = x+1 | S(n) = x, \text{ Passé}\right) &= 1 - \mathbb{P}\left(S(n+1) = x-1 | S(n) = x, \text{ Passé}\right) \\ &= f(l(n, x+1/2) - l(n, x-1/2)) \qquad \text{(I.1)}\end{aligned}$$

où f est la fonction décroissante exponentielle :

$$f(x) = \exp(-\beta x)/(\exp(-\beta x) + \exp(\beta x)).$$

Le premier résultat mathématique rigoureux a été démontré par B. Tóth en 1995 [57]. Il a prouvé un théorème limite pour les temps locaux à certains temps aléatoires, qui fait apparaître l'ordre de grandeur $n^{2/3}$ du déplacement à un instant $n \gg 1$. Ce théorème lui permet de déduire que la position de cette marche aléatoire observée à des temps géométriques indépendants de la marche et correctement renormalisée admet une limite en loi mais ne permet pas d'avoir directement le résultat pour des temps *déterministes*.

Plus précisément, pour tous $e \in \mathbb{Z} + 1/2$ et $h \in \mathbb{N}^*$, soit $t_{e,h}$ le premier instant (aléatoire) où le temps local $l(\cdot, e)$ atteint la valeur h en e.

Théorème 1.1 (B. Tóth [57]). *Fixons (x, h) dans le demi plan supérieur $\mathbb{R} \times \mathbb{R}_+^*$. Alors la convergence suivante a lieu dans l'espace fonctionnel $D(\mathbb{R})$ muni de la topologie de Skorokhod :*

$$\frac{1}{\sigma\, n^{1/3}} l(t_{[n^{2/3}x]+1/2, [n^{1/3}\sigma h]}, [n^{2/3}\cdot] + 1/2) \Longrightarrow_{n\to\infty} \Lambda'_{x,h}(\cdot)$$

où $\sigma^2 := \sum_{z\in\mathbb{Z}} z^2 \exp(-\beta z^2) / \sum_{z\in\mathbb{Z}} \exp(-\beta z^2)$ et $\Lambda'_{x,h}$ est le processus suivant : $\Lambda'_{x,h}(x) = h$, $(\Lambda'_{x,h}(x+y), y \geq 0)$ et $(\Lambda'_{x,h}(x+y), y \leq 0)$ sont deux mouvements browniens indépendants commençant au niveau h, le premier (resp. le second) coalesçant avec la demi droite $\mathbb{R}^+$ (resp. $\mathbb{R}^-$) et réfléchi sur $\mathbb{R}_-$ (resp. $\mathbb{R}^+$). Le dessin I.1 éclaircit cette définition.

Un point-clef de la preuve est un argument du type Ray-Knight (pour les papiers originaux sur le sujet, voir [41, 49]). Il est facile de déduire l'ordre de grandeur du déplacement à partir de ce théorème : pour n'importe quel x, à un instant d'ordre de grandeur n, la marche se trouve en $[n^{2/3}x]$ et a passé environ $n^{1/3}$ sur chacun des sites qu'elle a visités.

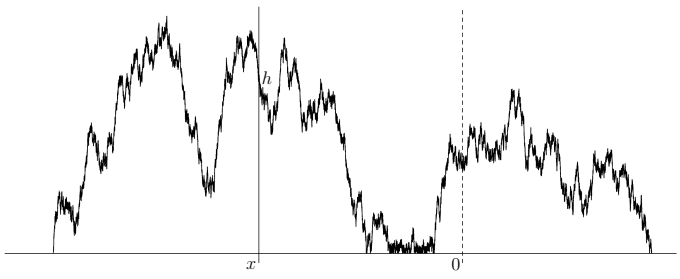

FIGURE I.1 – réalisation de $\Lambda'_{x,h}$

Notons que B. Tóth a en fait obtenu un résultat plus général, qui décrit la loi jointe de temps locaux pris à divers temps aléatoires du même type que ci-dessus. Soient $(x_1, h_1), \cdots, (x_k, h_k) \in \mathbb{R} \times \mathbb{R}_+^*$, alors on a

$$\Big(\frac{1}{\sigma n^{1/3}} l\Big(t_{[n^{2/3}x_1]+\frac{1}{2},[n^{1/3}\sigma h_1]}, [n^{2/3}\cdot] + 1/2\Big), \cdots, \frac{1}{\sigma n^{1/3}} l\Big(t_{[n^{2/3}x_k]+\frac{1}{2},[n^{1/3}\sigma h_k]}, [n^{2/3}\cdot] + 1/2\Big)\Big) \Longrightarrow_{n\to\infty} \Big(\Lambda'_{x_1,h_1}(\cdot), \cdots, \Lambda'_{x_k,h_k}(\cdot)\Big),$$

où les Λ'_{x_i,h_i} sont définis par récurrence de la façon suivante : $\Lambda_{0,0} := 0$ et sachant que les $\Lambda'_{x_i,h_i} : \mathbb{R} \to \mathbb{R}$ sont définis pour tout $i \in \{0, \cdots, j-1\}$, $(\Lambda'_{x_j,h_j}(y), y \geq x_j)$ (resp. $(\Lambda'_{x_j,h_j}(y), y \leq x_j)$) est un mouvement brownien indépendant de ces courbes jusqu'à ce qu'il rencontre une des courbes déjà tracées [1] : si c'est une courbe "allant vers la droite" i.e. si c'est une courbe du type $(\Lambda'_{x_i,h_i}(y),\ y \geq x_i)$ (resp. "allant vers la gauche"), il coalesce avec elle, si c'est une courbe "allant vers la gauche" i.e. du type $(\Lambda'_{x_i,h_i}(y),\ y \leq x_i)$ (resp. "allant vers la droite"), il se réfléchit sur elle.

Gardons en mémoire pour la suite que ce théorème fait apparaître une structure de browniens réfléchis coalescents pour les temps locaux limites de la marche auto-répulsive.

I.1.2 Le modèle jouet

Ce modèle a été introduit par B. Tóth et W. Werner dans [59]. Il a l'avantage d'être très simple et très visuel : un seul dessin permet de comprendre à la fois le mouvement de la marche aléatoire et ses temps locaux. Nous utilisons dans ce paragraphe les mêmes notations que dans l'article [17].

1. La courbe $\Lambda_{0,0}$ est prise en compte.

Définition de la marche Notre modèle jouet est noté $(\tilde{X}_n, n \geq 0)$. Comme précédemment, $l(n,e)$ représente le temps local sur l'arête e avant la n-ième étape :

$$l(n,e) = \#\left\{k \in \{0,\cdots,n-1\},\ \{\tilde{X}_k, \tilde{X}_{k+1}\} = \{e-1/2, e+1/2\}\right\}.$$

Nous ajoutons une condition initiale à ce temps local, c'est à dire qu'au lieu de considérer que la marche part avec un temps local égal à 0 sur toutes les arêtes, nous changeons sa valeur selon les règles suivantes :

$$\ell_n(e) = l(n,e) + a(e)$$

où $a(e)$ vaut 0 ou -1 si $|e| - 1/2$ est pair ou impair, respectivement (voir Fig. I.2).

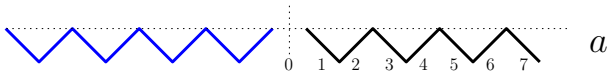

FIGURE I.2 – Tracé de l'initialisation a

La loi de la marche aléatoire $(\tilde{X}_n)$ est définie par $\tilde{X}_0 = 0$ et pour tout $n \geq 0$, en posant

$$\ell_n^- := \ell_n(\tilde{X}_n - 1/2) \text{ et } \ell_n^+ := \ell_n(\tilde{X}_n + 1/2),$$

nous avons

$$\mathbb{P}\left(\tilde{X}_{n+1} = \tilde{X}_n + 1 \middle| \tilde{X}_0, \cdots, \tilde{X}_n\right) = 1 - \mathbb{P}\left(\tilde{X}_{n+1} = \tilde{X}_n - 1 \middle| \tilde{X}_0, \cdots, \tilde{X}_n\right)$$
$$= \begin{cases} 1 & \text{si} \quad \ell_n^- > \ell_n^+ \\ 1/2 & \text{si} \quad \ell_n^- = \ell_n^+ \\ 0 & \text{si} \quad \ell_n^- < \ell_n^+. \end{cases}$$

En d'autres termes, à l'instant n, la marche choisit de sauter le long de l'arête voisine qu'il a visité le moins souvent dans le passé (en tenant compte de l'initialisation a), et dans le cas d'égalité, il tire à pile ou face pour choisir sa direction.

Notons que l'on peut choisir d'autres initialisations a pour lesquelles le modèle restera intéressant [2] : par exemple, on peut prendre une initialisation aléatoire telle que $(a(k+1/2), k \in \mathbb{N})$ et $(a(-k-1/2), k \in \mathbb{N})$ suivent des marches aléatoires simples indépendantes commençant en 0 (à la limite, ce modèle correspond au modèle stationnaire continu). Les propriétés qu'il est important de garder pour la configuration initiale a sont le fait que $|a(e) - a(e+1)| = 1$ pour toute arête e de $\mathbb{Z} + 1/2$, excepté l'arête $\{\tilde{X}_0 - 1/2\} = \{-1/2\}$ pour laquelle on a $a(-1/2) = a(1/2)$. Ainsi, il est facile de voir que pour tout temps n, nous aurons toujours $|\ell_n(e) - \ell_n(e+1)| = 1$ pour tout $n \in \mathbb{N}$ et tout $e \in \mathbb{Z} + 1/2$ sauf une seule, qui est l'arête $e = \tilde{X}_n - 1/2$: à ce

2. Notons par exemple que l'initialisation $a := 0$ donne une marche aléatoire triviale allant toujours vers la droite ou toujours vers la gauche selon le premier tirage.

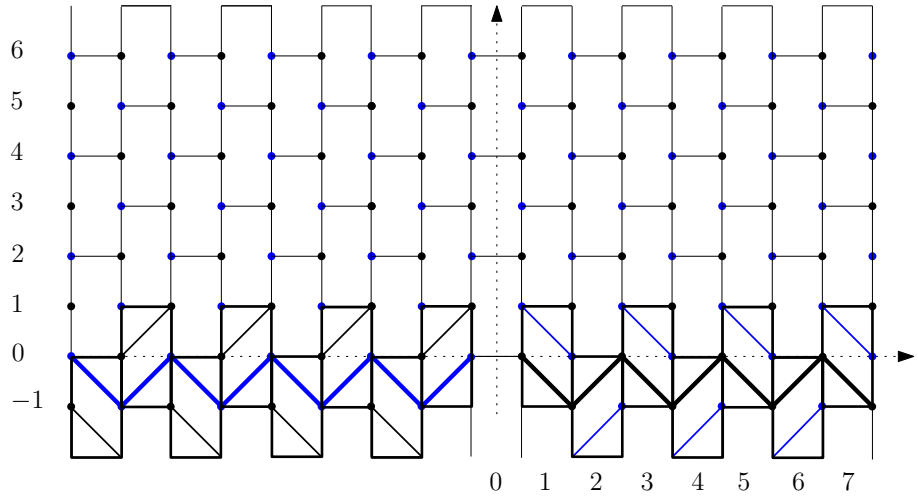

FIGURE I.3 – Les rectangles divisant le demi plan et les segments déterministes provenant de l'initialisation a (tracée en gras).

point, nous avons $\ell_n(e) - \ell_n(e+1) \in \{-2, 0, 2\}$. Nous venons d'expliciter le fait que $n \mapsto \ell_n(\cdot)$ est un processus de Markov : à partir de ces courbes, nous pouvons lire directement où se trouve la marche $\tilde{X}$.

Le labyrinthe ou BW discret Il s'avère que cette marche aléatoire peut aussi être vue comme un chemin qui parcourt un labyrinthe très proche de la toile brownienne définie partie I.2. (voir §11 de [59] pour la démonstration complète, mais ce fait est très facile à obtenir). La définition du labyrinthe paraît assez technique, mais elle se comprend facilement avec les figures I.3, I.4 et I.5. Soit $\mathbb{N}^{\#} := \mathbb{N} \cup \{-1\}$. Posons :

$$F := \{(x - 1/2, h) \in (\mathbb{Z} - 1/2) \times \mathbb{N}^{\#} \ : \ x + h \text{ est impair}\},$$
$$B := ((\mathbb{Z} - 1/2) \times \mathbb{N}^{\#}) \setminus F.$$

Nous divisons le demi-plan supérieur en rectangles de taille 1×2 et disposés comme suit : $(x - 1/2, x + 1/2) \times (h - 1, h + 1)$ pour $(x - 1/2, h) \in F$. Dans chaque rectangle défini ainsi avec $(x - 1/2, h) \in F$ tel que $h \notin \{-1, 0\}$, nous tirons à pile ou face indépendamment pour choisir l'une des deux configurations de la Fig. I.4 : soit nous traçons deux segments parallèles dirigés vers le haut de $(x - 1/2, h) \in F$ à $(x + 1/2, h + 1) \in F$ et de $(x - 1/2, h - 1) \in B$ à $(x + 1/2, h) \in B$ soit nous traçons deux segments vers le bas de $(x - 1/2, h) \in F$ à $(x + 1/2, h - 1) \in F$ et de $(x - 1/2, h + 1) \in B$ à $(x + 1/2, h) \in B$. Pour $h \in \{-1, 0\}$, les segments à tracer sont déterminés par l'initialisation a : pour tout $e \in \mathbb{Z} + 1/2 \setminus \{-1/2\}$, nous traçons une ligne de $(e, a(e))$ à $(e + 1, a(e + 1))$ et son segment parallèle dans le même rectangle

(voir Fig. I.3 pour plus de clarté). Lorsque $e = -1/2$, nous ne traçons rien (voir encore Fig. I.3, et Fig. I.5 pour une réalisation complète).

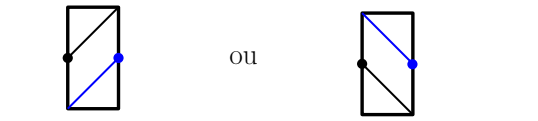

avec probabilité 1/2 avec probabilité 1/2

FIGURE I.4 – Choix entre les deux configurations à tirer à pile ou face.

Si nous regardons les lignes passant par les éléments de F, nous observons que nous avons ainsi défini une famille de marches aléatoires simples allant vers la droite, partant de tous les points de F, indépendantes, coalescentes et réfléchies au dessus de 0 sur la partie négative de l'axe des abscisses et absorbées par 0 sur la partie positive. De manière analogue, les lignes passant par les éléments de B créent une famille de marches aléatoires simples coalescentes allant vers la gauche, ne croisant jamais la première famille (voir Fig. I.5). Ces familles constituent l'analogue discret de la toile brownienne définie sur le demi plan supérieur (voir partie I.2).

Nous voyons dans la figure I.5 que les familles des marches aléatoires coalescentes forment un labyrinthe aléatoire. Le chemin commençant au point $(0, 0)$ qui explore ce labyrinthe (tracé Fig. I.6) peut être vu comme un chemin discret $(\tilde{X}_n, \tilde{H}_n) \in \mathbb{Z} \times \mathbb{N}$. Sa première coordonnée a en fait la même loi que la marche aléatoire jouet dans $\mathbb{Z}$ définie plus haut et sa seconde coordonnée est la moyenne des temps locaux (avec l'initialisation) au temps n des deux arêtes adjacentes à $\tilde{X}_n$, i.e., $\tilde{H}_n = (\ell_n^+ + \ell_n^-)/2$.

Notons qu'il est trivial de montrer pour ce modèle des théorèmes limites ana-

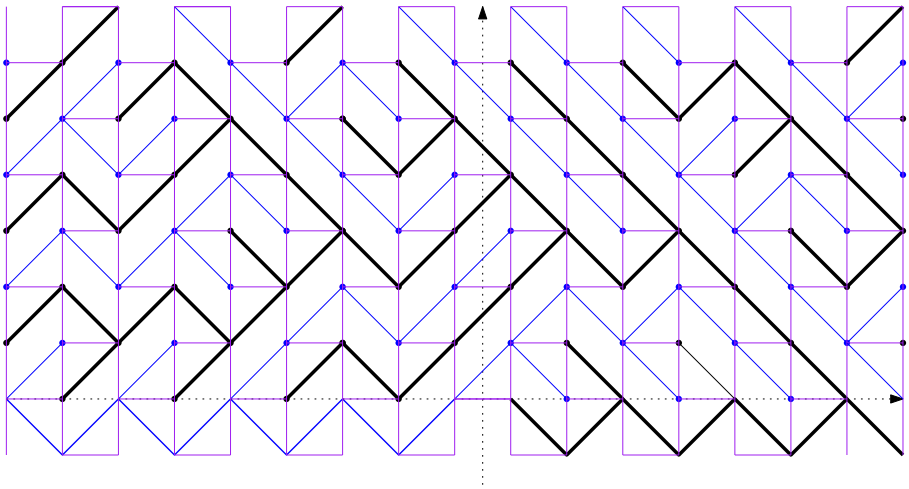

FIGURE I.5 – Réalisation des marches aléatoires coalescentes (en gras celles passant par F)

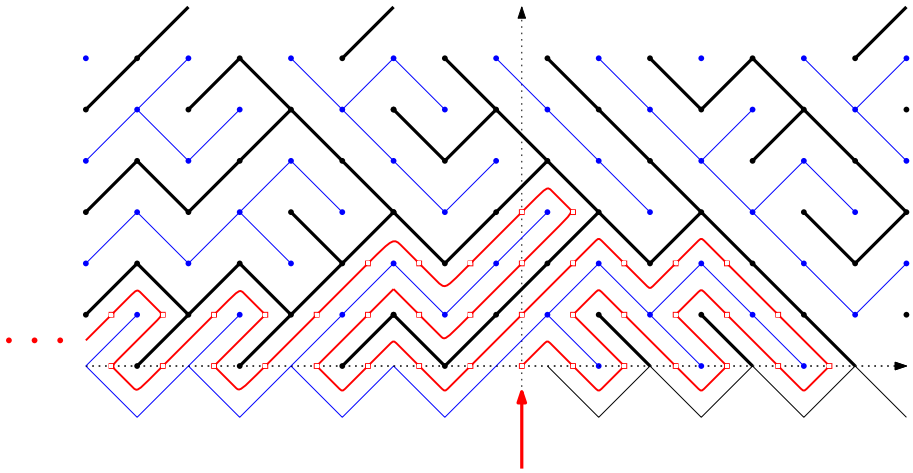

FIGURE I.6 – Réalisation des 39 premières étapes de $(\tilde{X}_n, \tilde{H}_n)$

logues à ceux de B. Tóth pour la TSRW. En effet, pour tout $(x,h) \in \mathbb{Z}\times\mathbb{N}$, le temps local de cette marche au temps d'atteinte de (x,h) est simplement la réunion des marches aléatoires partant de $(x-1/2, \ell_n^-)$ (allant vers la droite) et $(x+1/2, \ell_n^+)$ (allant vers la gauche). Cette description très simple des temps locaux nous a été utile pour déduire des informations sur la loi conditionnelle du déplacement du TSRM au temps 1 connaissant son temps local à cet instant, pour plus de détails, voir le paragraphe I.4.4 et l'article [17].

Ainsi, nous avons vu un lien entre des marches aléatoires coalescentes discrètes du demi plan et une marche aléatoire auto-répulsive dans $\mathbb{Z}$ (le modèle jouet). Une idée pour construire le modèle continu est donc de trouver l'analogue continu des marches aléatoires coalescentes discrètes, c'est à dire de définir une famille de Browniens, partant de tous les points du plan (cela sera la toile brownienne) et cette construction étant effectuée, de regarder s'il est possible de définir un processus 1+1 dimensionnel faisant le tour de cet arbre. C'est cette procédure qui a été appliquée dans [59] et que nous allons décrire dans les parties I.2 et I.3 de l'introduction.

I.1.3 Quelques modèles reliés

Il est naturel de se demander ce qu'il se passe pour des modèles plus généraux d'interaction, où les probabilités de transition de la marche aléatoire ne dépendent plus seulement des temps locaux des arêtes voisines, mais par exemple des temps locaux des k arêtes les plus proches. Une première généralisation intéressante est le cas où $k=2$ et la loi est la suivante : soit a et b deux réels et pour toute fonction $\ell : \mathbb{Z}+1/2 \to \mathbb{R}$, soit $\omega(\ell) := \exp\left(a\ell(-3/2) + b\ell(-1/2) - b\ell(1/2) - a\ell(3/2)\right)$, alors

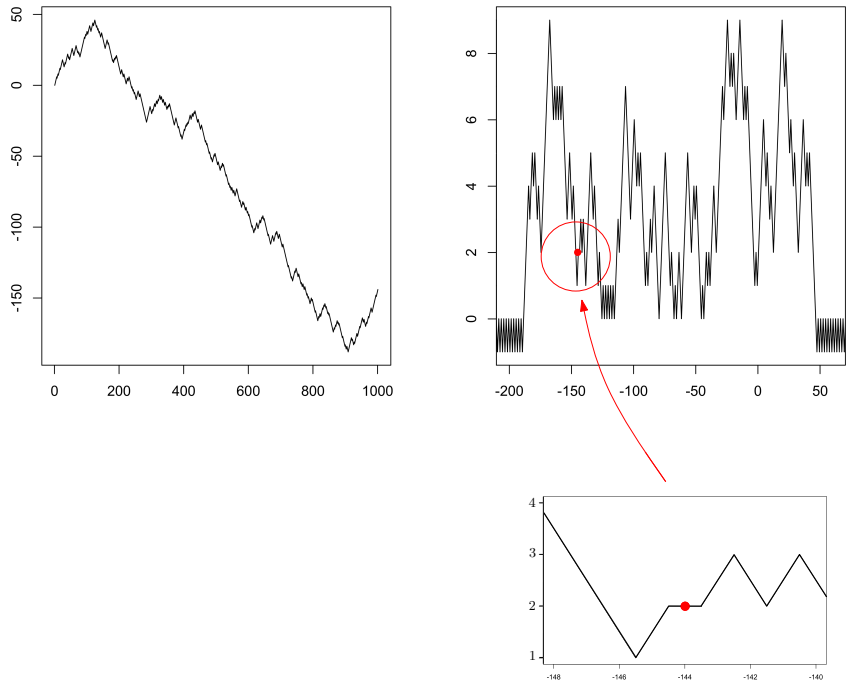

FIGURE I.7 – Réalisation du modèle jouet jusqu'au temps $n = 1000$. Sur la gauche, $k \mapsto \tilde{X}_k$; sur la droite, son temps local au temps n et la position $(\tilde{X}_n, \tilde{H}_n)$ zoomée

les lois de transitions de S vérifient :

$$\mathbb{P}(S(n+1) = x+1 | S(n) = x, \text{ Passé}) = \frac{\omega(l(n, x+\cdot))}{\omega(l(n, x+\cdot)) + \omega(-l(n, x+\cdot))}$$

où l désigne comme précédemment le temps local de S.

Ce modèle a été introduit et étudié par A. Erschler, B. Tóth et W. Werner dans [24]. Notons que lorsque $b > 0$ et $a = 0$, c'est le cas précédemment mentionné de la TSRW, paragraphe I.1.1. Lorsque $b > 0$ et $|a|$ est petit, nous pouvons donc voir cette marche comme une perturbation de la TSRW. Les auteurs de [24] ont décrit quelques propriétés de ce modèle suivant les valeurs de a et b. Ils ont en particulier montré un comportement au premier abord peu intuitif : la répulsion par les deuxièmes voisins n'a pas toujours le même effet que la répulsion par les voisins immédiats car des pièges peuvent apparaître.

Les preuves des théorèmes limites de [57] (et des papiers plus récents) s'appuient sur des arguments combinatoires qui rendent l'extension des résultats à des classes plus générales de marches auto-répulsives unidimensionnelles difficile. Il est conjecturé que lorsque $b > 0$ et $a \in (-b/3, b)$, cette nouvelle marche aléatoire renormalisée par $n^{2/3}$ converge vers le TSRM (dans [24], les auteurs ont prouvé que le gradient

des temps locaux admet une mesure stationnaire de type Gaussien).

Ce modèle discret est fortement lié au modèle continu de polymère brownien, introduit par R. Durrett et C. Rogers en 1992 [21]. Ce polymère est un processus stochastique dont la dérive est une moyenne pondérée de son temps local. Plus précisément, si nous le notons $(Y(t))_{t\geq 0}$, sa loi est donnée par $Y(0) = 0$ et

$$Y(t) = B(t) + \int_0^t \int_0^s (f(Y(s) - Y(u))du)\, ds,$$

où B est un mouvement Brownien unidimensionnel, f une fonction à valeurs réelles suffisamment régulière. Il est instructif de retranscrire cette égalité avec la densité du temps d'occupation (le temps local) $L(t, x)$ du processus Y :

$$Y(t) = B(t) + \int_0^t \int_{-\infty}^{\infty} f(z)L(s, Y(s) - z)dzds.$$

Il est conjecturé dans [21] que si $f(-x) = -f(x)$, $\mathrm{sgn}(f(x)) = \mathrm{sgn}(x)$ (condition de répulsion) et f décroit suffisamment vite en l'infini, alors presque sûrement $Y_t/t \to_{t\to\infty} 0$, et même plus tard dans [59] que $Y_{t\cdot}/t^{2/3}$ converge en loi vers le TSRM. Des résultats allant dans ce sens ont été obtenus par P. Tarrés, B. Tóth et B. Valkó en 2009 [56]. Ces auteurs ont prouvé des bornes super diffusives pour un large ensemble de fonctions f : $\liminf_{t\to\infty} t^{-5/4}\mathbb{E}(Y(t)^2) > 0$, et $\limsup_{t\to\infty} t^{-3/2}\mathbb{E}(Y(t)^2) < \infty$. Ces résultats sont encore loin du $t^{2/3}$ attendu, mais ils ont le mérite d'être "robustes" : la classe des modèles unidimensionnels auto-répulsifs pour lesquels ils s'appliquent ne dépend pas des particularités microscopiques.

I.2 La toile brownienne (BW)

La toile brownienne ("Brownian Web", notée BW dans cette thèse) est un objet central dans la construction et l'étude du processus qui nous intéresse (nous verrons plus loin que le TSRM est une fonction déterministe du BW). Nous pouvons déduire de nombreuses informations sur le comportement du TSRM en observant certaines des courbes qui constituent le BW.

Il existe plusieurs façons d'appréhender le BW, comme une famille (aléatoire) de fonctions ou comme un objet topologique. Dans un premier temps, nous allons voir le BW simplement comme une famille de courbes aléatoires coalescentes du plan, qui peut être définie dans *différents domaines du plan*. En ce qui nous concerne, nous utiliserons essentiellement le plan tout entier et le demi plan supérieur. Il est néanmoins possible de définir le BW au dessus de n'importe quelle courbe suffisamment sympathique (notons que la continuité n'est pas suffisante, voir [53] pour plus

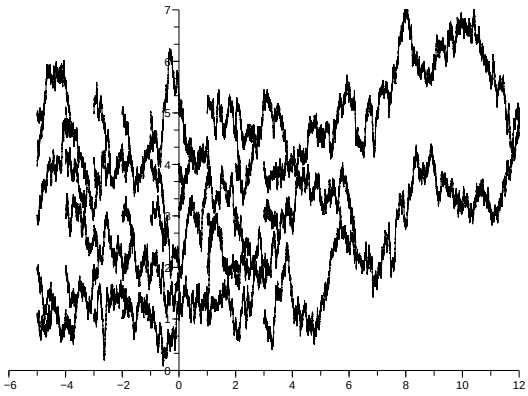

FIGURE I.8 – Quelques courbes de l'arbre $\mathcal{T}_f$

de détails). Pour plus de clarté, nous allons nous restreindre dans ce paragraphe à la version définie dans *tout le plan*, qui est aussi la plus classique.

L'idée de sa construction est la suivante : de chaque point du plan, on fait partir deux mouvements browniens unidimensionnels, un vers la droite de type f (pour "forward"), un vers la gauche de type b ("backward"), de telle sorte que ces trajectoires sont indépendantes tant qu'elles restent disjointes mais qu'elles coalescent dès qu'elles rencontrent une courbe du même type (f ou b) et se réfléchissent l'une sur l'autre si elles appartiennent à des types différents. On obtient ainsi une famille aléatoire de trajectoires browniennes partant de tous les points du plan. Le mouvement brownien est récurrent et deux trajectoires finissent toujours par se rencontrer. Si nous regardons seulement les courbes de type f, nous obtenons ainsi une structure - complexe car dense dans le plan - d'arbre enraciné en $+\infty$. C'est l'arbre $\mathcal{T}_f$ ("forward") des courbes qui vont vers la droite (voir Fig. I.8). De même pour les courbes de type b, elles forment un arbre $\mathcal{T}_b$ enraciné en $-\infty$.

Précisons avant d'entrer plus dans les détails que cette famille a été introduite par R. Arratia en 1979 [4] qui s'intéressait à cette structure pour étudier les asymptotiques du modèle de vote ("voter model") en dimension 1 et les flux stochastiques. Elle a été ensuite étudiée par B. Tóth et W. Werner pour le TSRM en 1998 [59], puis reprise par L. Fontes, M. Isopi, C. Newmann et K. Ravishankar en 2004 dans [30] qui lui ont donné son nom ("brownian web") et sa structure topologique, nécessaire pour prouver la convergence des marches coalescentes vers ce objet. La définition exacte du BW varie d'un papier à l'autre et nous veillerons dans les parties suivantes à être toujours précis sur la version que nous utiliserons (qui est celle du papier de B. Tóth et W. Werner [59]) tout en explicitant les points de différence avec les autres définitions. Une première divergence mineure - mais très visible dans les dessins ! -

est l'orientation du BW. Nous avons choisi l'orientation horizontale pour le temps, mais certains auteurs préfèrent l'orientation verticale.

I.2.1 Construction de la toile brownienne

Nous allons rapidement expliquer la construction du BW. Pour plus de détails, le lecteur se réfèrera à [59].

Construction du squelette Pour commencer, choisissons n'importe quelle famille de points Q déterministe, dénombrable et dense dans le plan, on peut penser par exemple à $Q = \mathbb{Q}^2$. Il est possible de définir la loi jointe de la famille $(\Lambda_{\tilde{x},\tilde{h}}(y), y \in \mathbb{R}\ ;\ (\tilde{x},\tilde{h}) \in Q)$ telle que pour tout $(\tilde{x},\tilde{h}) \in Q$, $(\Lambda_{\tilde{x},\tilde{h}}(y), y \in \mathbb{R})$ est une fonction de $\mathbb{R}$ dans $\mathbb{R}$ qui a la loi d'un mouvement brownien partant des deux côtés de condition initiale $\Lambda_{\tilde{x},\tilde{h}}(\tilde{x}) = \tilde{h}$. Ainsi la courbe $(\Lambda_{\tilde{x},\tilde{h}}(y), y \geq \tilde{x})$ appartient à $\mathcal{T}_f$ selon le critère introduit ci-dessus (elle va vers la droite), et la courbe $(\Lambda_{\tilde{x},\tilde{h}}(y), y \leq \tilde{x})$ est dans $\mathcal{T}_b$. L'interaction entre les éléments de cette famille est définie comme suit : les règles principales sont que les trajectoires sont indépendantes avant de se toucher et qu'elles ne peuvent pas se croiser. Définissons par récurrence les éléments de la famille. Soit $(\tilde{x}_i,\tilde{h}_i)_{i\in\mathbb{N}}$ un ordre quelconque de Q. Supposons que les courbes $(\Lambda_{\tilde{x}_i,\tilde{h}_i}(y),\ y \in \mathbb{R}\ ;\ i < j)$ soient déjà définies. Le processus $(\Lambda_{\tilde{x}_j,\tilde{h}_j}(y), y \geq \tilde{x}_j)$ appartenant à $\mathcal{T}_f$ (resp. $(\Lambda_{\tilde{x}_j,\tilde{h}_j}(y), y \leq \tilde{x}_j) \in \mathcal{T}_b$) est un mouvement brownien indépendant des courbes déjà tracées jusqu'à ce qu'il en rencontre une : s'il touche une courbe de $\mathcal{T}_f$ (resp. $\mathcal{T}_b$), il coalesce avec elle ; si c'est une courbe de $\mathcal{T}_b$ (resp. $\mathcal{T}_f$), il est réfléchi sur elle à la manière de Skorokhod [3]. On peut montrer que cette procédure est bien définie car les coalescences et réflexions ne dépendent pas de l'ordre que l'on choisit pour construire la famille. Pour les coalescences, c'est simplement du à la propriété de Markov fort. Le cas des réflexions est plus complexe mais a été résolu dans [53], grâce à un argument combinatoire dans le discret et à un principe d'invariance. Notons que comme Q est dense dans le plan, le tracé de toutes ces trajectoires est lui aussi dense. Cette famille dénombrable est parfois appelée *squelette* du BW.

Le BW sur $\mathbb{R}^2$ Maintenant que la construction est effectuée pour un nombre de points conséquent, il est naturel de se demander si l'on peut étendre cette construction à une famille de courbe $(\Lambda_{x,h}(y), y \in \mathbb{R}\ ;\ (x,h) \in \mathbb{R}^2)$ partant de tous les points du plan en utilisant les courbes du squelette déjà tracées. Ici, l'extension de la famille dénombrable à la famille issue du plan tout entier laisse un *choix* sur la régularité,

3. La réflexion de Skorokhod est définie comme suit : si f et g sont deux fonctions continues définies sur $[0,T]$, telles que $f(0) > g(0)$ alors la réflexion de f sur g est donnée par $f_g(t) := f(t) + \sup_{s\leq t}(f(s) - g(s))_-$ où $x_- := -x\mathbf{1}_{\{x<0\}}$.

et les différentes versions du BW utilisent des régularités différentes selon les besoins des auteurs. Dans [59], la courbe issue de (x,h) de type f, $(\Lambda_{x,h}(y), y \geq x)$, correspond au supremum des $\Lambda_{\tilde{x},\tilde{h}}(y)$ tels que $(\tilde{x},\tilde{h})$ appartient à l'ensemble

$$\left\{(\tilde{x},\tilde{h}) \in Q \ : \ \tilde{x} < x, \ \Lambda_{\tilde{x},\tilde{h}}(x) < h\right\},$$

c'est à dire que les courbes $\Lambda_{\tilde{x},\tilde{h}}$ considérées commencent avant x et passent sous h en x. La courbe de type b issue de (x,h) i.e. $(\Lambda_{x,h}(y), y \leq x)$ est définie de manière analogue comme le supremum des $\Lambda_{\tilde{x},\tilde{h}}(y)$ tels que $(\tilde{x},\tilde{h})$ appartient à

$$\left\{(\tilde{x},\tilde{h}) \in Q \ : \ \tilde{x} > x, \ \Lambda_{\tilde{x},\tilde{h}}(x) < h\right\}.$$

Remarquons que la dualité entre $\mathcal{T}_f$ et $\mathcal{T}_b$, c'est à dire le fait que $\mathcal{T}_f$ a la même loi que $(\Lambda_{-x,h}(-y), \ y \geq -x, \ (x,h) \in \mathbb{R}^2)$ découle directement des définitions.

Remarque. Dans l'article [59], les auteurs ont procédé en fait un peu différemment : ils ont construit tout d'abord toutes les courbes de $\mathcal{T}_f$ (avec l'aide d'un squelette ne contenant que des éléments de $\mathcal{T}_f$; la construction est ainsi simplifiée car il n'y a pas à se préoccuper du problème des réflexions) et ensuite défini de façon *déterministe*, à partir des courbes de $\mathcal{T}_f$, les courbes de $\mathcal{T}_b$:

$$\forall (x,h) \in \mathbb{R}^2, \ \forall y \leq x, \quad \Lambda_{x,h}(y) := \sup\{h' > 0 \ : \ \Lambda_{y,h'}(x) < h\}.$$

La dualité n'est plus triviale et constitue l'objet de leur Théorème 2.3. Ainsi, les deux constructions sont équivalentes.

Le théorème 2.1 de [59] montre que la famille $\mathcal{T}_f$ ainsi définie vérifie les propriétés suivantes :

(i) Pour tout ensemble fini déterministe $(x_1,h_1),\cdots,(x_n,h_n) \in \mathbb{R}^2$, la famille $(\Lambda_{x_i,h_i}(y), \ y \geq x_i, \ i \in \{1\cdots n\})$ suit la loi de mouvements browniens indépendants coalescents,

(ii) presque sûrement, pour tout $(x,h) \in \mathbb{R}^2$, $\Lambda_{x,h}(x) = h$,

(iii) presque sûrement, pour tout $(x_1,h_1),(x_2,h_2) \in \mathbb{R}^2$, Λ_{x_1,h_1} et Λ_{x_2,h_2} ne se croisent jamais,

(iv) presque sûrement, pour tout $x < y$, la fonction $h \mapsto \Lambda_{x,h}(y)$ est continue à gauche,

et que ces quatre propriétés caractérisent sa loi [4]. Notons que la première (i) nous montre que le choix de Q ne change pas la loi de Λ. La dernière propriété est présente

4. Ces propriétés ont été établies pour le BW défini sur le demi plan supérieur, mais les démonstrations s'appliquent aisément au cas du plan tout entier.

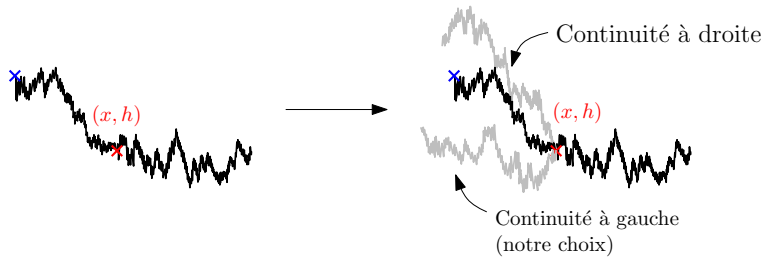

FIGURE I.9 – Choix pour un point sur une courbe f déjà tracée

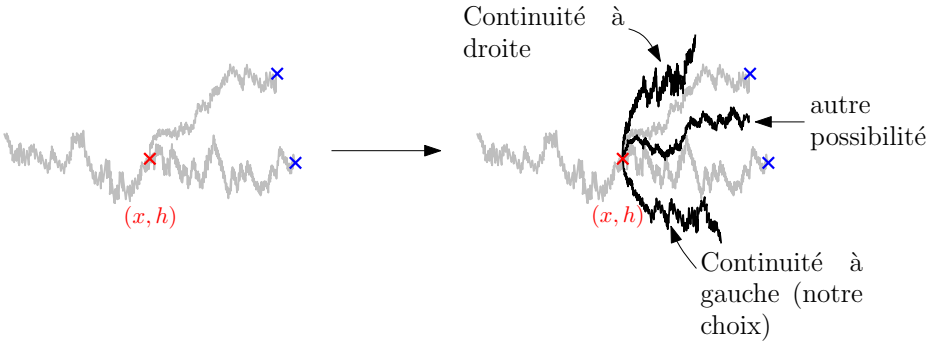

FIGURE I.10 – Choix pour un point de coalescence de deux courbes b

pour choisir une des différentes courbes possibles issue de (x,h) : cette condition est suffisante pour en obtenir une seule, celle qui est "la plus basse". On aurait bien entendu pu remplacer cette dernière condition par une continuité à droite, ce qui reviendrait à choisir la courbe "la plus haute" parmi les courbes possibles. Une autre option naturelle choisie par R. Arratia est de "conserver le flot" i.e. de remplacer (iv) par "presque sûrement, pour tout $(x,h) \in \mathbb{R}^2$ et $x \leq y \leq z$, $\Lambda_{x,h}(z) = \Lambda_{y,\Lambda_{x,h}(y)}(z)$ et pour tout $x \leq y$ fixés, $h \to \Lambda_{x,h}(y)$ est presque sûrement continue à gauche (ou, de façon alternative, continue à droite)". Voir comme exemple les figures I.9, I.10 et I.11.

Comme échauffement pour le lecteur, nous montrons une petite partie de ce théorème (la preuve complète se trouve dans [59], p. 420 à 424) car cette démonstration illustre bien les méthodes utilisées pour l'étude du BW.

Preuve de la continuité de $\Lambda_{x,h}$ pour (x,h) fixé. Fixons $(x,h) \in \mathbb{R}^2$. Nous allons montrer que $\Lambda_{x,h}$ est bien définie et est continue (c'est la première étape pour montrer (i) du théorème). L'idée est que pour tout $\varepsilon > 0$, la courbe issue de (x,h) coalesce avec une des courbes du squelette avant $x + \varepsilon$. Plus précisément :

Fait 1.2. *Il existe une suite $(\tilde{x}_n, \tilde{h}_n)$ (déterministe) d'éléments de Q avec $\tilde{x}_n < x$ tendant vers (x,h) telle que presque sûrement pour tout $\varepsilon > 0$, à partir d'un certain*

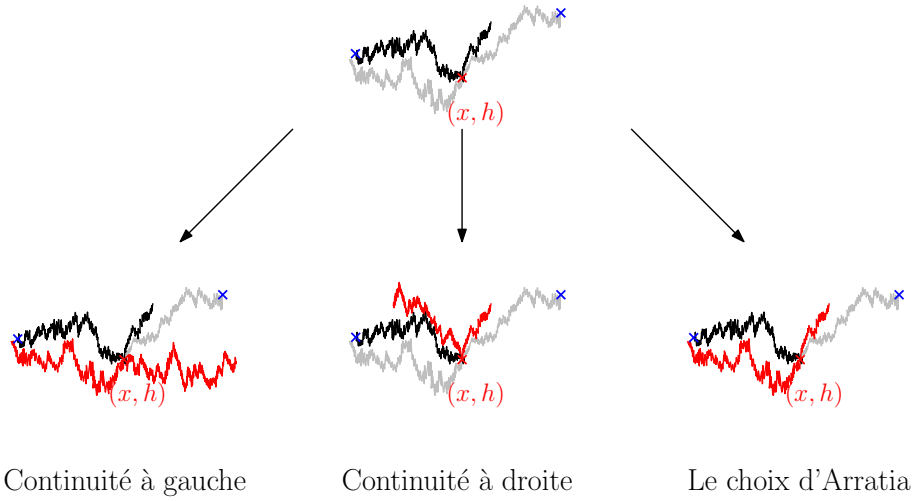

FIGURE I.11 – Choix pour un point de réflexion entre deux courbes f et b

$n_0 = n_0(\varepsilon)$, *on a* $\Lambda_{x,h}(y) = \Lambda_{\tilde{x}_n,\tilde{h}_n}(y)$ *pour tout* $y \geq x + \varepsilon$ *et tout* $n \geq n_0$.

En effet, nous pouvons encadrer la courbe $\Lambda_{x,h}$ par deux familles de courbes du squelette bien choisies qui commencent avant x et qui ont une probabilité faible de coalescer avant x et forte de coalescer avant $x + \varepsilon$ (si ces événements se produisent simultanément, les courbes du squelette commençant avant x et passant sous h en x se retrouvent bloquées entre ces deux familles de courbes). A cet effet, choisissons une courbe du squelette commençant dans le rectangle $(x-5^{-k}, x) \times (h-2\cdot 2^{-k}, h-2^{-k})$ et une autre dans $(x-5^{-k}, x) \times (h+2^{-k}, h+2\cdot 2^{-k})$ et notons $\mathcal{A}_k$ l'événement "elles restent chacune respectivement dans les rectangles $(x-5^{-k}, x+5^k) \times (h-3\cdot 2^{-k}, h)$ et $(x-5^{-k}, x+5^k) \times (h, h+3\cdot 2^{-k})$ et elles coalescent avant $x+\varepsilon$" (voir dessin I.12). Des estimées browniennes classiques permettent de voir que cette probabilité est plus grande que $1-u_k$ où la série des u_k est convergente. Le lemme de Borel Cantelli nous donne le fait 1.2.

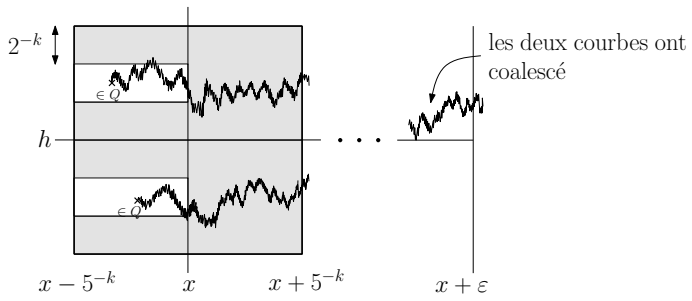

FIGURE I.12 – Encadrement de la courbe issue de (x, h) par deux courbes du squelette

Le même encadrement et le lemme de Borel Cantelli permettent de montrer que presque sûrement,

$$\Lambda_{x,h}(x) = \lim_{y \downarrow x} \Lambda_{x,h}(y) = h$$

(car $\sup_{y \in [x, x+5^{-k}]} |\Lambda_{x,h}(y) - h| < 3 \cdot 2^{-k}$ est inclu dans $\mathcal{A}_k$).

Ceci permet de conclure sur la continuité de $\Lambda_{x,h}$. □

Remarque. Une autre possibilité intéressante pour la définition du BW est de garder toutes les courbes possibles en (x, h) (en certains points exceptionnels, plusieurs courbes du squelette passent). C'est l'option choisie par Fontes et al dans [30] et c'est aussi la plus naturelle pour montrer la convergence des marches aléatoires coalescentes discrètes vers le BW (à la limite, il y a effectivement plusieurs courbes en certains points du plan). Une façon de toutes les considérer est de définir le BW comme la fermeture du squelette défini plus haut pour une métrique bien choisie de l'espace dans lequel les courbes coalescentes vivent.

I.2.2 Propriétés du BW

BW et son squelette Une première propriété assez rassurante du BW est la coalescence immédiate vers un nombre localement fini de courbes : il n'y a pas assez de place dans le plan pour qu'un nombre infini de courbes subsiste. Plus précisément, définissons par $M(x, y)$ la trace en y de toutes les courbes de $\mathcal{T}_f$ qui commencent avant x, c'est à dire :

$$M(x, y) := \{\Lambda_{z,h}(y) \ : \ (z, h) \in \mathbb{R}^2, \ z < x\}.$$

Alors, presque sûrement, pour tout $x < y$, l'ensemble $M(x, y)$ est localement fini et non borné (Proposition 2.2 (ii) de [59]). Une propriété similaire établit que presque sûrement, pour tout $(x, h) \in \mathbb{R}^2$, il existe une suite (y_n) décroissant vers x et une suite $(\tilde{x}_n, \tilde{h}_n)$ de points dans Q telle que

$$\Lambda_{x,h}(y) = \Lambda_{\tilde{x}_n, \tilde{h}_n}(y) \quad \text{pour tout } y \geq y_n \text{ et tout } n \geq 0.$$

Autrement dit, quelle que soit la courbe choisie, elle coalesce "immédiatement" avec le squelette du BW (Proposition 2.2 (iv) de [59]).

Différents types de points Nous savons qu'en chaque point du plan, une courbe du BW est définie. La trajectoire de chacune de ces courbes passe par un nombre infini de points dans le plan (ce sont des courbes browniennes, leur trace a donc une dimension de Hausdorff égale à 3/2), ce qui implique que certains points sont touchés

plusieurs fois par des courbes du BW (chaque point (x,h) est au moins touché par la courbe qui part de ce point et par celles qui partent d'un autre endroit et qui passent exactement par (x,h)). Nous allons analyser les différentes configurations qui peuvent se produire. Le tableau I.13. résume les cas possibles.

Pour tout $(x,h) \in \mathbb{R}^2$, définissons par $I(x,h)$ le nombre de courbes de $\mathcal{T}_f$ coalesçant exactement en (x,h), i.e.

$$I(x,h) = \limsup_{y \uparrow x} \Big\{ p \in \mathbb{N} \ : \exists (x_1,h_1), \cdots, (x_p,h_p) \in \mathbb{R}^2, \text{telle que} \\ \forall i = 1, \cdots, p, \ x_i \leq y, \ \Lambda_{x_i,h_i}(x) = h \text{ et} \\ \forall z \in [y,x), \ \Lambda_{x_1,h_1}(z) < \cdots < \Lambda_{x_p,h_p}(z) \Big\}.$$

De même, $I^*(x,h)$ désigne le nombre de courbes de $\mathcal{T}_b$ coalesçant exactement en (x,h). La proposition suivante décrit en détail les différents types de points possibles. Pour alléger l'écriture, nous désignons par $[I(x,h), I^*(x,h)]$ le type du point (x,h). Cette proposition est issue de la Proposition 2.4 de [59].

Proposition 1.3 (sur les types de points du BW)**.**

1. *Pour tout $(x,h) \in \mathbb{R}^2$ fixé, presque sûrement, $I(x,h) = 0$ et $I^*(x,h) = 0$.*
2. *Presque sûrement, tout point (x,h) appartient à l'un des types de points suivants :* $[0,0]$, $[1,0]$, $[0,1]$, $[2,0]$, $[1,1]$, $[0,2]$.

Les points de type différent de $[0,0]$ joueront un rôle particulier pour les trajectoires du TSRM, nous renvoyons le lecteur à la partie I.4.2. pour plus de détails.

I.2.3 Applications diverses et développements

Le BW est un objet très naturel et de ce fait constitue un sujet d'étude important à plusieurs titres, au delà du contexte du TSRM qui nous a principalement intéressé au cours de cette thèse. Il est par exemple une illustration simple de "bruit noir" (voir le cours de B. Tsirelson [63]). Il est aussi la limite de l'arbre Poissonien en dimension deux ("Two-dimensional Poisson Trees") introduit par Ferrari, Landim et Thorisson dans [27], voir [26]. Cet arbre Poissonien est notamment lié à un modèle de "drainage network" de Gangopadhyay, Roy et Sarkar [32]. Quant aux auteurs de [30], ils se sont intéressés à cette structure pour étudier le phénomène de vieillissement dans des modèles unidimensionnels discrets de spin [29].

Récemment, des perturbations du BW ont été étudiées. Une manière simple de perturber le BW est de modifier le modèle discret vu paragraphe I.1.2. et de voir comment cette perturbation se propage à la limite. Une autre possibilité est de perturber directement le modèle continu en utilisant ses points spéciaux. Nous décrivons brièvement deux exemples.

$I(x,h)$	$I^*(x,h)$	Dessin	Description	Dimension de Hausdorff
0	0	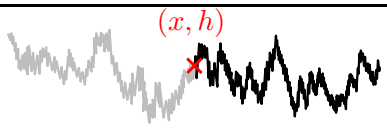	-	2
1	0	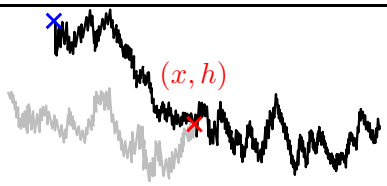	Point sur une courbe f	3/2
0	1	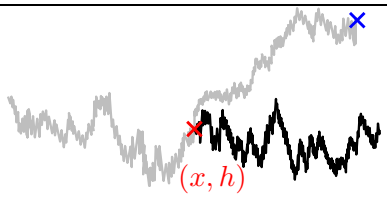	Point sur une courbe b	3/2
2	0	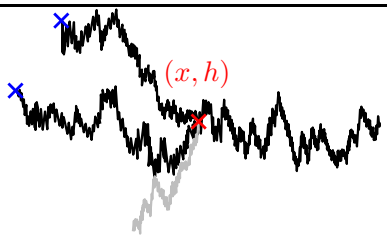	Point de coalescence de deux courbes f	0 (dénombrable, dense)
0	2	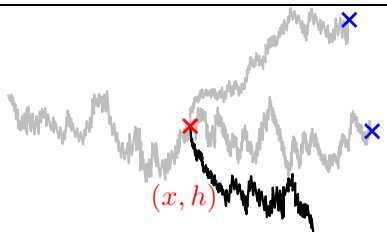	Point de coalescence de deux courbes b	0 (dénombrable, dense)
1	1	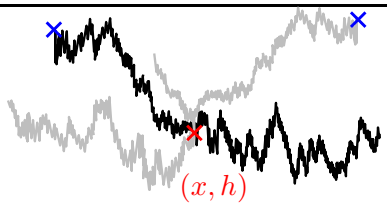	Point de réflexion	1
1	1	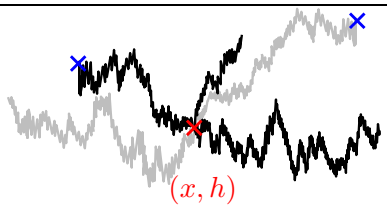	Point de réflexion	1

FIGURE I.13 – Les différents types de points du BW. Pour les dessins, les croix représentent les points dont sont issues les courbes. Les courbes de l'arbre $\mathcal{T}_f$ sont en noir, et celles de $\mathcal{T}_b$ sont en gris.

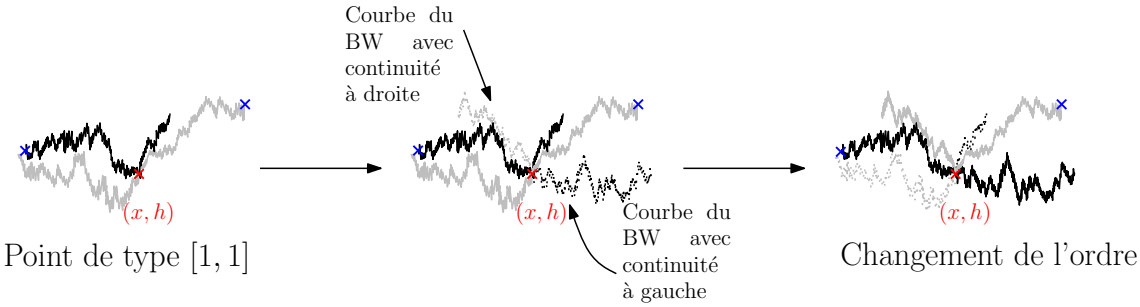

FIGURE I.14 – Point $[1,1]$ marqué dans le BW dynamique

Pour le premier cas, considérons l'arbre coalesçant discret vu dans I.1.2 que l'on définit dans le plan tout entier (l'initialisation a est abandonnée et tous les rectangles suivent les mêmes règles) et supposons que dans chaque rectangle, et de façon indépendante les uns des autres, le dessin choisi évolue selon une chaîne de Markov stationnaire sur l'espace $\{-1,+1\}$ où $+1$ désigne la configuration à gauche de la figure I.4 (lignes vers le haut) et -1 la configuration à droite (lignes vers le bas) et qui saute entre les états -1 et $+1$ avec un taux 1. Cette dynamique a été introduite par C. Howitt et J. Warren dans [34]. Il n'est pas difficile de voir que lorsque l'on fixe deux temps u_1 et u_2, et que l'on fait tendre la maille du réseau discret vers 0 alors les deux BW obtenus seront indépendants l'un de l'autre (c'est une manifestation de la sensibilité au bruit des marches aléatoires coalescentes, et est lié au fait que le BW soit un bruit noir). Pour obtenir une loi jointe plus intéressante, on peut réduire la vitesse des perturbations en même temps que l'on fait tendre la maille du réseau vers 0. C'est ce qui est étudié dans l'article [35]. En particulier, ses auteurs définissent de cette manière un couplage de paramètre θ de deux BW. Dans ce couplage, les courbes respectives du couple partant d'un point fixé du plan sont des mouvements browniens couplés de paramètre θ (voir [34]) où les deux mouvements browniens évoluent indépendamment lorsqu'ils sont séparés, et interagissent lorsqu'ils se touchent (ils restent ensemble un moment).

Un autre perturbation possible consiste à autoriser plusieurs branches à partir d'un même site, c'est l'étude de [54] : reprenons les marches aléatoires coalescentes discrètes et considérons seulement celles allant vers la droite. Dans chaque rectangle, de façon indépendante et avec une probabilité $\beta > 0$, on choisit la configuration avec deux branches (nous aurons à la fois le segment qui part vers le haut et celui qui part vers le bas). Si l'on fait tendre la maille du réseau ε vers 0 en même temps que β de sorte que $\beta/\varepsilon \to b$ pour un certain $b \geq 0$, alors la limite est appelée "brownian net" de paramètre b (lorsque $b = 0$, on retrouve le BW). Les auteurs de [54] ont montré cette convergence et étudié certaines des propriétés de l'objet limite.

Ces deux perturbations peuvent être construites directement dans le modèle

continu en marquant un nombre Poissonien des points de type $[1, 1]$, c'est l'objet de l'article [44]. La Figure I.14 représente un point marqué et le changement effectué pour le BW dynamique.

I.3 Le vrai processus auto-répulsif (TSRM)

I.3.1 Qu'est-ce qu'un processus auto-répulsif ?

Avant d'entrer dans les détails de la construction (complexe) du TSRM, intéressons-nous à l'objet que nous désirons obtenir. Soit $(X_t)_{t\geq 0}$ un processus continu à valeurs réelles quelconque : comment détecter que ce processus est auto-répulsif ? De manière analogue aux modèles discrets, nous avons besoin d'introduire la mesure du temps d'occupation μ_t qui mesure le temps passé avant l'instant t dans chacune des régions de $\mathbb{R}$:

$$\forall A \text{ borélien de } \mathbb{R}, \quad \mu_t(A) := \int_0^t \mathbf{1}_{\{X_s \in A\}} ds.$$

Supposons que cette mesure d'occupation de notre processus admette (pour tout temps t) une densité par rapport à la mesure de Lebesgue, que l'on appelle par analogie avec les semi-martingales *temps local* et que l'on note $L_t(\cdot)$. Intuitivement, nous dirons qu'un processus est auto-répulsif s'il est repoussé par les endroits x où $L_t(x)$ est élevé. Il aura donc une longue mémoire et sera non-markovien. Cependant, il est naturel d'imposer en plus que $(X_t, L_t(\cdot))$ soit un processus de Markov (avec son temps local, le processus a assez d'information pour savoir comment il va évoluer). Nous considérerons souvent le processus 1+1 dimensionnel $(X_t, H_t) := (X_t, L_t(X_t))$. La figure I.15 présente une visualisation du paysage à un instant t.

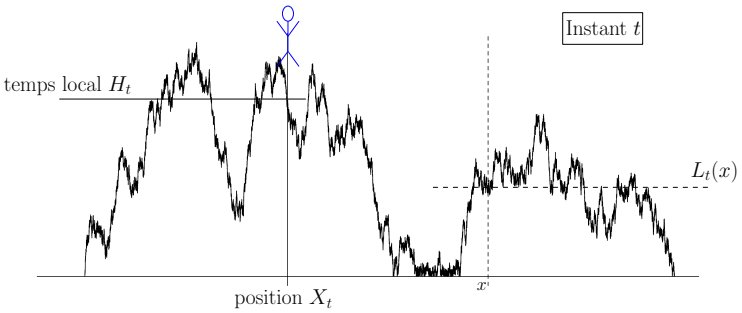

FIGURE I.15 – Photographie de l'instant t : X_t et son temps local $L_t(\cdot)$

Le "vrai" processus auto-répulsif de B. Tóth et W. Werner possède en outre une autre propriété : son auto-interaction est *locale*. C'est à dire que le processus

ne considère que les valeurs de L_t autour de X_t à l'instant t pour décider où il va diriger (il est dit "myope").

I.3.2 Construction et propriétés du TSRM

Nous avons déjà évoqué dans la partie I.1 sur les modèles discrets qu'une méthode possible pour construire le modèle continu associé (et donc un processus *a priori* auto-répulsif) est de faire le tour de l'arbre correspondant à l'analogue continu des marches aléatoires discrètes. Nous allons donc définir le TSRM comme le processus qui commence au point $(0,0)$, qui trace le tour de l'arbre $\mathcal{T}_f$ (en le laissant sur sa droite)[5] et qui se dirige vers le haut (c'est à dire au dessus de $\Lambda_{0,0}$ et vers $+\infty$), sa paramétrisation étant donnée par l'aire parcourue. Le TSRM construit à partir du BW défini sur le plan tout entier est appelé TSRM *stationnaire* car pour presque tout instant $t > 0$, la loi de $(X_{t+s} - X_t)_{s\geq 0}$ est égale à la loi du TSRM $(X_s)_{s\geq 0}$. Nous parlerons essentiellement du TSRM stationnaire excepté §I.4.3.

Tous les résultats présentés dans cette partie sont issus de l'article de B. Tóth et W. Werner [59] ; les numéros des lemmes, propositions et théorèmes réfèrent à cet article.

Définition du TSRM et ses premières propriétés Pour définir le TSRM plus précisément, nous avons besoin de notations supplémentaires. Pour tout $(x,h) \in \mathbb{R}^2$, soit $S_{x,h}$ l'aire entre $\Lambda_{x,h}$ et $\Lambda_{0,0}$:

$$S_{x,h} := \int_{-\infty}^{+\infty} (\Lambda_{x,h}(y) - \Lambda_{0,0}(y))\, dy.$$

Presque sûrement, pour tout (x,h) au dessus de la courbe $\Lambda_{0,0}$, le processus (X,H) vaut (x,h) au temps aléatoire $S_{x,h}$ et à cet instant, il a visité tous les points se trouvant entre $\Lambda_{x,h}$ et $\Lambda_{0,0}$. Plus précisément,

$$(X_t, H_t) := \bigcap_{\varepsilon>0} \overline{\{(x,h) \in \mathbb{R}^2 \ : \ S_{x,h} \in (t-\varepsilon, t+\varepsilon)\}}. \tag{I.2}$$

Les auteurs de [59] ont prouvé que cela définissait effectivement un processus $(X_t, H_t)_{t\geq 0}$, c'est à dire que le membre de droite de (I.2) est bien un singleton (Lemme 3.4), et ils ont montré la continuité de ce processus. Grâce à la structure brownienne de l'arbre, on peut aisément déduire quelques premières propriétés du processus comme sa récurrence dans $\mathbb{R}$ ou son invariance d'échelle : pour tout $a > 0$, $(X_{at}, H_{at})_{t\geq 0}$ et $(a^{2/3}X_t, a^{1/3}H_t)_{t\geq 0}$ ont la même loi (Proposition 3.5). Ce processus admet également

5. C'est le même processus que celui qui trace le tour de l'arbre dual $\mathcal{T}_b$ en le laissant sur sa gauche.

une variation finie d'ordre 3/2 (contrairement aux semi-martingales dont la variation quadratique est finie). Pour simplifier l'écriture, nous désignerons par TSRM à la fois le couple $(X_t, H_t)_{t\geq 0}$ et sa première coordonnée $(X_t)_{t\geq 0}$.

Il est important de noter que l'ensemble des temps aléatoires

$$D := \{S_{x,h},\ (x,h) \in \mathbb{R}^2,\ h > \Lambda_{0,0}(x)\}$$

est dense dans $\mathbb{R}_+$ (et même son complémentaire a une mesure de Lebesgue nulle, voir Proposition 4.4) mais qu'il ne remplit pas tout $\mathbb{R}_+$: il existe des temps exceptionnels pour lesquels le processus ne se trouve pas au point de départ d'une courbe du BW. Par exemple, le temps pour lequel il atteint pour la première fois $x \neq 0$ fixé *n'est pas* dans D (voir le paragraphe ci-dessous sur les points spéciaux du TSRM pour une discussion plus détaillée de ce point).

Autres propriétés fondamentales du TSRM Le TSRM parcourt la frontière entre les arbres $\mathcal{T}_f$ et $\mathcal{T}_b$. Le modèle jouet et les théorèmes limites de [57] nous laissent supposer que ce processus aura des propriétés auto-répulsives. Pour montrer cette répulsion mathématiquement, nous nous intéressons à la mesure du temps d'occupation de $(X_t)_{t\geq 0}$. Notre objectif sera de montrer que le processus X est effectivement repoussé par les endroits qu'il a le plus visités de façon locale. Rappelons la définition de la mesure du temps d'occupation :

$$\forall A \text{ borélien de } \mathbb{R}, \quad \mu_t(A) = \int_0^t \mathbf{1}_{\{X_s \in A\}} ds.$$

Tout comme dans le cas des semi-martingales, cette mesure pour le TSRM admet une densité par rapport à la mesure de Lebesgue que l'on appelle aussi *temps local* et que l'on note $L_t(\cdot)$ (voir théorème 4.2). De plus, la fonction $t \mapsto L_t(\cdot)$ est une fonction croissante continue de $\mathbb{R}_+$ dans l'espace des fonctions continues réelles à support compact muni de la topologie de la convergence uniforme sur les compacts. La famille des temps locaux $(L_t(\cdot))$ peut en fait être retrouvée à partir de la famille $(S_{x,h}, (x,h) \in \mathbb{R}^2)$ grâce à la relation suivante :

$$L_t(x) := \sup\{h > 0\ :\ S_{x,h} < t\}.$$

(Autrement dit, $t \mapsto L_t(x)$ est l'inverse généralisé de $h \mapsto S_{x,h}$). Cette relation implique notamment $L_t(X_t) = H_t$.

Réciproquement, avec les propriétés de régularité de $h \mapsto S_{x,h}$, on en déduit un théorème de Ray-Knight très puissant pour la loi des temps locaux : presque sûrement, pour tout $(x,h) \in \mathbb{R}^2$ et $y \in \mathbb{R}$,

$$L_{S_{x,h}}(y) = \Lambda_{x,h}(y) - \Lambda_{0,0}(y).$$

Ainsi, le processus X et l'initialisation $\Lambda_{0,0}$ contiennent toute l'information nécessaire pour retrouver le BW entier.

De plus, le processus $(X_t, L_t(\cdot))_{t\geq 0}$ est bien un *processus de Markov*, et même la loi de X juste après t ne dépend que de L_t restreinte au voisinage immédiat du point X_t.

Maintenant que les définitions nécessaires pour discuter de répulsion par les temps d'occupation sont posées, nous pouvons décrire l'équation dynamique qui régit le TSRM. Cette équation peut sembler paradoxale au premier abord car elle ne fait intervenir aucun bruit aléatoire : nous avons un système déterministe d'équations différentielles dont la solution est pourtant aléatoire ! En fait, les régularités ne sont pas suffisantes pour que ce système soit bien défini ($L_t(\cdot)$ n'est pas dérivable, il possède la même régularité qu'un mouvement brownien) et les limites à considérer sont à entendre dans le sens "limite en probabilité".

Théorème 1.4 (Théorème 6.1)**.** *Le TSRM vérifie l'équation dynamique suivante : pour tout $t > 0$ fixé,*

$$X_t = - \boldsymbol{P}\text{-}\lim_{\varepsilon\to 0} \int_0^t \frac{L_s(X_s+\varepsilon) - L_s(X_s-\varepsilon)}{2\varepsilon} ds.$$

Nous voyons ainsi très clairement que le TSRM est repoussé par le "gradient" du temps local au point où il se trouve : il est bien auto-répulsif.

Points spéciaux du TSRM Les trajectoires du TSRM sont très différentes de celles du mouvement brownien. En particulier, en certains temps exceptionnels, le TSRM peut être strictement monotone, ce qui n'est jamais le cas pour le mouvement brownien. Cela signifie que le TSRM n'accumule aucun temps local au point de stricte monotonie (et à l'instant de stricte monotonie).

Plus précisément, nous disons que $t > 0$ est un temps de *stricte monotonie* pour X s'il existe $\varepsilon > 0$, tel que pour tout $u \in (0, \varepsilon)$, $X_{t-u} < X_t < X_{t+u}$ (stricte croissance) ou pour tout $u \in (0, \varepsilon)$, $X_{t-u} > X_t > X_{t+u}$ (stricte décroissance). Alors, l'ensemble des points (X_t, H_t) tel que t est un temps de stricte monotonie pour X correspond aux points de type $[1, 1]$ (voir les dessins de ces points dans le tableau I.13, le premier dessin correspond à une stricte croissance, le deuxième à une stricte décroissance). De manière analogue, on peut voir que les points du BW de type $[0, 2]$ correspondent aux minima locaux, les points du type $[2, 0]$ aux maxima locaux (pour ce cas, voir la figure I.16), et que les points de type $[0, 1]$ désignent les temps pour lesquels le processus commence une excursion (en dessous de x pour le premier dessin, au dessus de x pour le deuxième).

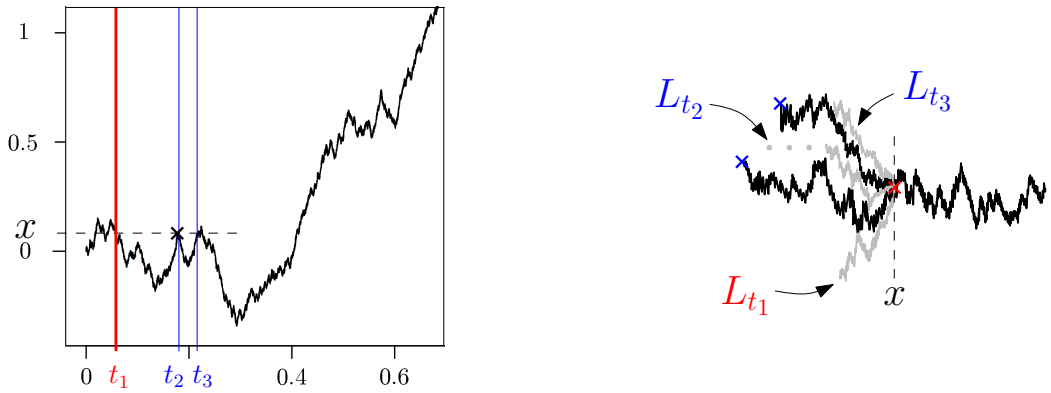

FIGURE I.16 – Un maximum local de la trajectoire du TSRM et schéma de quelques courbes du BW associées. Le dernier temps d'atteinte t_1 de x avant le temps t_2 où le processus effectue le maximum local est dans D. Les deux autres temps (t_2 = temps du maximum local et t_3 = premier temps d'atteinte de x après avoir effectué le maximum local) ne sont pas dans D. Ils correspondent aux deux autres choix possibles pour la courbe du BW issue du point de maximum local.

I.4 Nos contributions sur le TSRM

I.4.1 Propriétés de grandes déviations

Dans ce paragraphe, nous décrivons comment déduire simplement des informations sur certains comportements du TSRM à partir de quelques courbes du BW bien choisies. Ce genre de méthode a été utilisé dans l'article [16] et le but de ce paragraphe est de les expliciter dans un cas simple.

A titre d'exemple, fixons $x \gg 1$ et étudions l'événement "$X_1 > x$". Nous ne calculerons pas sa probabilité exacte avec les courbes du BW (pour une expression exacte voir le paragraphe I.4.3.), mais il est possible de trouver une approximation suffisamment bonne pour évaluer correctement son ordre de grandeur.

Tout d'abord, remarquons que "$X_1 > x$" implique que le premier temps d'atteinte de x, que l'on note σ_x, a lieu avant 1. Une difficulté déjà soulignée est que ce temps n'est pas dans D, c'est à dire que la courbe du temps local en cet instant n'est pas donnée par une courbe du BW. En fait, il correspond à l'infimum des temps pour lesquels $L_\cdot(x)$ est strictement positif[6]. Si $\Gamma_x(\cdot) := L_{\sigma_x}(\cdot) + \Lambda_{0,0} = \lim_{\varepsilon\to 0} \Lambda_{x,\Lambda_{0,0}(x)+\varepsilon}$, alors on connait la loi de Γ_x : il est facile de montrer que sur $[x,\infty)$, $\Gamma_x(\cdot)$ coalesce immédiatement avec $\Lambda_{0,0}$ et sur $(-\infty, x]$, elle suit la loi d'un mouvement brownien (allant vers la gauche), réfléchi sur $\Lambda_{0,0}$ entre 0 et x et absorbé par $\Lambda_{0,0}$ sur $\mathbb{R}_-$ (voir

6. Ce n'est pas vrai pour tous les x simultanément car il existe des points exceptionnels tels que les extrema locaux ou les points de stricte monotonie, voir le paragraphe I.4.2.

Lemme 2.1 de [16]). Or le TSRM X touche x avant 1 lorsque l'aire de $\Gamma_x(\cdot) - \Lambda_{0,0}$ est inférieure à 1. Nous nous sommes ainsi ramené à l'étude d'une aire brownienne. Si $\mathcal{A}$ désigne l'aire d'un mouvement brownien réfléchi entre 0 et 1, le changement d'échelle du brownien nous donne

$$\mathbb{P}(X_1 > x) \leq \mathbb{P}\left(\mathcal{A} < 1/(\sqrt{2}x^{3/2})\right) = \exp\left(-\frac{4|a_1'|^3}{27}x^3 + O(\ln(x))\right).$$

où a_1' désigne la première racine négative de la dérivée de la fonction d'Airy Ai (voir le paragraphe IV.3.2). L'égalité asymptotique concernant l'aire brownienne $\mathcal{A}$ peut être trouvée dans [36].

Pour trouver un événement contenu dans $X_1 > x$, une première idée est d'étudier le processus après le temps d'atteinte σ_x. Mais il est difficile de savoir ce qu'il se passe pour le processus après ce temps (bien sûr, pas de propriété de Markov fort ici !). Il est donc plus simple d'évaluer la probabilité que X dépasse d'une certaine distance $\delta > 0$ la valeur x et qu'il reste ensuite au dessus de x pendant un temps suffisamment grand pour assurer $X_1 > x$. Il est préférable de travailler avec des courbes du BW : nous remplaçons donc le premier temps d'atteinte de $y := x + \delta$ par un instant où X a accumulé un peu de temps local en y, par exemple une quantité $\delta' > 0$. Ainsi, la courbe du BW qui nous intéresse est $\hat{\Lambda} := \Lambda_{y,\Lambda_{0,0}(y)+\delta'}$ (voir dessin I.17). Une manière d'obtenir $X_1 > x$ est d'imposer l'existence d'un *point de stricte croissance* entre x et y à un temps inférieur à 1 et de s'assurer ensuite que le TSRM reste à droite de ce point pendant une durée supérieure à 1 : comme les points de stricte monotonie sont exceptionnels, il est impossible pour le processus d'être strictement monotone plusieurs fois au même point et nous lisons directement sur la courbe du BW $\hat{\Lambda}$ si effectivement (X, H) est repassé par ce point avant de toucher $(y, \Lambda_{0,0}(y) + \delta')$ ou non : il repasse par ce point *ssi* $\hat{\Lambda} - \Lambda_{0,0}$ est strictement positif en ce point. Pour résumer, pour avoir $X_1 > x$, il suffit qu'il existe un point z dans $[x, y]$ tel que $\hat{\Lambda}(z) = \Lambda_{0,0}(z)$ et $\int_{-\infty}^{y} \hat{\Lambda} - \Lambda_{0,0} \leq 1$ (le point de stricte croissance est donc atteint avant l'instant 1) et $\int_{y}^{\infty} \hat{\Lambda} - \Lambda_{0,0} \geq 1$ (X reste à droite de z après l'avoir touché au moins jusqu'au temps $\int_{-\infty}^{\infty} \hat{\Lambda} - \Lambda_{0,0} \geq 1$).

En choisissant convenablement δ et δ' et à l'aide d'estimées sur les aires browniennes, nous obtenons une borne inférieure de la probabilité de cet événement d'ordre de grandeur

$$\exp\left(-\frac{4|a_1'|^3}{27}x^3 + O(\ln(x))\right)$$

correspondant à la borne supérieure. □

Des raisonnements similaires (mais plus délicats car plusieurs courbes du BW interviennent) permettent d'évaluer les queues de la loi de H_1 (de manière moins précise que pour X car ces événements sont plus complexes, le temps local initial

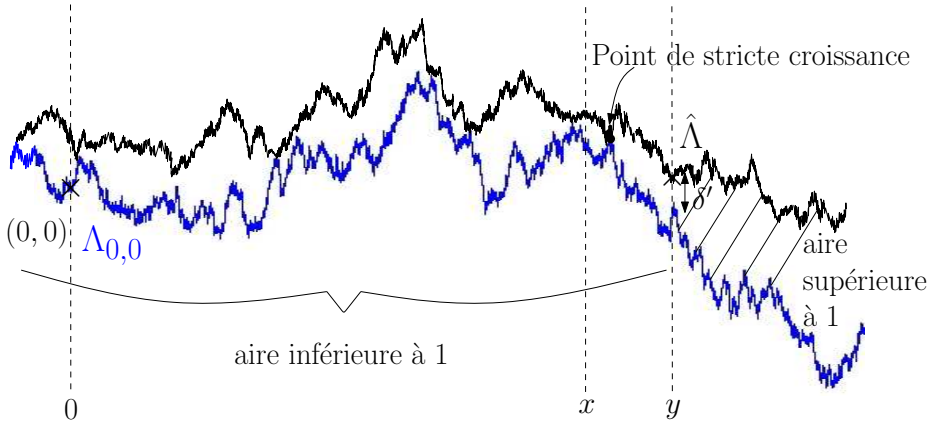

FIGURE I.17 – Dessin représentant l'événement étudié

joue un rôle crucial), de même que des lois du logarithme itéré pour les processus X et H (voir paragraphe I.4.2).

Nous résumons dans la proposition suivante les résultats que nous avons ainsi obtenus sur les grandes déviations du TSRM dans [16]. Ils sont présentés pour le temps 1 mais il est facile de généraliser ces formules pour n'importe quel temps fixé, grâce à la propriété de changement d'échelle.

Proposition 1.5. *Nous avons les asymptotiques suivantes pour le TSRM (X, H). Lorsque $x \to \infty$,*

$$\mathbb{P}(X_1 > x) = \exp\left(-\frac{4|a_1'|^3}{27}x^3 + O(\ln(x))\right) \tag{I.3}$$

où a_1' est la première racine négative de la dérivée de la fonction d'Airy Ai. Et il existe deux constantes strictement positives η et η' telles que pour tout h assez grand,

$$\exp\left(-\eta h^{3/2}\right) \leq \mathbb{P}(H_1 \leq -h) \leq \mathbb{P}\left(\inf_{t\in[0,1]} H_t \leq -h\right) \leq \exp\left(-\frac{1}{\eta}h^{3/2}\right)$$
$$\exp\left(-\eta' h^{3/2}\right) \leq \mathbb{P}(H_1 \geq h) \leq \mathbb{P}\left(\sup_{t\in[0,1]} H_t \geq h\right) \leq \exp\left(-\frac{1}{\eta'}h^{3/2}\right).$$

I.4.2 Lois du logarithme itéré

En développant les raisonnements suivis pour trouver les grandes déviations du TSRM, nous pouvons obtenir des lois du logarithme itéré pour les processus X et H. Les résultats asymptotiques pour X étant assez précis, nous pouvons identifier la constante pour X. Ce n'est pas le cas pour H pour lequel nous utilisons une loi du 0-1 pour montrer son existence. Notons qu'il est facile de prédire les puissances intervenant dans ces formules : la puissance de t provient du changement d'échelle

et celle de $\ln\ln(t)$ des grandes déviations ($1/\alpha$ si décroissance en $\exp(-O(x^\alpha))$). La proposition suivante a été montrée dans l'article [16].

Proposition 1.6. *Presque sûrement,*

$$\limsup_{t\to+\infty} \frac{X_t}{t^{2/3}\left(\ln\ln(t)\right)^{1/3}} = \limsup_{t\to 0+} \frac{X_t}{t^{2/3}\left(\ln\ln(1/t)\right)^{1/3}} = 3/(2^{2/3}|a_1'|),$$

où a_1' désigne toujours la première racine négative de la dérivée de la fonction d'Airy Ai. De plus, il existe quatre constantes l^+, l^-, l_0^+, l_0^- telles que, presque sûrement,

- $\limsup_{t\to\infty} t^{-1/3}(\ln\ln(t))^{-2/3}\, H_t = l^+$
- $\liminf_{t\to\infty} t^{-1/3}(\ln\ln(t))^{-2/3}\, H_t = l^-$
- $\limsup_{t\to 0} t^{-1/3}(\ln\ln(1/t))^{-2/3}\, H_t = l_0^+$
- $\liminf_{t\to 0} t^{-1/3}(\ln\ln(1/t))^{-2/3}\, H_t = l_0^-$.

I.4.3 Calculs de lois marginales

Dans ce paragraphe, nous nous intéressons non plus au TSRM stationnaire, mais au TSRM commençant avec un temps local initial identiquement égal à zéro. La définition du modèle "temps local plat" se fait facilement à l'aide d'une toile brownienne définie dans le demi-plan supérieur. Pour éviter les confusions, nous notons ce BW $(\Lambda'_{x,h}, (x,h) \in \mathbb{R}\times\mathbb{R}_+^*)$ et le TSRM associé $(X'_t, H'_t)_{t\geq 0}$. Concrètement, cela signifie remplacer la courbe $\Lambda_{0,0}$ par la fonction identiquement nulle : $\Lambda'_{0,0} := 0$. Les définitions restent les mêmes en considérant $\Lambda'_{0,0}$ comme une courbe à part entière ($\Lambda'_{0,0}(y), y \geq 0$) est une courbe de type f, ($\Lambda'_{0,0}(y), y \leq 0$) est une courbe de type b et les autres courbes du BW coalescent et se réfléchissent sur elle de la même manière.

Nous présentons dans ce paragraphe les résultats que nous avons obtenus en collaboration avec B. Tóth dans [18]. Dans cet article, nous donnons des expressions explicites pour les densités des lois de X'_1 et H'_1 [7], notées respectivement ν_1 et ν_2.

Nous avons établi le théorème suivant :

Théorème 1.7. *Les densités de X'_1 et H'_1 vérifient les formules suivantes :*

$$\forall x \in \mathbb{R}, \quad \nu_1(x) = \sum_{k=1}^{\infty} \frac{3^{2/3}}{2^{7/3}} \left(\frac{\Gamma(2/3)}{\Gamma(1/3)}\right)^2 |a_k'|^{-3}\, f_{2/3}(-2^{-1/3} a_k' |x|)$$

$$\forall h \in \mathbb{R}_+, \quad \nu_2(h) = \frac{2\cdot 6^{1/3}\sqrt{\pi}}{\Gamma(1/3)^2} e^{-(8h^3)/9} U(1/6, 2/3; (8h^3)/9).$$

7. Comme remarqué précédemment, ces résultats se généralisent facilement pour n'importe quel temps $t > 0$ fixé à la place de 1 grâce à l'invariance d'échelle des processus X' et H'

où $f_{2/3}$ est la fonction de Mittag-Leffler définie IV.3.3, les facteurs a'_k sont les zéros (ordonnés de façon décroissante) de la dérivée de la fonction d'Airy Ai, et $U(1/2, 4/3; \cdot)$ est la fonction confluente hypergéométrique du second type (ou fonction de Tricomi), donnée par la représentation integrale (IV.52) dans la sous-section IV.3.4.

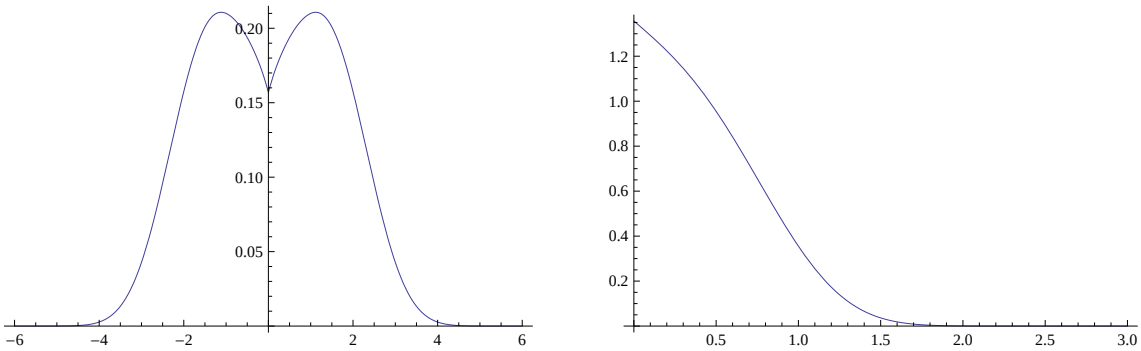

FIGURE I.18 – Tracé des densités de X_1 (sur la droite) et de H_1 (sur la gauche)

Remarque. Il existe une relation entre le déplacement *à un instant donné* du processus stationnaire et celui partant d'un profil plat. Leur construction nous donne facilement $X_1 = 2^{-1/3} X'_1$. Ceci permet de retrouver l'asymptotique de X_1 (I.3) démontrée par d'autres méthodes plus haut. Précisons qu'il n'y a aucune relation de la sorte entre H_1 et H'_1 (et les asymptotiques sont complètement différentes).

Notons que la densité obtenue pour X_1 est très particulière : elle n'est pas dérivable en 0 ce qui signifie que le point de départ est très singulier par rapport aux autres pour le processus, même après un temps macroscopique.

Dans la suite de ce paragraphe, nous décrivons l'idée de départ qui permet d'obtenir ces formules. Soit $T_{x,h}$ l'aire sous la courbe $\Lambda'_{x,h}$, qui correspond aussi au temps de passage en (x, h) de (X', H') (voir Fig. I.19) et soit $t \in \mathbb{R}_+ \mapsto \rho(t; x, h)$ sa densité. Calculons la densité de (X'_t, H'_t) pour $t > 0$. Pour cela, il est utile de considérer le processus à des *temps aléatoires indépendants*. Soit θ_s une variable aléatoire exponentielle de paramètre s indépendante du TSRM et $f : \mathbb{R} \times \mathbb{R}_+ \to \mathbb{R}$ une fonction continue bornée,

$$\begin{aligned}\mathbb{E}(f(X'(\theta_s), H'(\theta_s))) &= \int_0^\infty s\, e^{-st} \mathbb{E}(f(X'_t, H'_t)) dt \\ &= \int_{-\infty}^\infty \int_0^\infty s\, \mathbb{E}\left(e^{-sT_{x,h}}\right) f(x,h) dx dh,\end{aligned}$$

où l'on a effectué le changement de variable "$t = T_{x,h}$" préservant (presque sûrement) la mesure de Lebesgue (voir Proposition 4.1 (iii) de [59]). Ainsi la densité

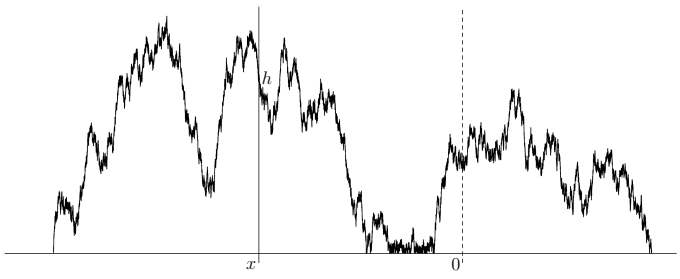

FIGURE I.19 – L'aire $T_{x,h}$

de $(X'(\theta_s), H'(\theta_s))$ vaut $(x,h) \in \mathbb{R} \times \mathbb{R}_+ \mapsto s\,\mathbb{E}(\exp(-sT_{x,h}))$. Ceci implique notamment que la densité de (X'_t, H'_t) est égale à $(x,h) \in \mathbb{R} \times \mathbb{R}_+ \mapsto \rho(t;x,h)$ (la densité de $T_{x,h}$ en t). Nous étudions tout d'abord la densité de $(X'(\theta_s), H'(\theta_s))$. Les propriétés de changement d'échelle nous indiquent qu'il suffit de regarder le temps 1. Soit $(B_t, t \geq 0)$ un mouvement brownien standard, $\tau := \inf\{t \geq 0,\ B_t = 0\}$, et $u(h) := \mathbb{E}(\exp(-\int_0^\tau B_t dt))$. Avec la propriété de Markov simple appliquée au temps 0 et les propriétés d'indépendance des courbes de type f et b, on obtient :

$$\mathbb{E}\left(e^{-T_{x,h}}\right) = u(h)\,\mathbb{E}\left(e^{-\int_0^x |B_t| dt} u\left(|B_x|\right)\right)$$

La formule de Feynman-Kac nous donne une équation aux dérivées partielles vérifiée par cette fonction. Une étude plus poussée permet d'en déduire les résultats du théorème 1.7.

I.4.4 Le voleur auto-répulsif, ou l'étude de la loi conditionnelle du déplacement au temps 1 sachant son temps local L_1

Dans ce paragraphe, nous décrivons le résultat principal de [17]. Nous nous sommes intéressés à une question déjà abordée par J. Warren et M. Yor [65] et D. Aldous [2] dans le cas du mouvement brownien. Une manière ludique de présenter ce problème est d'imaginer la situation suivante : un voleur se déplace sur un espace unidimensionnel et cherche la meilleure stratégie pour échapper à la police, qui ne connait que les endroits qu'il a visités et le temps qu'il a passé à chacun de ces endroits (elle dispose par exemple juste des factures d'hôtel, et pas des dates). Nous avons montré dans [17] qu'une assez bonne solution consiste à suivre une trajectoire du TSRM : mis à part les points de stricte monotonie, qui donnent une indication sur son passage, le voleur ne laisse aucune information derrière lui. En

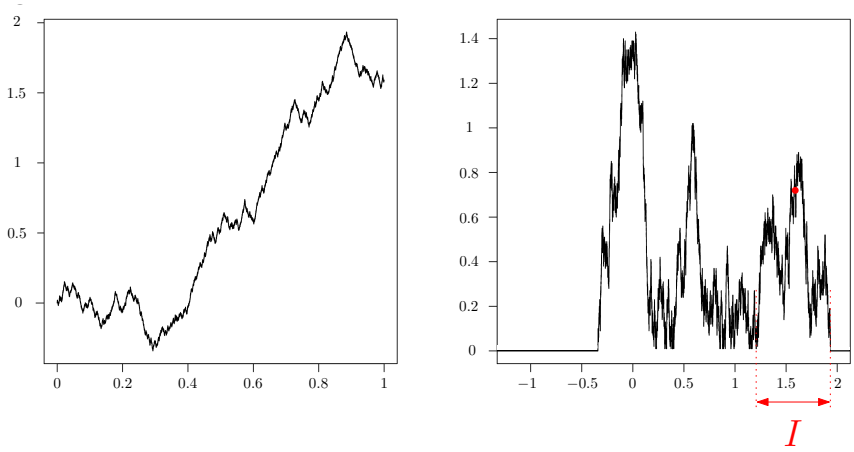

FIGURE I.20 – Réalisation d'une trajectoire du TSRM jusqu'au temps $t = 1$, à droite son temps local au temps 1 et l'intervalle I du théorème.

langage mathématique, nous nous intéressons à la loi conditionnelle de X_1 sachant le temps local L_1 et le résultat est le suivant :

Théorème 1.8. *Soit I l'intervalle contenant X_1 délimité par $\sup\{x \leq X_1 \ : \ L_1(x) = 0\}$ et $\inf\{x \geq X_1 \ : \ L_1(x) = 0\}$. La loi conditionnelle de X_1 sachant L_1 est la loi uniforme sur l'intervalle I.*

Remarque. Il se peut que l'intervalle I soit l'intervalle de l'ensemble des points visités tout entier, auquel cas le voleur est parfaitement caché. Nous avons calculé dans [17] la probabilité de cet événement, qui vaut à peu près $22,5\%$.

Intuitivement, ce résultat provient d'un fait très simple mais très vague : supposons qu'une courbe, réalisation d'un certain temps local à un temps appartenant à D, soit fixée. Alors, "la probabilité" [8] que cette courbe soit issue d'un point fixé dans l'intervalle I est la même pour tous les points (car ce sont des courbes browniennes).

Pour donner un sens à cette observation, nous avons utilisé le modèle jouet défini §I.1.2. Ce modèle est très pratique car la description des temps locaux est assez simple pour trouver les probabilités des événements qui nous intéressent. Cependant, une difficulté apparaît dans le modèle discret car les courbes de type f et b n'appartiennent pas au même réseau et l'information de l'endroit où l'on se trouve se lit directement sur le temps local (voir la figure I.7). Une idée exploitée dans l'article est d'effacer cette information, et de montrer le résultat pour le temps local discret ainsi modifié. Nous utilisons ensuite un argument d'invariance pour en déduire le résultat dans le continu.

8. Bien entendu, ici le mot probabilité n'a pas de sens car ces probabilités sont nulles

CHAPITRE II

La loi de Tracy Widom et les β-ensembles

Dans ce chapitre, nous nous intéressons à la loi de Tracy-Widom-β, introduite par C. Tracy et H. Widom en 1994 [61, 62] dans le contexte des matrices aléatoires pour $\beta = 1, 2$ et 4. Cette loi, tout comme la loi gaussienne, a des propriétés d'universalité : elle apparaît dans de nombreux modèles probabilistes *a priori* différents, comme la plus grande valeur propre de certains ensembles de matrices aléatoires, la longueur de la plus grande sous-suite strictement croissante de permutations aléatoires [6], les fluctuations du système de particules ASEP (Asymmetric Simple Exclusion Process) [37, 60], les polymères dirigés ou les modèles de croissance (voir par exemple les notes de cours de S. Majumdar [42]). Dans ce chapitre, nous allons définir tout d'abord très brièvement les ensembles de matrices aléatoires qui entrent en jeu dans sa définition (§II.1). Ensuite, nous décrirons l'étude de la plus grande valeur propre de ces ensembles de matrices, dont la loi limite est la loi de Tracy-Widom (§II.2). Elle fait apparaître un opérateur stochastique SAE_β qui permet en particulier de calculer les premiers termes du développement asymptotique des queues de la loi de Tracy-Widom. Dans l'article [19] écrit en collaboration avec B. Virág (correspondant au chapitre VI de cette thèse), nous nous sommes intéressés à la queue droite. Avec des outils comme la formule de Cameron-Martin-Girsanov, nous avons pu déterminer l'exposant polynomial de son développement asymptotique.

II.1 Quelques mots sur les matrices aléatoires

L'étude des matrices aléatoires est apparue dans les années 30, avec les travaux de statisticiens comme J. Wishart, et se développa dans les années 50 sous l'impulsion de physiciens (F. Dyson et E. Wigner). Dans le contexte de la physique nucléaire [66],

E. Wigner a proposé de modéliser les propriétés statistiques des positions des niveaux d'énergie des noyaux lourds excités par les valeurs propres de très grandes matrices aléatoires symétriques ayant des entrées indépendantes identiquement distribuées. Depuis lors, la théorie des matrices aléatoires constitue un domaine très actif de recherche en probabilités et elle possède de multiples applications dans des contextes très divers tels que la théorie des nombres (avec la fonction zeta de Riemann), la combinatoire, les algèbres d'opérateurs, ou en physique le chaos quantique, les systèmes désordonnés (les verres, verres de spins...) et dans de nombreux autres domaines.

II.1.1 Définition des ensembles Gaussiens

Les premiers ensembles de matrices aléatoires apparus historiquement sont les ensembles Gaussiens GOE (Gaussian Orthogonal Ensemble), GUE (Gaussian Unitary Ensemble) et GSE (Gaussian Symplectic Ensemble). Ces trois modèles ont été introduits par F. Dyson [22] et ils font partie des matrices aléatoires les plus classiques et les plus étudiées. Nous définissons ici les deux premiers ensembles.

Très simplement, une matrice aléatoire appartient l'ensemble GOE ($\beta = 1$) s'il existe une dimension n telle qu'elle s'écrive sous la forme

$$\begin{bmatrix} \sqrt{2}\, g_{1,1} & g_{1,2} & \cdots & g_{1,n} \\ g_{1,2} & \sqrt{2}\, g_{2,2} & \cdots & g_{2,n} \\ \vdots & \ddots & \ddots & \vdots \\ g_{1,n} & \cdots & g_{n-1,n} & \sqrt{2}\, g_{n,n} \end{bmatrix},$$

où les $(g_{i,j},\ i \leq j,\ (i,j) \in \{1, \cdots, n\}^2)$ sont des variables aléatoires indépendantes de loi gaussienne centrée réduite.

Pour toute matrice orthogonale O fixée et toute matrice aléatoire A de l'ensemble GOE, on a

$$OAO^{-1} \overset{(d)}{=} A. \tag{II.1}$$

et réciproquement, toute matrice aléatoire symétrique vérifiant la stabilité (II.1) et dont les entrées triangulaires supérieures sont i.i.d. est nécessairement dans l'ensemble GOE.

Les matrices de l'ensemble GUE ($\beta = 2$) s'écrivent :

$$\begin{bmatrix} g_{1,1} & \frac{1}{\sqrt{2}}(g_{1,2} + i\, h_{1,2}) & \cdots & \frac{1}{\sqrt{2}}(g_{1,n} + i\, h_{1,n}) \\ \frac{1}{\sqrt{2}}(g_{1,2} + i\, h_{1,2}) & g_{2,2} & \cdots & \frac{1}{\sqrt{2}}(g_{2,n} + i\, h_{2,n}) \\ \vdots & \vdots & \ddots & \vdots \\ \frac{1}{\sqrt{2}}(g_{1,n} + i\, h_{1,n}) & \frac{1}{\sqrt{2}}(g_{2,n} + i\, h_{2,n}) & \cdots & g_{n,n} \end{bmatrix},$$

où les $(g_{i,j},\ i \leq j,\ (i,j) \in \{1,\cdots,n\}^2)$ et $(h_{i,j},\ i \leq j,\ (i,j) \in \{1,\cdots,n\}^2)$ sont des variables aléatoires indépendantes de loi gaussienne centrée réduite.

De même que pour les matrices GOE, les matrices GUE possèdent des propriétés de symétrie : pour toute matrice unitaire U fixée et toute matrice aléatoire GUE A, on a

$$UAU^{-1} \overset{(d)}{=} A. \tag{II.2}$$

et réciproquement, toute matrice aléatoire hermitienne vérifiant la stabilité (II.2) et dont les entrées triangulaires supérieures sont i.i.d. est nécessairement dans l'ensemble GUE.

Les premiers objets d'investigation sur les matrices aléatoires sont les valeurs propres et leurs propriétés statistiques. La loi jointe des valeurs propres des matrices GOE, GUE, et GSE admet pour densité :

$$\forall \lambda_1 \geq \lambda_2 \geq \cdots \geq \lambda_n \in \mathbb{R},\ \mathbb{P}_n^\beta(\lambda_1,\ \lambda_2,\ \cdots,\ \lambda_n) = \frac{1}{Z_n^\beta} \exp\left(-\beta \sum_{k=1}^n \lambda_k^2\right) \prod_{j>k} |\lambda_j - \lambda_k|^\beta, \tag{II.3}$$

où Z_n^β est la constante de renormalisation et le facteur β vaut 1 pour les matrices GOE, $\beta = 2$ pour GUE et $\beta = 4$ pour GSE. Notons que cette densité correspond à la loi jointe de variables aléatoires gaussiennes à laquelle nous ajoutons un terme de répulsion provenant des $|\lambda_j - \lambda_k|^\beta$.

II.1.2 Généralisation : les β-ensembles

La loi (II.3) a un sens physique pour tous les β (et pas seulement pour $\beta = 1$, 2 ou 4) car elle décrit un gaz de Coulomb dont la température vaut $1/\beta$ (voir par exemple le chapitre 1, Section 1.4 de [31]). Cette famille de lois est appelée *β-ensemble*. I. Dumitriu et A. Edelman dans [20] ont effectué une avancée majeure dans ce domaine lorsqu'ils ont découvert en 2002 que (II.3) suit la distribution des valeurs propres des *matrices tridiagonales* suivantes :

$$H_n^\beta = \frac{1}{\sqrt{\beta}} \begin{bmatrix} \sqrt{2}\, g_1 & \chi_{(n-1)\beta} & & & \\ \chi_{(n-1)\beta} & \sqrt{2}\, g_2 & \chi_{(n-2)\beta} & & \\ & \ddots & \ddots & \ddots & \\ & & \chi_{2\beta} & \sqrt{2}\, g_{n-1} & \chi_\beta \\ & & & \chi_\beta & \sqrt{2}\, g_n \end{bmatrix},$$

où les variables aléatoires $g_1, g_2, \cdots, g_n$ sont des gaussiennes centrées réduites et $\chi_\beta, \chi_{2\beta}, \cdots, \chi_{(n-1)\beta}$ sont des variables aléatoires indépendantes suivant une loi χ dont le paramètre est l'indice de χ.

II.2 Comportement des valeurs propres et loi de Tracy-Widom-β

Lorsque $n \to \infty$, les valeurs propres renormalisées par $\sqrt{n}$ se répartissent selon la célèbre loi du demi-cercle de Wigner (voir Fig. II.1) qui admet pour densité la fonction

$$x \in [-2, 2] \mapsto \frac{1}{2\pi}\sqrt{4 - x^2}.$$

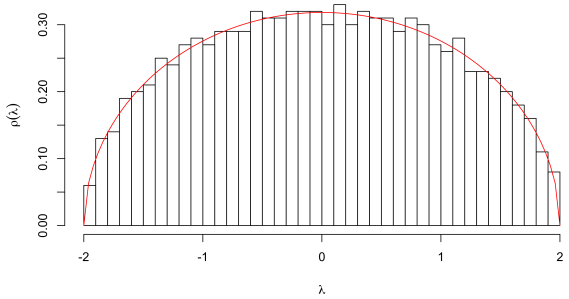

FIGURE II.1 – Le demi-cercle de Wigner et la répartition en histogramme des valeurs propres pour une simulation d'une matrice GOE de taille $n = 1000$.

Nous pouvons nous intéresser au comportement des valeurs propres à l'intérieur du spectre ou au bord du spectre. La partie qui nous intéresse ici est le bord du spectre. Lorsque $n \to \infty$, la plus grande valeur propre divisée par $\sqrt{n}$ centrée en 2 et renormalisée par $n^{2/3}$ converge en loi vers la loi de Tracy-Widom-β. Cela a d'abord été montré dans les cas $\beta = 1, 2$ et 4 dans les papiers [61, 62], où des formules exactes existent (la loi de Tracy-Widom est définie via l'équation différentielle de Painlevé II). J. A. Ramírez and B. Rider and B. Virág ont étendu ce résultat pour tous les β. Dans [48], les auteurs ont montré que l'opérateur renormalisé :

$$\tilde{H}_n^\beta := n^{2/3}\left(2I_n - \frac{H_n^\beta}{\sqrt{n}}\right) \tag{II.4}$$

converge vers l'opérateur stochastique d'Airy (SAE_β) :

$$\mathcal{H}_\beta := -\frac{d^2}{dx^2} + x + \frac{2}{\sqrt{\beta}}B'_x \tag{II.5}$$

dans un certain sens (ici, B' désigne un bruit blanc). En particulier, les plus petites valeurs propres de $\tilde{H}_n^\beta$ convergent en loi vers celles de $\mathcal{H}_\beta$.

Remarque. Il est en fait facile grâce à la loi du demi-cercle de deviner la puissance 2/3 qui apparaît dans la renormalisation (II.4). Les valeurs propres se raréfient au bord du spectre (la densité devient nulle), il faut donc effectuer une dilatation pour obtenir une limite non triviale lorsque $n \to \infty$. Pour $\delta > 0$ petit, le nombre de valeurs propres entre $2-\delta$ et 2 est équivalent à

$$\frac{n}{2\pi}\int_{2-\delta}^{2}\sqrt{4-x^2}dx = O(n\,\delta^{3/2}).$$

Ceci nous indique qu'il faut prendre δ de l'ordre de grandeur $n^{-2/3}$ pour avoir un nombre fini non nul de valeurs propres dans la fenêtre $[2-\delta, 2]$.

L'argument heuristique La convergence établie dans [48] provient de conjectures et d'arguments heuristiques solides d'Alan Edelman et Brian Sutton [55, 23]. Expliquons en quelques lignes d'où provient l'opérateur II.5. Les matrices tridiagonales sont considérées comme des opérateurs différentiels discrets. Pour tout $\alpha \leq 1$, nous dirons qu'une suite de matrices $(A_n, n \in \mathbb{N})$ converge vers un opérateur A (agissant sur les fonctions) et noterons $A_n \overset{n^\alpha}{\to} A$ lorsque pour tout f "régulière" [1] à support compact et à valeurs positives, on a

$$\|A_n f(\cdot/n^\alpha) - Af(\cdot/n^\alpha)\|_\infty \to 0$$

(pour chaque n, f est identifiée au vecteur $(f(1/n^\alpha), \cdots, f(n/n^\alpha))$ et A_n agit sur ce vecteur. Le notation $Af(\cdot/n^\alpha)$ représente le vecteur $(Af(1/n^\alpha), \cdots, Af(n/n^\alpha)))$.

Ainsi avec ces notations,

$$\begin{bmatrix} 2 & 0 & \cdots & 0 \\ 0 & 2 & \ddots & \vdots \\ \vdots & \ddots & \ddots & 0 \\ 0 & \cdots & 0 & 2 \end{bmatrix} \overset{\sqrt{n}}{\to} \times \text{ par } 2 \quad ; \quad \begin{bmatrix} 0 & 2 & \cdots & 0 \\ 0 & 0 & 2 & \vdots \\ \vdots & \ddots & \ddots & 2 \\ 0 & \cdots & 0 & 0 \end{bmatrix} \overset{\sqrt{n}}{\to} \times \text{ par } 2$$

$$\frac{1}{\sqrt{n}}\begin{bmatrix} 1 & 0 & \cdots & 0 \\ 0 & 2 & \ddots & \vdots \\ \vdots & \ddots & \ddots & 0 \\ 0 & \cdots & 0 & n \end{bmatrix} \overset{\sqrt{n}}{\to} \times \text{ par } x \; ; \quad \sqrt{n}\begin{bmatrix} -1 & 1 & 0 & \cdots & 0 \\ 0 & -1 & 1 & \ddots & \vdots \\ \vdots & \ddots & \ddots & \ddots & 0 \\ 0 & \cdots & 0 & -1 & 1 \end{bmatrix} \overset{\sqrt{n}}{\to} \frac{d}{dx}$$

1. Nous sommes volontairement flous sur cette définition car nous ne présentons que des arguments heuristiques.

$$n\begin{bmatrix} -2 & 1 & 0 & \cdots & 0 \\ 1 & -2 & 1 & \ddots & \vdots \\ 0 & \ddots & \ddots & \ddots & 0 \\ \vdots & 0 & 1 & -2 & 1 \end{bmatrix} \overset{\sqrt{n}}{\to} \frac{d^2}{dx^2}\,; \quad n^{1/4}\begin{bmatrix} g_1 & 0 & \cdots & 0 \\ 0 & g_2 & \ddots & \vdots \\ \vdots & \ddots & \ddots & 0 \\ 0 & \cdots & 0 & g_n \end{bmatrix} \text{ " } \overset{\sqrt{n}}{\to} \text{ " } \times \text{ par } B'$$

où pour la dernière convergence, les g_k sont des variables aléatoires indépendantes de loi gaussienne centrée réduite.

Considérons enfin comme dernier exemple la matrice (II.4) qui nous intéresse :

$$n^{1/6}\left[2\sqrt{n}I_n - H_n^\beta\right].$$

Pour trouver vers quel opérateur elle converge (au sens défini ci-dessus), nous utilisons une approximation de la loi χ lorsque son paramètre est très grand. Nous avons en effet lorsque $k \ll n$,

$$\chi_{\beta(n-k)} \sim \sqrt{\beta(n-k)} + \frac{h_k}{\sqrt{2}} \sim \sqrt{\beta n} - \frac{\sqrt{\beta}}{2\sqrt{n}}k + \frac{h_k}{\sqrt{2}}.$$

où les h_k désignent des variables aléatoires indépendantes de loi gaussienne centrée réduite. Ainsi, nous pouvons approximer les premières lignes de la matrice (II.4) de la façon suivante :

$$-n^{2/3}\begin{bmatrix} -2 & 1 & & \\ 1 & -2 & 1 & \\ & \ddots & \ddots & \ddots \end{bmatrix} + \frac{1}{2n^{1/3}}\begin{bmatrix} 0 & 1 & & \\ 1 & 0 & 2 & \\ & 2 & \ddots & \ddots \\ & & \ddots & \end{bmatrix} - \frac{n^{1/6}}{\sqrt{2\beta}}\begin{bmatrix} 2g_1 & h_1 & & \\ h_1 & 2g_2 & h_2 & \\ & \ddots & \ddots & \ddots \end{bmatrix}$$

En utilisant les convergences vues dans les exemples plus haut, nous voyons apparaître le résultat suivant qui correspond à la convergence voulue :

$$n^{1/6}\left[2\sqrt{n}I_n - H_n^\beta\right] \overset{n^{1/3}}{\longrightarrow} \quad -\frac{d^2}{dx^2} + x + \frac{2}{\sqrt{\beta}}B' = \mathcal{H}_\beta.$$

Étude de la loi de Tracy-Widom-β Pour tout $\beta > 0$, la plus grande valeur propre renormalisée de H_n^β converge donc vers une loi limite, appelée loi de Tracy-Widom-β. Nous avons déjà mentionné que cette loi a été très étudiée dans les cas où $\beta = 1, 2$ et 4, mais nous connaissons encore assez peu la loi pour β général. Mentionnons tout de même un résultat récent d'A. Bloemendal et de B. Virág en 2010 [8]. Ces auteurs ont trouvé une caractérisation de la loi de Tracy-Widom pour tous les β comme limite de la solution bornée d'une équation aux dérivées partielles.

Nous nous intéressons ici plutôt au développement asymptotique des queues de cette loi.

Grâce à la transformée de Ricatti, les valeurs propres de SAE_β peuvent être réinterprétées en terme de probabilités d'explosion d'une diffusion unidimensionnelle. En particulier, Ramírez et al. [48] ont montré que

$$\mathbb{P}(TW_\beta > a) \quad = \quad \mathbb{P}(X \text{ explose en un temps fini}), \tag{II.6}$$

où X est la diffusion

$$\begin{cases} dX(t) = (t + a - X^2(t))dt + \frac{2}{\sqrt{\beta}} dB(t), \\ X(0) = \infty. \end{cases} \tag{II.7}$$

Dans le papier [19], nous utilisons cette représentation pour obtenir des estimées précises sur la queue de la loi de Tracy-Widom. Notre outil principal est la formule de Cameron-Martin-Girsanov qui nous permet de changer la dérive d'une diffusion pour évaluer la probabilité d'explosion à l'aide du nouveau processus. Notre principal théorème est le suivant :

Théorème 2.1. *Lorsque a tend vers l'infini, nous avons :*

$$\mathbb{P}\left(TW_\beta > a\right) = a^{-3\beta/4} \exp\left(-\frac{2}{3}\beta a^{3/2} + O\left(\sqrt{\ln a}\right)\right).$$

Ceci généralise, avec une moindre précision, des résultats déjà connus dans les cas $\beta = 1, 2$ et 4 qui provenaient directement de sa représentation en terme de solution de l'équation de Painlevé II. Plus récemment, le développement asymptotique des queues de la loi de Tracy-Widom-β a été l'objet des articles [10] (pour la queue gauche) et [11] (pour la queue droite). En particulier, dans l'article [11], les auteurs sont capables d'obtenir par récurrence tous les termes du développement asymptotique en utilisant un argument (non rigoureux) de grande déviation (voir l'équation 1-29 de [11]). Les premiers termes sont en accord avec ceux que nous avons obtenus.

Le “vrai” processus auto-répulsif

CHAPITRE III

Grandes déviations et propriétés des trajectoires du TSRM

LES RÉSULTATS DE CE CHAPITRE ONT ÉTÉ SOUMIS POUR PUBLICATION.

We derive some large deviation bounds for events related to the "true self-repelling motion", a one-dimensional self-interacting process introduced by Tóth and Werner, that has very different path properties than usual diffusion processes. We then use these estimates to study certain of these path properties such as its law of iterated logarithms for both small and large times.

III.1 Introduction

In the present paper, we study some features of a self-interacting one-dimensional process called the true self-repelling motion, defined by Tóth and Werner in [59]. Let us first very briefly recall the intuitive definition of this process and describe the motivations that lead to our study.

The true self-repelling motion denoted by TSRM is a continuous real-valued process $(X_t, t \geq 0)$ that is locally self-interacting with its past occupation-time. More precisely, for each positive time t, define its occupation-time measure μ_t that assigns to each interval $I \subset \mathbb{R}$, the time spent in it by X before time t :

$$\mu_t(I) = \int_0^t 1_{X_s \in I} \, ds.$$

It turns out that for this particular process X, almost surely for each t, the measure μ_t has a continuous density $L_t(x)$. By analogy with semi-martingales, where such occupation-time densities also exist, the curve $x \mapsto L_t(x)$ is called the "local-time"

profile of X at time t. Heuristically, the dynamics of X_t is such that the TSRM is locally pushed in the direction of the negative "gradient" of the local time at its current position. Loosely formulated, one can write $dX_t = -\nabla_x L_t(X_t)dt$ (even if $(X_t, t \geq 0)$ is a random process). For more details and comments on this description, we refer to [59]. It turns out that this process is of a very different type than diffusions. For example (see again [59]), its quadratic variation almost surely vanishes whereas its variation of power $3/2$ is positive and finite. Similarly, it does not have the Brownian scaling property, it has instead a $2/3$ scaling behavior i.e., for any positive λ, $(X_{\lambda t}, t \geq 0)$ has the same law as $(\lambda^{2/3} X_t, t \geq 0)$.

This same exponent $2/3$ appears in various other models that can be interpreted as continuous height-fluctuations of $1+1$-dimensional models in the Khardar-Parisi-Zhang universality class (such as the Tracy-Widom distribution for eigenvalues of large random matrices, the movement of the second-class particle in a TASEP etc.). TSRM seems however at present to be one of the few such "non-diffusive" continuous processes that probabilists can define (see also [24] for related questions). All this gives us some motivation to study in more detail its behavior, in order to see what features it shares with the other previously-mentioned models, and also for its own independent interest.

Let us now describe briefly the results of the present paper : Both for the process $(X_t, t \geq 0)$ itself as for the height process $(H_t, t \geq 0)$, we give the rate of decay of the probability that their value at a given time is very large (with more precision for X). This enables us to derive almost sure fluctuation results (of the type of the law of the iterated logarithm) for these two processes (adding 0-1 law arguments for H). For instance, we shall see that $\limsup_{t\to\infty} X_t/(t^{2/3}(\log\log t)^{1/3})$ is almost surely equal to a finite positive constant we express in terms of the first negative zero of the derivative of the Airy function, and a similar result when $t \to 0$.

The construction of the process X_t is based on a family of coalescing one-dimensional Brownian motions starting from all points in the plane. Such families had been constructed by Arratia in [4], and further studied in [59, 53, 30, 43] and are called "Brownian web" in the latter papers. As a consequence, the estimates on the TSRM will follow from results concerning this Brownian web. In Section III.2, we will recall some aspects of the construction of TSRM and some features of the Brownian web. In Section III.3, we will focus on the large deviation estimates concerning X_1, we then derive the LIL for X in Section III.4, and we finally focus on the fluctuations of the height-process in the final Section III.5.

Acknowledgement : I am grateful to my supervisors Bálint Tóth and Wendelin Werner for their guidance throughout this work. Special thanks go to Wendelin Werner for his careful reading of successive versions of this paper.

III.2 Preliminaries and notations

In this section, we put down some notation, and collect some elementary estimates that will be useful later on.

III.2.1 Versions of the Brownian web

The true self-repelling motion (TSRM) is a deterministic function of a certain family of coalescing one-dimensional Brownian motions. There are two natural variants of TSRM, that respectively correspond to such Brownian families in the entire plane (this is the "stationary" TSRM, this version has stationary increments) or in the upper half-plane (this is the TSRM with "zero-initial conditions"). Other initial conditions are also possible, see Section 4 of [53] for examples.

Let us briefly first recall the construction in the **stationary** case which will be the main focus of this paper. To start with, choose any deterministic countable dense family Q of points $(\tilde{x}, \tilde{h})$ in the plane, say $Q = \mathbb{Q}^2$. It is then possible to define the joint law of a family $(\Lambda_{\tilde{x},\tilde{h}}(y), y \geq \tilde{x}\,;\, (\tilde{x}, \tilde{h}) \in Q)$ in such a way that, for each $(\tilde{x}, \tilde{h}) \in Q$, $\Lambda_{\tilde{x},\tilde{h}}$ is a function from $[\tilde{x}, \infty)$ into $\mathbb{R}$, that is distributed like a Brownian motion started from height $\tilde{h}$ at time $\tilde{x}$. Furthermore (see e.g. [59] for details), different curves are "independent until their first meeting time" and they coalesce after this meeting time (and follow the same Brownian evolution). Recall that Q is dense in the plane, so that the picture of all these lines is dense in the plane. The coalescent structure nevertheless defines a tree-like structure rooted "at $x = +\infty$". This type of curves is often referred to as the "forward lines".

If we are given a countable dense family $\tilde{Q}$ in the plane, then one can almost surely define the family of "backward" lines $(\Lambda_{\tilde{x},\tilde{h}}(y), y \leq \tilde{x}\,;\, (\tilde{x}, \tilde{h}) \in \tilde{Q})$ such that each $\Lambda_{\tilde{x},\tilde{h}}$ is now a function defined on $(-\infty, \tilde{x}]$ in such a way that the backward lines can be viewed as the "dual tree" of the previous dense tree (it is therefore a *deterministic* function of all forward lines). It is proved in [59] that this family of backward lines has the same law as the reversed image (changing x into $-x$) of the law of the forward lines (choosing $\tilde{Q}$ to be the symmetric image of Q).

There is an alternative construction where one does not have to first define the whole dense family of forward lines to construct the backward ones : Instead, one can construct the forward and the backward paths one by one for each $(\tilde{x}, \tilde{h}) \in Q$ inductively, applying a reflection/coalescence rule explained in the section 3.1.4 of [53]. Roughly, the rule is that when two curves meet, there is coalescence if they are of the same type (both backward or both forward), and otherwise, the two curves are "reflected on each other". Note that the proofs in [53] use the discrete model (with reflecting/coalescing random walks) and an invariance principle.

Both constructions define (for each Q) a family of curves $\Lambda_{\tilde{x},\tilde{h}}(\cdot)$ (from $\mathbb{R}$ to $\mathbb{R}$) indexed by $(\tilde{x},\tilde{h}) \in Q$, such that for each $(\tilde{x},\tilde{h})$ in Q, $\Lambda_{\tilde{x},\tilde{h}}(\tilde{x}) = \tilde{h}$ almost surely. It is then natural to wonder whether there exists certain "versions" of the process $(\Lambda_{x,h},\ (x,h) \in \mathbb{R}^2)$, defined simultaneously for all points (x,h) in the plane, with some additional regularity properties. It turns out that the situation is reminiscent of that of real-valued Lévy processes, where one can choose a right-continuous or a left-continuous version, except that time is here replaced by the h-variable.

In [59], the authors choose to define the forward line starting at $(x,h) \in \mathbb{R}^2$ denoted $\Lambda_{x,h}(y), y \geq x$ by taking the supremum of all $\Lambda_{\tilde{x},\tilde{h}}(y)$ over the countable family of lines

$$\{(\tilde{x},\tilde{h}) \in Q \ :\ \tilde{x} < x,\ \Lambda_{\tilde{x},\tilde{h}}(x) < h\}$$

that is to say over the lines in the countable family that are starting before x and passing below h at time x. Their Theorem 2.1 states that this family Λ then verifies :

- for any finite set $(x_1,h_1),\cdots,(x_n,h_n) \in \mathbb{R}^2$, a.s. $(\Lambda_{x_i,h_i},\ i \in \{1,\cdots,n\})$ is distributed as independent coalescing Brownian motions,
- a.s., for all $(x,h) \in \mathbb{R}^2$, $\Lambda_{x,h}(x) = h$,
- a.s., for all $(x_1,h_1),(x_2,h_2) \in \mathbb{R}^2$, Λ_{x_1,h_1} and Λ_{x_2,h_2} do not cross each other,
- a.s., for all $x < y$, the mapping $h \mapsto \Lambda_{x,h}(y)$ is left-continuous,

and that those four properties characterize its distribution. Note that the first one tells us that the choice of Q does not change the distribution of Λ. The last "left-continuity" means that for those (x,h) where there might be some choice, one chooses the lowest one. Throughout our paper, the notation $(\Lambda_{x,h})_{(x,h)\in\mathbb{R}^2}$ corresponds to this version of the coalescing family.

Clearly, there is another natural choice, that one can obtain by considering the symmetric picture (upwards down) i.e. to define

$$\Lambda^+_{x,h} = \inf\{\Lambda_{\tilde{x},\tilde{h}}(y),\ \tilde{x} < x,\ \Lambda_{\tilde{x},\tilde{h}}(x) > h,\ (\tilde{x},\tilde{h}) \in Q\}.$$

This family Λ^+ verifies the same properties as Λ, except that left-continuity with respect to h is replaced by right-continuity.

Another option proposed by Fontes, Isopi, Newman, and Ravishankar in [30] is to define a metric on a natural space on which the coalescing family lives and to consider the closure of $(\Lambda_{x,h}(y), y \geq x\ ;\ (x,h) \in Q)$ in this topological space. Note that you can now have more than one curve starting from certain (exceptional) points. In fact, the curves of the families Λ and Λ^+ correspond to the two extremal choices for the curves of their family. This construction is useful in order to state the convergence of the discrete model with coalescing random walks towards the coalescing Brownian motions. The family is called in their paper Brownian Web (Double Brownian Web if you add the backward lines). By a slight abuse of terminology, we will just call our family $(\Lambda_{x,h}(y),\ y \in \mathbb{R}\ ;\ (x,h) \in \mathbb{R}^2)$ "Brownian Web" (BW).

III.2.2 TSRM and the Brownian web

The intuitive link between the TSRM and the BW goes as follows : Let us consider the process (X_t, H_t) started at $(0, 0)$ which traces the contour of the "forward tree" moving upwards, that is to say above $\Lambda_{0,0}$ and towards $+\infty$. It is in fact the same contour as that of the "backward tree". This process visits all the points above the curve $\Lambda_{0,0}$ (it is plane-filling). The time-parametrization will be chosen in such a way that the area swept by (X, H) during the interval $[0, t]$ is exactly t and its first coordinate X will be the "true" self-repelling motion.

In order to be more precise, we need some additional notations. For each $(x, h) \in \mathbb{R}^2$, let $S_{x,h}$ denotes the (algebraic) area between $\Lambda_{x,h}$ and $\Lambda_{0,0}$:

$$S_{x,h} := \int_{-\infty}^{+\infty} (\Lambda_{x,h}(y) - \Lambda_{0,0}(y))\, dy.$$

Almost surely, for every (x, h) above the initial curve $\Lambda_{0,0}$, the process (X, H) is equal to (x, h) at the random time $S_{x,h}$ and has visited all the points between $\Lambda_{x,h}$ and $\Lambda_{0,0}$. Tóth and Werner proved that this indeed defines a continuous process $(X_t, H_t)_{t\geq 0}$ (see Lemma 3.4 of [59]). Thanks to the Brownian structure of the tree and the correspondence between area in the tree and time for the process, one can then easily deduce basic properties for (X, H) such as the recurrence of X in $\mathbb{R}$, or the scaling property : for every $a > 0$, $(X_{at}, H_{at})_{t\geq 0}$ and $(a^{2/3}X_t, a^{1/3}H_t)_{t\geq 0}$ are identical in law (Proposition 3.5 of [59]).

Another important observation is that together with the initial profile $\Lambda_{0,0}$, the first coordinate X contains enough information in order to recover both the process H and the upper part of the BW $(\Lambda_{x,h},\ x \in \mathbb{R},\ h \geq \Lambda_{0,0}(x))$. Indeed, as we already mentioned in the introduction, the occupation-time measure of X turns out (for each time t) to have a continuous density with respect to Lebesgue measure, denoted by $L_t(\cdot)$. Moreover, the definition of (X, H) readily shows that when $t = S_{x,h}$, then

$$\Lambda_{0,0}(\cdot) + L_t(\cdot) = \Lambda_{x,h}(\cdot)$$

i.e. that the random area $S_{x,h}$ corresponds to the first time t at which the local time at x, $L_t(x)$, reaches the level $h - \Lambda_{0,0}(x)$, and the curve of the BW from $\Lambda_{x,h} - \Lambda_{0,0}$ is the local time curve at $S_{x,h}$. It is a stronger analog to Ray-Knight Theorems for Brownian motion.

For each fixed (deterministic) $x \in \mathbb{R}$, we will denote by σ_x the first hitting time of x by the TSRM X. It is easy to see that $a.s$, this time equals the infimum of the set of times at which $L_\cdot(x)$, is positive. That is to say, for every given $x \neq 0$, σ_x is almost surely equal to the infimum of $S_{x,h}$ over all $h > \Lambda_{0,0}(x)$ (note that this is

not true for all x simultaneously because of the existence of "fast points" or of local maxima).

In the sequel, we shall simply denote by $\Gamma_x(\cdot)$, the profile at this time σ_x :

$$\Gamma_x(\cdot) := L_{\sigma_x}(\cdot) + \Lambda_{0,0}(\cdot).$$

Remark that almost surely for every $x \in \mathbb{R}$ this curve is equal to $\Lambda^+_{x,\Lambda_{0,0}(x)}(\cdot)$, coming from the right-continuous version of the BW (this is contained in Theorem 4.3 (ii) in [59]). Note also that with this definition Γ_0 is just the same as the initial profile $\Lambda_{0,0}$.

The following Lemma describes the joint law of Γ_0 and Γ_x. In fact, we will use a slightly stronger version and describe the law of Γ_Y, when Y is some Γ_0-measurable random variable :

Lemma 3.1. *Let Y denote a Γ_0-measurable random variable. Then, conditionally on Γ_0, the distribution of Γ_Y is that of a coalescing-reflecting Brownian motion started from $(Y, \Gamma_0(Y))$, that is reflected on Γ_0 in the interval between 0 and Y and coalescing with it outside of this interval.*

As the "starting point" $(Y, \Gamma_0(Y))$ of Γ_x is random, this fact is not totally straightforward. Our proof uses features of the BW established in [59].

Démonstration. We already know that for a **fixed** point (x, h) in the plane and conditionally on Γ_0, $\Lambda_{x,h}$ has the distribution of a Brownian motion reflected on Γ_0 between 0 and x and coalescing with it outside this interval. As the point $(Y, \Gamma_0(Y))$ is Γ_0-measurable, conditionally on Γ_0, the distribution of the increments of $\Lambda_{Y,\Gamma_0(Y)}$ remains those of a Brownian motion starting at this point, reflected on Γ_0 between 0 and Y and coalescing with it outside this interval. It remains to use Proposition 2.2 (v) in [59] which tells us that $\Lambda_{Y,\Gamma_0(Y)}$ is continuous to deduce that the distribution of this process corresponds indeed to the above description. □

A consequence of this lemma is that the distribution of σ_x itself can be simply expressed in terms of areas under Brownian curves : For every (deterministic) $x > 0$,

$$\sigma_x \overset{(d)}{=} \sqrt{2}\left(\int_0^x |B_t|dt + \int_x^{\tau'} |B_t|dt\right) \tag{III.1}$$

where B is a Brownian motion started at the origin and τ' denotes its first hitting time of 0 after time x. Indeed, the initial curve $\Gamma_0(x - \cdot)$ has the distribution of a Brownian motion starting at $\Gamma_0(x)$ and the distribution of $\Gamma_x(x-\cdot)$ conditionally on Γ_0 is given by Lemma 3.1, thus the difference $\Gamma_x(x-\cdot)-\Gamma_0(x-\cdot)$ has the distribution of a reflected Brownian motion multiplied by $\sqrt{2}$, absorbed at its first hitting of 0 after time x.

III.2.3 Brownian estimates

As shown by the example of the law of σ_x, the construction of the TSRM via the Brownian web makes it possible to express the probability of TSRM-events in terms of Brownian motions and areas under Brownian curves. We now collect some results concerning the law of Brownian motion integrals that we will need later in the paper.

Throughout this paper, B will denote a standard Brownian motion, and $\tilde{B}$ a reflected Brownian motion (that has the same law as $|B|$), P_x will denote the law of these processes started at x. When $x = 0$, we will sometimes simply write P instead of P_0. For each $y \in \mathbb{R}$, the first hitting time of the level y by B (respectively $\tilde{B}$) after time t will be denoted by $\tau_y^{(t)}$ (resp. $\tilde{\tau}_y^{(t)}$), when $t = 0$, we simply write τ_y (resp. $\tilde{\tau}_y$).

In order to derive our estimates about the tail of X_1 and H_1, we will build on the following rather classical asymptotics about the areas under a Brownian motion and a Brownian bridge. The first two results can for instance be found in [36] and the very classical third one in [40]. Here and throughout the paper,

$$\kappa := 2|a_1'|^3/27$$

where a_1' denotes the first (negative) zero of the derivative of the Airy function Ai.

Proposition 3.2. *1. For some positive constant γ, when $\varepsilon \to 0$,*

$$P_0\left(\int_0^1 |B_t|dt \le \varepsilon\right) \sim \gamma\,\varepsilon \exp\left(-\frac{\kappa}{\varepsilon^2}\right).$$

2. In the case of the Brownian bridge,

$$P_0\left(\int_0^1 |B_t - tB_1|dt \le \varepsilon\right) \sim \gamma' \exp\left(-\frac{\kappa}{\varepsilon^2}\right)$$

as $\varepsilon \to 0$ for some positive constant γ'.

3. The law of the area under a Brownian motion starting at 1 stopped at its first hitting of 0 is given by

$$P_1\left(\int_0^{\tau_0} B_t dt \le u^{-3}\right) = \frac{\int_u^\infty e^{-2y^3/9}dy}{\int_0^\infty e^{-2y^3/9}dy}.$$

This last statement follows in fact directly from the fact that the function $F(x, A) := P_x(\int_0^{\tau_0} B_t dt \le A)$ is a function of $x/A^{1/3}$ that satisfies the PDE $(\partial_x^2 - 2x\partial_A)F = 0$ (because $F(B_{t\wedge\tau_0}, A - \int_0^{t\wedge\tau_0} B_s ds)$ is a martingale).

Suppose that U_1 and U_2 are independent copies of the random variable $\int_0^{\tau_0} B_t dt$ in statement 3. A simple consequence of that estimate that we shall use at some point is that when $x \to 0$,

$$P_1(U_1 + U_2 \le x) = \exp\left(-8/(9x) + O(\log(1/x))\right). \tag{III.2}$$

Indeed a lower bound of $P_1(U_1+U_2\leq x)$ is simply given by $(P_1(U_1\leq x/2))^2$. For the upper bound, a possible proof consists in dividing the interval $[0,x]$ into $[1/x]+1$ intervals of length x^2 and to examine the probability that $U_1+U_2\leq x$ according to which portion U_1 belongs to :

$$P_1(U_1+U_2\leq x)\leq \sum_{j=0}^{[1/x]+1} P_1(U_1\in[jx^2,(j+1)x^2])\,P_1(U_2\leq x-jx^2+x^2)$$

Using Proposition 3.2-3, we deduce :

$$P_1(U_1+U_2\leq x)\leq \sum_{j=0}^{[1/x]+1}\exp\left(-\frac{2}{9\,x}\left[\frac{1}{(j+1)x}+\frac{1}{1+x(1-j)}\right]+O(\log(1/x))\right)$$

The minimum over $j\in\{0,\cdots,[1/x]+1\}$ of the function between the brackets takes the form $4(1+O(x))$. It gives the desired upper bound. □

III.3 Tail estimates for the distribution of X_1

The main goal of the present section is to derive the following facts :

Proposition 3.3. *When $x\to\infty$,*

$$\mathbb{P}(X_1\geq x)=\exp\left(-2\kappa\,x^3+O(\ln(x))\right)$$

and

$$\mathbb{P}\left(\sup_{s\in[0,1]}X_s\geq x\right)=\exp\left(-2\kappa\,x^3+O(\ln(x))\right)\quad \textit{as well.}$$

Note that X_1 and $-X_1$ have the same distribution, so that this also describes the behavior of $\mathbb{P}(X_1<-x)$ when $x\to+\infty$. We would like to also point out that our proof can be easily adapted to the case when the initial condition is flat. The only difference is that the coefficient 2κ in front of x^3 is replaced by κ (because the corresponding Brownian motion is not multiplied by $\sqrt{2}$). Note that in a recent preprint [18] by Bálint Tóth and the author, explicit formulas have been obtained for the density of the distribution of X_1 (and H_1) for the flat initial condition case which permits to derive the tails expansion. In a sense this new result supersedes the Propositions 3.3 (and 3.6 concerning the H_1 tail). However, the arguments presented in this paper are short and self-contained.

Démonstration. Recall the representation of the law of σ_x from the end of Section III.2.2. It follows that

$$\mathbb{P}\left(\sup_{s\in[0,1]}X_s\geq x\right)=\mathbb{P}(\sigma_x\leq 1)\leq P\left(\sqrt{2}\int_0^x\tilde{B}_u du\leq 1\right)=P\left(\int_0^1\tilde{B}_u du\leq\frac{1}{\sqrt{2x^3}}\right).$$

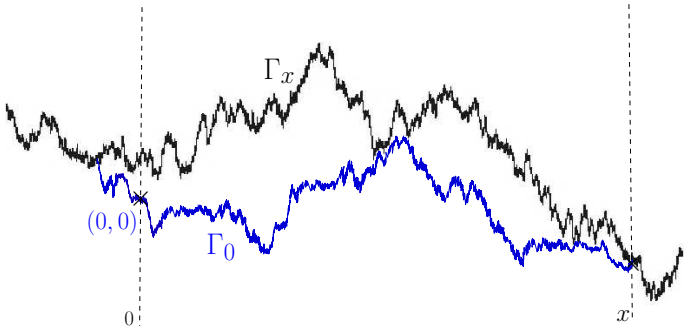

FIGURE III.1 – The two reflected-coalescing curves Γ_x and Γ_0

Combined with Proposition 3.2-1, this proves immediately the upper bound.

For the lower bound, it is sufficient to estimate the probability of a well-chosen subset of the event $\{X_1 > x\}$, that can be easily described using the Brownian web. In order to ensure that $X_1 > x$, it would for instance suffice that $\sigma_{x+1/x^2} < 1$ and that X stays to the right of x during a time-interval of length 1 after σ_{x+1/x^2}. We will use a slight variation of this idea : Let $\tilde{\Gamma}_x$ denote the line corresponding to the first time at which the local time $L_t(x)$ of X at x exceeds $1/x$. Let $\hat{\Gamma}_{x+1/x^2}$ denote the line corresponding to the first time at which the local time at $x + 1/x^2$ exceeds $1/(2x)$, and finally let Γ'_0 be the line corresponding to the first time at which the local time at 0 reaches $1/x$. Note that using Lemma 3.1, the joint distribution of those three processes together with Γ_0 is known. We will evaluate the probability that the following four events hold simultaneously (see Figure III.2. for a representation of those events) :

- The integral of $\tilde{\Gamma}_x - \Gamma_0$ over $[0, x]$ does not exceed $1 - 2/x^3$ and $\tilde{\Gamma}_x(0) < 1/x^4$.
- The integral of $\Gamma'_0 - \Gamma_0$ on $(-\infty, 0)$ does not exceed $1/x^3$.
- $\hat{\Gamma}_{x+1/x^2}(x) - \Gamma_0(x) \leq 1/x$ and $\hat{\Gamma}_{x+1/x^2} - \Gamma_0$ hits 0 on $[x, x + 1/x^2]$, and the integral of this function on $[x, x + 1/x^2]$ does not exceed $1/x^3$.
- The integral of $\hat{\Gamma}_{x+1/x^2} - \Gamma_0$ on $[x + 1/x^2, \infty)$ is greater than one.

It is easy to check just using monotonicity of the BW that if these four events hold then X_1 will be bigger than x – i.e. to the right of x in the two-dimensional picture (the first, second and third one imply $\sup_{s\leq 1} X_s \geq x + 1/x^2$, the third and last one ensure that X_1 stays above x during the time-interval $[\sigma_{x+1/x^2}, \sigma_{x+1/x^2} + 1]$). Notice also that these four events are independent as the processes defining them (restricted to the appropriate time-intervals) correspond to different parts of the BW (and this is why we chose to work with these events). Let us evaluate the probability of each of them. Thanks to Brownian scaling, the second and the third one are equal to positive constants independent of x.

If the process $\hat{\Gamma}_{x+1/x^2} - \Gamma_0$ stays above $1/(4x)$ in the time interval of length $4x$ starting at $x + 1/x^2$, then the fourth event is satisfied. It implies that the probability

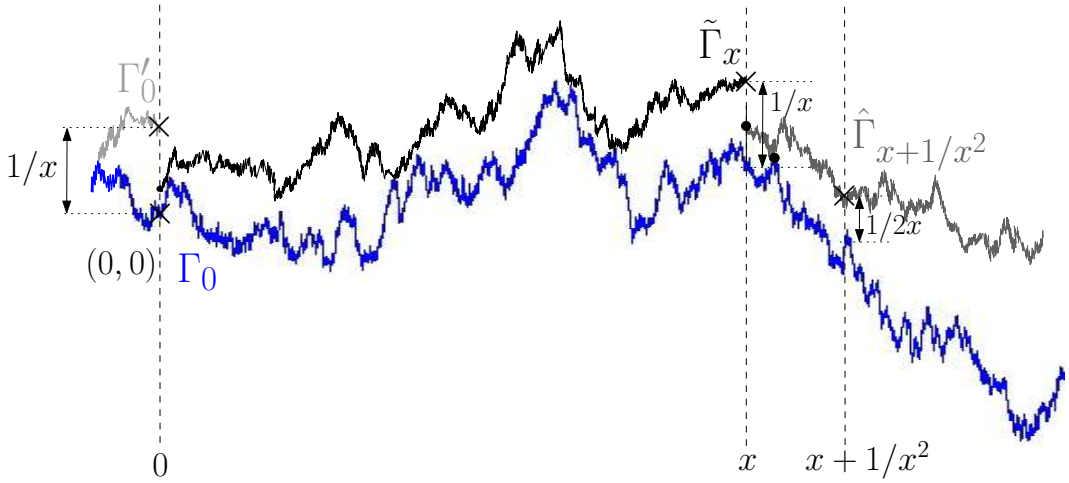

FIGURE III.2 – The BW-curves Γ_0, Γ'_0, $\tilde{\Gamma}_x$ and $\hat{\Gamma}_{x+1/x^2}$

of the fourth event is bounded from below by

$$P_0\left(\inf_{s\le 4x} B_s \ge -1/(4\sqrt{2}x)\right) = P_0\left(|B_1| \le 1/(8\sqrt{2}x^{3/2})\right) \ge c/x^{3/2} \qquad \text{(III.3)}$$

for some absolute constant c.

It remains to deal with the first event. Its probability is responsible for the main exponential term : The strong Markov property applied at the first hitting time of 0 by $\tilde{\Gamma}_x - \Gamma_0$ together with the fact that $y \mapsto P_0(\int_0^y |B_t|dt \le A,\ |B_y| \le B)$ (for any positive A and B) is decreasing with y show that it is bounded from below by

$$P_{1/(\sqrt{2}x)}\left(\tau_0 < 1/x^2,\ \sqrt{2}\int_0^{\tau_0} B_t dt \le 1/x^3)\right) P_0\left(\sqrt{2}\int_0^x |B_t|dt \le 1-3/x^3,\ \sqrt{2}|B_x| \le 1/x^4\right).$$

The scaling property shows again that the first term in this product does not depend on x. The second term can be evaluated thanks to the Brownian bridge. Scaling shows that it is bounded from below by :

$$\begin{aligned} &P_0\left(\int_0^1 |B_t - tB_1|dt \le \frac{1}{\sqrt{2}x^{3/2}}\left(1-3/x^3\right) - \frac{|B_1|}{2},\ |B_1| \le \frac{1}{\sqrt{2}x^{9/2}}\right) \\ &\ge P_0\left(\int_0^1 |B_t - tB_1|dt \le \frac{1}{\sqrt{2}x^{3/2}}\left(1-4/x^3\right)\right) \times P_0\left(|B_1| \le \frac{1}{\sqrt{2}x^{9/2}}\right) \end{aligned}$$

because of the independence between $(B_t - tB_1,\ t \in [0,1])$ and B_1. Putting the pieces together, we get finally that

$$P(X_1 \ge x) \ge \frac{c'}{x^6} \times P_0\left(\int_0^1 |B_t - tB_1|dt \le \frac{1}{\sqrt{2}x^{3/2}}\left(1-4/x^3\right)\right) \qquad \text{(III.4)}$$

where c' is some absolute constant. Proposition 3.2-2 then allows to conclude. □

III.4 Law of the iterated logarithm for X

The main goal of this section is to use the previous estimates in order to derive the analogue for X of the law of the iterated logarithm :

Proposition 3.4. *Almost surely*

$$\limsup_{t\to+\infty} \frac{X_t}{t^{2/3}\left(\ln\ln(t)\right)^{1/3}} = \limsup_{t\to 0+} \frac{X_t}{t^{2/3}\left(\ln\ln(1/t)\right)^{1/3}} = 1/(2\kappa)^{1/3}.$$

Stationarity shows that this also describes the almost sure fluctuations at any given positive time t_0 i.e. that almost surely,

$$\limsup_{t\to 0+} \frac{X_{t_0+t} - X_{t_0}}{t^{2/3}\left(\ln\ln(1/t)\right)^{1/3}} = 1/(2\kappa)^{1/3}.$$

The same type of local result will hold for the TSRM with flat initial condition at any given positive time. However, if X is the TSRM with flat initial conditions, then the result stated in the proposition does not hold anymore. The proof can however be directly adapted and then shows that one just has to replace the constant $1/(2\kappa)^{1/3}$ by $1/\kappa^{1/3}$.

III.4.1 Proof of the upper bounds

Let us now first briefly derive the upper bounds in this proposition i.e. the fact that these limsups are not greater than $1/(2\kappa)^{1/3}$. This part of the proof will go along similar lines as the standard proof of the LIL for the Brownian motion (see e.g., Chapter II p. 56 of [51]) based on Borel-Cantelli Lemmas. Let us first focus on the $t \to \infty$ part. Clearly, it suffices to show that for every $\lambda > 1$ and $\varepsilon > 0$, there almost surely exists some N such that for all $n \geq N$,

$$\sup_{t\in[0,\lambda^n]} X_t \leq \frac{1+\varepsilon}{(2\kappa)^{1/3}} \lambda^{2n/3} \left(\ln\ln(\lambda^n)\right)^{1/3}.$$

If we define

$$x_n := \frac{1+\varepsilon}{(2\kappa)^{1/3}} \left(\ln\ln(\lambda^n)\right)^{1/3},$$

we get (because $\sup_{t\in[0,\lambda^n]} X_t/\lambda^{2n/3}$ and $\sup_{t\in[0,1]} X_t$ have the same law) from Proposition 3.3 that

$$\mathbb{P}\left(\lambda^{-2n/3} \sup_{t\in[0,\lambda^n]} X_t \geq x_n\right) = \mathbb{P}\left(\sup_{t\in[0,1]} X_t \geq x_n\right) = e^{-2\kappa\, x_n^3 + O(\ln(x_n))}.$$

Our choice for x_n ensures that

$$\sum_n \mathbb{P}\left(\lambda^{-2n/3} \sup_{t\in[0,\lambda^n]} X_t \geq x_n\right) < \infty.$$

Note that λ can be chosen arbitrarily close to one and ε arbitrarily small which implies the result when $t \to \infty$.

The proof for $t \to 0$ is almost identical, except that we now have to choose $\lambda \in (0,1)$. □

III.4.2 Proof of the lower bounds

The purpose of this subsection is to derive the lower bounds in Proposition 3.4. Let us stress that some caution is needed because the process X does not have independent increments, so that the standard proof of the LIL for Brownian motion cannot be adapted directly.

We again first focus on the case where $t \to +\infty$. Let us fix any small δ. Our goal is to show that for $c := 1/(2\kappa)^{1/3}$ one can almost surely find a sequence of times $t_n \to +\infty$, such that

$$X_{t_n} \geq (c-\delta)\, t_n^{2/3} \left(\ln\ln(t_n)\right)^{1/3}. \tag{III.5}$$

We will choose t_n to be some first hitting times. More precisely, let us choose $\lambda > 1$, $\varepsilon \in (0, 2/3)$ and define for each $n \geq 1$,

$$\lambda_n = \lambda^{n^{1+\varepsilon}},$$

and let

$$\tilde{\sigma}_n := \sigma_{\lambda_n} = \inf\{t \geq 0 \ : \ X_t = \lambda_n\}.$$

Our sequence (t_n) will be a subsequence of $(\tilde{\sigma}_n)$.

Note that $\lambda_n/\lambda_{n-1} \sim \lambda^{(1+\varepsilon)n^\varepsilon}$ increases quite rapidly when $n \to \infty$, but not too fast either (both facts will be useful in our proof). Define

$$\gamma_n := c'\, \lambda_n^{3/2} \Big/ \sqrt{\ln\ln(\lambda_n^{3/2})}$$

where the positive constant c' will be chosen later.

Our goal is to prove that $\tilde{\sigma}_n \leq \gamma_n$ (i.e. that the area between Γ_{λ_n} and Γ_0 does not exceed γ_n) infinitely often as soon as $c' > \sqrt{2\kappa}$, which indeed implies (III.5).

Let us define the boxes $L_n := [-\lambda_n, \lambda_n] \times [-\eta_n, \eta_n]$ with $\eta_n := 3\sqrt{\lambda_n \ln(n)}$. As the sequence (λ_n) increases fast, the box L_{n-1} is really small compared to L_n when n is large.

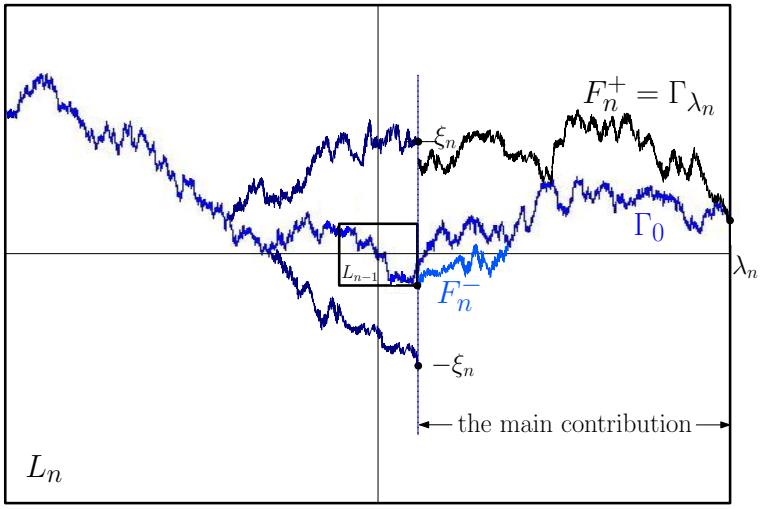

FIGURE III.3 – Boxes L_n and L_{n-1} and the curves involved in $\mathcal{A}_n$ and $\mathcal{B}_n$

Our choice for η_n ensures that if we define

$$\mathcal{D}_n := \{\Gamma_0([-\lambda_n, \lambda_n]) \in [-\eta_n, \eta_n]\}$$

then

$$\sum_n \mathbb{P}(\mathcal{D}_n^c) < \infty,$$

so that almost surely, $\mathcal{D}_n$ holds for all large enough n. Similarly, one can also for instance see that

$$\Gamma_{\lambda_n}([\lambda_{n-1}, \lambda_n]) \in [-\eta_n, \eta_n]$$

almost surely for all large enough n.

The fact that the events $\{\tilde{\sigma}_n \leq \gamma_n\}$ for $n \geq 1$ are not independent leads us to define closely related events that happen to be independent, so that we will be able to apply Borel-Cantelli arguments. The events that we are going to focus on will be defined in terms of the Brownian Web in the disjoint portions $(L_n \setminus L_{n-1})$. One minor technical difficulty is that in order to recognize where Γ_0 is in $L_n \setminus L_{n-1}$, one needs information about the Brownian web in L_{n-1}. We will circumvent this problem by considering instead the forward line in the web denoted by F_n^- started from the bottom right corner of L_{n-1}. Then, we define F_n^+ to be the backward line in the web that is started from $F_n^-(\lambda_n)$ reflected above this curve F_n^-.

Now, we define the event $\mathcal{A}_n$ that the following three events hold :

– The area between F_n^+ and F_n^- is small i.e.

$$\int_{\lambda_{n-1}}^{\lambda_n} (F_n^+(u) - F_n^-(u))\, du \leq (1-\varepsilon)\gamma_n.$$

– $F_n^+(\lambda_{n-1}) \in [\eta_{n-1}, \xi_n]$ with $\xi_n := \varepsilon c' \sqrt{\lambda_n / \ln(\ln(\lambda_n^{3/2}))}$.

– F_n^- and F_n^+ stay in L_n during the interval $[\lambda_{n-1}, \lambda_n]$.

The last event ensures that $\mathcal{A}_n$ is indeed measurable with respect to the Brownian web in L_n. Note that, as before, the probability of this third event is very close to 1 for n large, and in fact equal to $1 - a_n$ for some summable a_n.

We can use the same trick as in the proof of the lower bound of the tail of X_1 in order to get a lower bound for the probability that the first two events involved in this definition happen : Indeed, using scaling and then the independence between $t \in [0,1] \mapsto B_t - tB_1$ and B_1, we get that

$$\begin{aligned}\mathbb{P}(\mathcal{A}_n) + a_n &\geq P\left(\int_0^1 |B_u|\, du \leq (1-\varepsilon)c'\alpha_n,\ \sqrt{2}\eta_{n-1}/\sqrt{\lambda_n - \lambda_{n-1}} \leq |B_1| \leq \varepsilon c'\alpha_n\right) \\ &\geq P\left(\int_0^1 |B_u - uB_1|\, du \leq (1-\frac{3}{2}\varepsilon)c'\alpha_n\right) \times P\left(|B_1| \in \left[\frac{\sqrt{2}\eta_{n-1}}{\sqrt{\lambda_n - \lambda_{n-1}}}, \varepsilon c'\alpha_n\right]\right)\end{aligned}$$

where $\alpha_n := 1/\sqrt{2\,\ln\ln(\lambda_n^{3/2})}$. Part 2 of Proposition 3.2 then shows that

$$\sum \mathbb{P}(\mathcal{A}_n) = \infty$$

as soon as $c' \geq (1+\varepsilon)^{1/2}/(1-3\varepsilon/2) \times \sqrt{2\kappa}$ (this is where we used that the sequence (λ_n) is not increasing too fast, in the sense $\ln(\lambda_n) = 0\,(n^{1+\varepsilon})$).

Consider now the two backward lines started at (λ_{n-1}, ξ_n) and $(\lambda_{n-1}, -\xi_n)$. Define the event $\mathcal{B}_n$ that the area between these two curves does not exceed ξ_n^3, that they coalesce in the interval $[\lambda_{n-1} - 2\xi_n^2, \lambda_{n-1} - \xi_n^2]$, that they do not enter the box $[\lambda_{n-1} - \xi_n^2, \lambda_{n-1}] \times [-\xi_n/3, \xi_n/3]$ and do not exit the box $[\lambda_{n-1} - 2\xi_n^2, \lambda_{n-1}] \times [-2\xi_n, 2\xi_n]$. Clearly, scaling shows that the probability of this event does not depend on n. Furthermore, our definition of ξ_n ensures that for large enough n, one can check whether this event holds by just looking at the Brownian web in the part of $L_n \setminus L_{n-1}$ that is to the left of λ_{n-1}, which implies in particular that $\mathcal{B}_n$ is independent of $\mathcal{A}_n$.

Hence, it also follows that the events $(\mathcal{A}_n \cap \mathcal{B}_n)$ are independent, so that almost surely, $\mathcal{A}_n \cap \mathcal{B}_n$ holds for infinitely many values of n. As $\mathcal{D}_n$ holds almost surely for all large n, we conclude that almost surely $\mathcal{A}_n \cap \mathcal{B}_n \cap \mathcal{D}_{n-1}$ occurs infinitely often. But we can notice that when this last event holds, then, due to the monotonicity properties of the Brownian web, we get that $F_n^- \leq \Gamma_0$, F_n^- coalesces with Γ_0 in the interval $[\lambda_{n-1}, \lambda_n]$ (because $F_n^+(\lambda_{n-1})$ is bigger than η_{n-1}) and thus $F_n^+ = \Gamma_{\lambda_n}$. Moreover, $\{F_n^+(\lambda_{n-1}) \leq \xi_n\} \cap \mathcal{D}_{n-1}$ implies that the backward lines involved in $\mathcal{B}_n$ enclose Γ_0 and Γ_{λ_n}. As ξ_n^3 is much smaller than $\varepsilon\gamma_n$, it permits to conclude that $\mathcal{A}_n \cap \mathcal{B}_n \cap \mathcal{D}_{n-1}$ is included in $\tilde{\sigma}_n \leq \gamma_n$ as soon as c' is greater than $(1+\varepsilon)^{1/2}/(1-3\varepsilon/2) \times \sqrt{2\kappa}$. Taking the limit $\varepsilon \to 0$ gives the result.

The proof of the lower bound when $t \to 0$ is almost identical. The very same proofs goes through without modification, one just has to take λ smaller than 1 instead of larger than 1. □

III.5 Fluctuations of the height

III.5.1 Statement of tail-estimates

In this section, we will mostly study the tails of the distribution of the height H_t. Again, we can restrict ourselves to $t = 1$ thanks to the scaling property. The estimates that we will derive are the following :

Proposition 3.5. *There exists two positive constants η and η' such that for all large h,*

$$\begin{array}{ccccccc} \exp(-\eta h^{3/2}) & \leq & \mathbb{P}(H_1 \leq -h) & \leq & \mathbb{P}\left(\inf_{t\in[0,1]} H_t \leq -h\right) & \leq & \exp(-\frac{1}{\eta}h^{3/2}) \\ \exp(-\eta' h^{3/2}) & \leq & \mathbb{P}(H_1 \geq h) & \leq & \mathbb{P}\left(\sup_{t\in[0,1]} H_t \geq h\right) & \leq & \exp(-\frac{1}{\eta'}h^{3/2}). \end{array}$$

We use here two different constants η and η' to stress that, unlike the case of X, the distribution of H is **not** symmetric (i.e. the distributions of $-H_1$ and H_1 are quite different). See Fig. III.4.

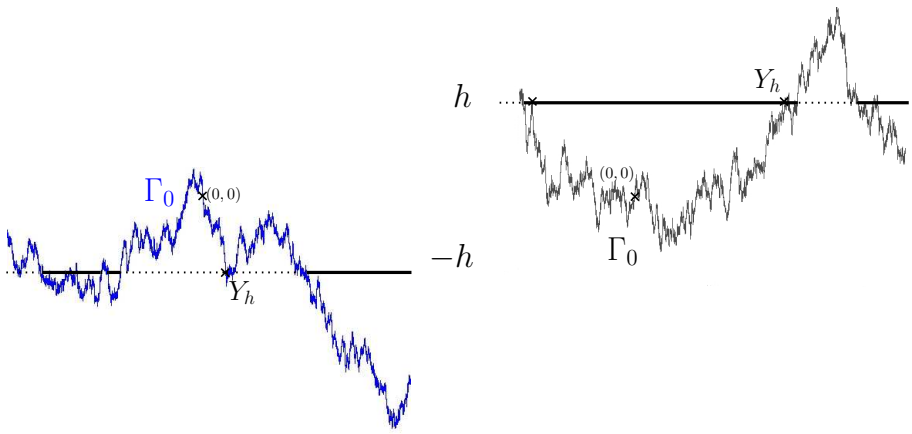

FIGURE III.4 – The initial configuration Γ_0 and the lines $-h$ and h (the thick lines represent the possible places (X_1, H_1) where one can have $H_1 < -h$ (on the left hand side) and $H_1 > h$ (on the right hand side) knowing Γ_0

In fact the derivation of the tail-estimates for H_1 are very different than those for X_1, because the initial profile will now play a key-role. Roughly speaking, the exceptional events that we will focus on will require a combination of a very favorable initial profile Γ_0 and a particular behavior of the TSRM between time 0 and 1.

The next three subsections are devoted to the proof of Proposition 3.5.

III.5.2 Lower bounds

We will first derive the lower bound for the probability that $H_1 \leq -h$ and we will in fact focus on the sub-event $\{H_1 \leq -h \text{ and } X_1 > 0\}$. To guess what configuration

to consider, we can imagine that for the initial profile, the random variable

$$Y_{-h} := \inf\{y \geq 0 \ : \ \Gamma_0(y) \leq -h\}$$

is exceptionally small. Then, on $[0, Y_{-h}]$, Γ_0 will at first glance look like a non-horizontal line with negative strong slope $-\alpha$ (to be determined), and one can compute the cost for another Brownian motion going backwards and reflected on this slope, starting at the point $(h/\alpha, -h)$ in order to create an area less than 1. One has to find a compromise between the cost of creating this initial configuration (which is roughly $P(\tau_{-h} < h/\alpha)$) and the cost of creating this small area with this slope. A back-of-the envelope calculation shows that a slope α of the order of $\sqrt{h}$ is close to optimal. In other words, we will roughly ask the initial profile Γ_0 to go down to level $-h$ during the interval $[0, \sqrt{h}]$ (recall that the "natural" Brownian scaling would give an interval of length h^2), and then the TSRM to run exceptionally fast down this slope.

More precisely, let us describe the events that we will require to hold (Figures III.5. and III.6. can help to quickly see what is going on). Define

$$\varepsilon_h := 1/(5\sqrt{h+2}),$$

and the function $f_h(\cdot)$ to be the linear function defined on $[0, \sqrt{h+2}]$ such that $f_h(0) = 0$ and $f_h(\sqrt{h+2}) = -h-2$. Define U_h to be the tube of vertical width ε_h around f_h, and V_h to be the same tube, but shifted vertically by $2\varepsilon_h$ so that V_h lies just above U_h. In other words,

$$\begin{aligned} U_h &= \{(x,l) \ : \ x \in [0, \sqrt{h+2}] \text{ and } |l - f_h(x)| < \varepsilon_h\} \\ V_h &= \{(x,l) \ : \ x \in [0, \sqrt{h+2}] \text{ and } |l - f_h(x) - 2\varepsilon_h| < \varepsilon_h\}. \end{aligned}$$

Then, we will require that

- The initial profile Γ_0 stays within U_h for all $x \in [0, \sqrt{h+2}]$.
- The backward line starting at $(\sqrt{h+2}, -h-2+2\varepsilon_h)$ stays in V_h for all $x \in [0, \sqrt{h+2}]$.
- The backward lines starting at $(0,0)$ and at $(0,1)$ coalesce in such a way that the area between them is less than $1/5$, i.e. $\int_{-\infty}^{0}(\Lambda_{(0,1)}(y) - \Lambda_{(0,0)}(y))dy \leq 1/5$.
- The forward lines starting at $(\sqrt{h+2}, -h-3)$, $(\sqrt{h+2}, -h-1)$ and at $(\sqrt{h+2}, -h-1/2)$ do coalesce before reaching the height $-h$, and the area between the last two curves is greater than 1.
- The backward line starting at $(\sqrt{h+2}, -h-1/2)$ and at $(\sqrt{h+2}, -h-2+2\varepsilon_h)$ do coalesce before reaching the height $-h$, and in a horizontal time-span smaller than one.

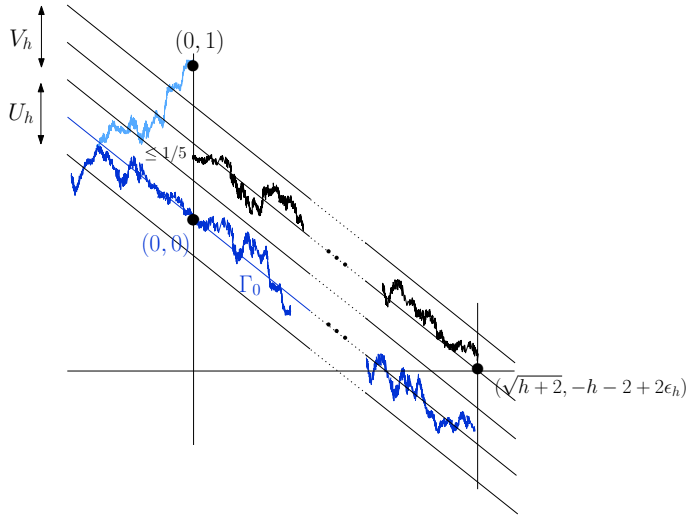

FIGURE III.5 – Realization of the first three events

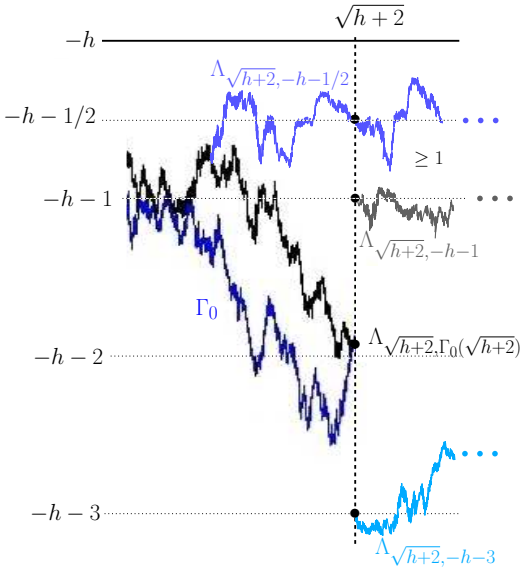

FIGURE III.6 – Zoom around $t = \sqrt{h+2}$ with the lines involved for the realization of the fourth and fifth events

All these definitions may seem somewhat messy, but it is easy to check, just using the monotonicity properties of the Brownian web, that if all these events occur, then H_t will hit $-h-2$ before time 1, and that the process (X_t, H_t) will stay under the horizontal line $-h$ for a time-interval of length at least one after this time. In particular, if the five events hold simultaneously, then $H_1 \leq -h$.

The first four events are independent, because they correspond to events dealing with the Brownian web in disjoint domains. The conditional probability of the last one given the first four turns out to be bounded from below by a positive constant

that does not depend on h. Indeed, it is independent on the third and fourth events. Moreover, the second event tells that the backward line started at $(\sqrt{h+2}, -h - 2 + 2\varepsilon_h)$ stays in the tube V_h. Therefore the conditional probability is bounded from below by the probability that a standard Brownian motion hits the affine function $-f_h - 3/2$ before reaching the height $1/2$ which clearly is positive (and bounded from below independently from h).

It remains to evaluate the probabilities of the first four events separately. The third and the fourth are positive and independent of h. The first two probabilities are equal. Note that $(\Gamma_0(x), x \leq \sqrt{h+2})$ is a Brownian motion and therefore $\Gamma^B(x) := \Gamma_0(x) - x\Gamma_0(\sqrt{h+2})/\sqrt{h+2}$ is a Brownian bridge independent from $\Gamma_0(\sqrt{h+2})$. Furthermore, if

$$\Gamma_0(\sqrt{h+2}) \in [-h-2-\varepsilon_h/2, -h-2+\varepsilon_h/2]$$

and

$$\sup_{x\in[0,\sqrt{h+2}]} |\Gamma^B(x)| \leq \varepsilon_h/2,$$

then the first event holds. The probabilities of each of these two independent events turns out of the type $\exp\big(-ch^{3/2}\big)$, which concludes the proof of the lower bound of $\mathbb{P}(H_1 < -h)$.

The proof of the lower bound for $\mathbb{P}(H_1 > h)$ is almost identical. The only difference is that the tubes now go upwards instead of downwards, and the reader can easily check that the same arguments work. □

III.5.3 Upper bound for $\mathbb{P}(\inf_{s\in[0,1]} H_s < -h)$

We define again for $l > 0$

$$Y_{-l} = \inf\{y > 0 \ : \ \Gamma_0(y) \leq -l\},$$

and we simply use Y for Y_{-h}. Clearly, by symmetry,

$$\begin{aligned}\mathbb{P}\left(\inf_{s\in[0,1]} H_s < -h\right) &= \mathbb{P}\left(\inf_{s\in[0,1]} H_s < -h,\ X_1 < 0\right) \ + \ \mathbb{P}\left(\inf_{s\in[0,1]} H_s < -h,\ X_1 > 0\right)\\ &= 2\mathbb{P}(\sigma_Y < 1)\\ &\leq 2\mathbb{P}\left(\int_0^Y (\Gamma_Y(y) - \Gamma_0(y))dy < 1\right).\end{aligned}$$

Recall from Lemma 3.1 that conditionally on Γ_0, the law of Γ_Y is that of a backward Brownian motion started at $(Y, \Gamma_0(Y))$ and reflected on Γ_0.

Note that Williams decomposition theorem (see for instance chapter 4 Corollary (4.6) p. 317 in [51]) states that the law of $(\Gamma_0(Y-y)+h, y \in [0,Y])$ is that of a three-dimensional Bessel process up to its last passage time at level h.

Recall that by the strong Markov property for the Brownian motion, if one defines (for a given $\epsilon > 0$)

$$\Gamma^j := (\Gamma_0(t + Y_{-j\epsilon}) + j\epsilon, t \in [Y_{-j\epsilon}, Y_{-(j+1)\epsilon}])$$

then $\Gamma^0, \Gamma^1, \Gamma^2, \ldots$ are i.i.d. Let us choose $\epsilon = c/h^{1/2}$ for some large c, and denote by N the integer part of h/ϵ.

Monotonicity properties readily imply (by comparing Γ_Y with the process where at each $Y_{-j\epsilon}$, the Brownian motion has to jump down to the actual location of Γ_0) that one can compare $\int_0^{Y_{-N\epsilon}}(\Gamma_Y(y) - \Gamma_0(y))dy$ with the sum of N i.i.d. copies of $\int_0^{Y_{-\epsilon}}(\Gamma_{Y_{-\epsilon}}(y) - \Gamma_0(y))dy$ (the latter being stochastically dominated by the former). Hence, it finally suffices to evaluate the probability that the sum of N copies of

$$\int_0^{Y_{-\epsilon}}(\Gamma_{Y_{-\epsilon}}(y) - \Gamma_0(y))dy$$

is smaller than 1. By scaling, this is exactly the same as the probability that the sum of N copies of

$$\int_0^{Y_{-c}}(\Gamma_{Y_{-c}}(y) - \Gamma_0(y))dy$$

is smaller than $h^{3/2}$ (which is smaller than $2cN$). Note that if we have chosen c sufficiently large, we made sure (because of scaling) that

$$E\left(\int_0^{Y_{-c}}(\Gamma_{Y_{-c}}(y) - \Gamma_0(y))dy\right) = c^3 E\left(\int_0^{Y_{-1}}(\Gamma_{Y_{-1}}(y) - \Gamma_0(y))dy\right) > 4c$$

and it therefore follows from the standard Cràmer Theorem for sums of i.i.d. positive random variables that for some positive constant a, the probability in question is bounded from above by $\exp(-ah^{3/2})$ for all large h, which concludes this part of the proof. □

III.5.4 Upper bound for $\mathbb{P}(\sup_{s\in[0,1]} H_s > h)$

Our goal is now to derive the upper bound for the probability that H_t reaches a large positive h before time 1. Recall $S_{x,h}$ denotes the area between $\Lambda_{x,h}$ and Γ_0. In other words, we want to evaluate the probability that there exists an x for which $S_{x,h} \in [0,1]$. Note that for symmetry reasons, this probability is bounded from above by twice the probability that there exists a positive x for which $S_{x,h} \in [0,1]$.

Note that the situation is different than in the previous section. Indeed, for H_t to be negative before time 1, the strategy had to be to find quickly a position where

the initial profile was negative. Here, it could a priori happen that the H_t is very large just because the TSRM spent some time in a tiny interval. So, the position at which this can happen is not a priori prescribed (see Figures III.7 and III.8).

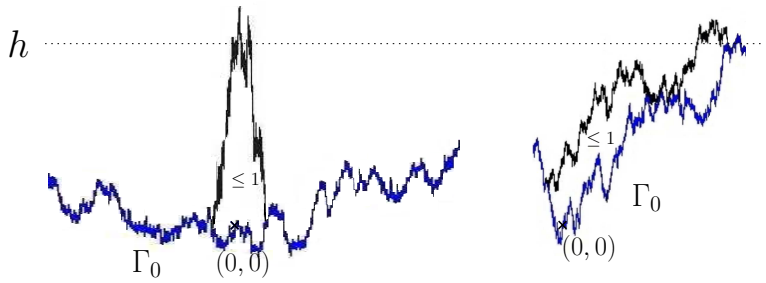

FIGURE III.7 – Possible configurations for $H_1 > h$

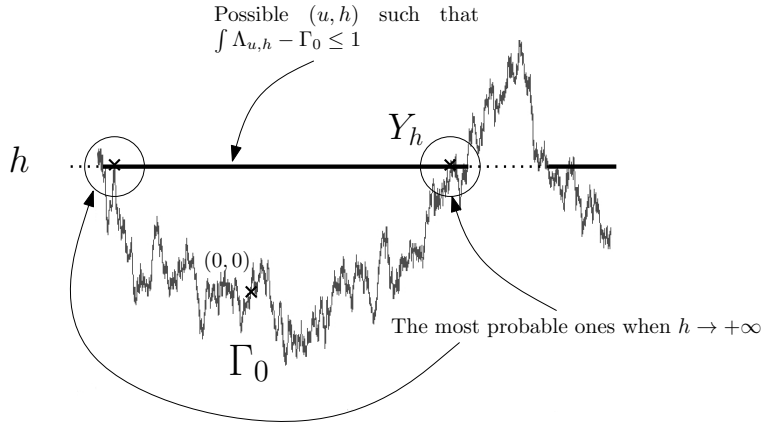

FIGURE III.8 – The initial local time with the possible positions for X when H first hits the level h

Recall from our earlier estimates that the probability that the TSRM X reaches $\sqrt{h}$ before time 1 is bounded by $\exp(-\kappa h^{3/2})$. It will therefore be sufficient to evaluate

$$\mathbb{P}(\exists x \in [0, \sqrt{h}],\ S_{x,h} \in [0, 1]).$$

Also, it is easy to check that the probability that $\Gamma[-\sqrt{h}, \sqrt{h}] \notin [-h/4, h/4]$ is also very small, and bounded from above by $\exp(-ch^{3/2})$ for some constant c and all large h.

It remains to bound the probability that $\Gamma[-\sqrt{h}, \sqrt{h}] \in [-h/4, h/4]$ and $S_{x,h} \leq 1$ for some $x \in [0, \sqrt{h}]$. In fact, we shall see that it is smaller than $\exp(-ch^3)$ for some constant c.

Indeed, if this holds for some $x \in [0, \sqrt{h}]$, it means that the backward line in the BW starting from (x, h) has to hit level $h/2$ in the interval $[x - 4/h, x]$. Indeed,

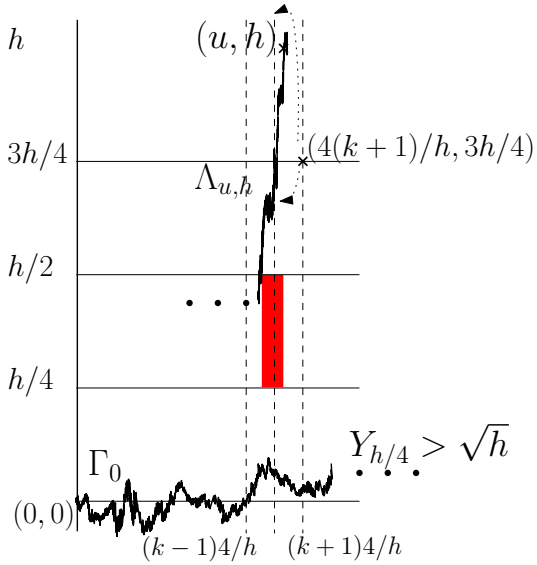

FIGURE III.9 – Representation of (u,h) verifying $S_{u,h} \leq 1$

otherwise, the domain in-between the initial profile and this backward line would contain a rectangle with area $(4/h) \times (h/4) = 1$.

Let us now suppose that for some $x \in [0, \sqrt{h}]$, the backward line in the BW starting from (x,h) has to hit level $h/2$ in the interval $[x - 4/h, x]$. Let us define j to be the smallest integer such that $\tilde{x} := 4j/h \geq x$. Then, the backwards line starting from $(\tilde{x}, 3h/4)$ has to either hit h or $h/2$ in the interval $[\tilde{x} - 2/h, \tilde{x}]$ (indeed, if it stays in the interval $[h/2, h]$, it would coalesce with the backward line starting from (x,h) and therefore hit $h/2$). See Fig. III.9.

The probability that a Brownian motion started from the origin hits level $h/4$ before time $2/h$ decays very fast when $h \to \infty$ (a possible upper bound is of the type $\exp(-ch^3)$). Note that there are of the order of $\sqrt{h} \times h/2$ possibilities for $\tilde{x}$.

Putting the pieces together, we obtain an upper bound of the type

$$\mathbb{P}(\Gamma[-\sqrt{h}, \sqrt{h}] \in [-h/4, h/4] \text{ and } \exists x \in [0, \sqrt{h}],\ S_{x,h} \leq 1) \leq C' h^{3/2} e^{-ch^3}.$$

The upper bound for $\mathbb{P}(\sup_{s \in [0,1]} H_s > h)$ follows. □

III.5.5 Flat initial condition

It is worthwhile to note that for the flat initial conditions i.e. when $\Gamma_0 = 0$, the situation is completely different. Indeed, clearly (H_t) is a non-negative process (so that there is no tail on the negative side...), and it is not possible to use a "favorable" initial profile to help constructing an event where H_1 becomes very large. In fact, the decay rate of the probability that H_1 is large is very different :

Proposition 3.6. *When $h \to \infty$, $\mathbb{P}(H_1 \geq h) = \exp\left(-8h^3/9 + O(\ln(h))\right)$*

Note again that it matches with the tail expansion obtained in [18].

Démonstration. Let us start with the lower bound. Let us study the stopping times S_{0,h_1} and S_{0,h_2} for $h_1 = h + 1/h^2$ and $h_2 = h + 5/h^2$ by (X, H). We would like to find an event that ensures that $S_{0,h_1} < 1$ and that H_t remains above h during a time at least 1 after this moment. We will consider the following four events (here Λ_1 and Λ_2 denote the BW lines that go through $(0, h_1)$ and $(0, h_2)$) :

- $\Lambda_1[-2/h^4, 2/h^4] \subset [h + 1/(2h^2), h + 3/(2h^2)]$.
- $\Lambda_2[-1/h^4, 1/h^4] \subset [h + 9/(2h^2), h + 11/(2h^2)]$.
- Λ_1 and Λ_2 coalesce in the vertical strip above $[1/h^4, 2/h^4]$ and in the vertical strip above $[-2/h^4, -1/h^4]$ (combined with the previous conditions, this implies that the area between Λ_1 and Λ_2 is greater than $6/h^6$ and that $H_t \geq h$ during the corresponding time-interval $[S_{0,h_1}, S_{0,h_2}]$).
- The integral of Λ_1 on the interval $[2/h^4, +\infty)$ and on the interval $(-\infty, -2/h^4]$ both belong to $[1/2 - 2/h^3 - 3/h^6, 1/2 - 2/h^3 - 2/h^6]$.

It is easy to see that $H_1 \geq h$ if those events hold simultaneously. Scaling shows that the probability that the first three are satisfied simultaneously is a constant that does not depend on h. Using the simple Markov property, conditionally on the first events, $(\Lambda_1(2/h^4 + s),\ s \geq 0)$ is a Brownian motion starting at some level in $[h + 1/(2h^2), h + 3/(2h^2)]$. With the expression of the density of the area under a Brownian motion until its first passage time at 0 given in Proposition 3.2-3, we have :

$$P_{h+u/h^2}\left(\int_0^{\tau_0} B_t dt \in [1/2 - 2/h^3 - 3/h^6, 1/2 - 2/h^3 - 2/h^6]\right) \geq \exp\left(-4h^3/9 + O(\ln(h))\right)$$

which is valid uniformly for every $u \in [1/2, 3/2]$.
Therefore,

$$\mathbb{P}(H_1 \geq h) \geq \left(\exp\left(-4h^3/9 + O(\ln(h))\right)\right)^2 = \exp\left(-8h^3/9 + O(\ln(h))\right)$$

For the upper bound, we can adapt the proof of the corresponding bound in the stationary case. The situation is at first sight simpler here, because we do not have to worry about the initial line.

Let us denote the Brownian web with flat initial data by $(\Lambda'_{x,h}, (x, h) \in \mathbb{R} \times \mathbb{R}^*_+)$ and $S'_{x,h}$ the integral of $\Lambda'_{x,h}(\cdot)$ over $\mathbb{R}$. First, notice that symmetry and the tail estimates for X_1 show that it is sufficient to find an upper bound for

$$\mathbb{P}(\exists y \in [0, Ch] \ :\ S'_{y,h} \leq 1)$$

for some given large enough C.

We now divide the interval $[0, Ch]$ into circa Ch^{10} smaller intervals $I_k := [x_k, x_{k+1}] = [k/h^9, (k+1)/h^9]$ and we wish to bound $\mathbb{P}(\exists y \in I_k,\, S'_{y,h} \leq 1)$ for each k.

We are going to consider two cases depending on whether $\Lambda'_{y,h}(I_k) \subset [h-1/h^2, \infty)$ or not :

- If $\Lambda'_{y,h}(I_k) \subset [h-1/h^2, \infty)$, then $\Lambda'_{x_{k+1},h-1/h^2}$ is below $\Lambda'_{y,h}$, so that $S'_{x_{k+1},h-1/h^2} \leq 1$.
- If $\Lambda'_{y,h}(I_k) \not\subset [h-1/h^2, \infty)$, then either the backward line started at $(x_{k+1}, h - 1/(2h^2))$ or the forward line started at $(x_k, h - 1/(2h^2))$ does not stay in $[h - 1/h^2, h)$ during the interval I_k.

The probability of the second case is very small, and can be bounded by a constant times $\exp(-Ch^6)$. The probability of the first case is bounded by the probability that the area under a two-sided Brownian motion starting at the level $h-1/h^2$ until the first hitting times of 0 (on both sides) is less than 1. One can then conclude using the estimate (III.2), and summing over the Ch^{10} values of k (that correspond to another $e^{O(\log(h))}$ term). □

III.5.6 Almost sure fluctuations

Our tail-estimates for H are less precise than those we obtained for X. However, let us say a few words on how to nevertheless deduce information about the almost sure behavior of the process $(H_t, t \geq 0)$:

Corollary 3.7. *There exists four constants $l^+ > 0$, $l_0^+ > 0$, $l^- < 0$ and $l_0^- < 0$ such that almost surely,*

$$\begin{aligned}
&\limsup_{t\to\infty} t^{-1/3}(\ln\ln(t))^{-2/3}\, H_t = l^+\\
&\liminf_{t\to\infty} t^{-1/3}(\ln\ln(t))^{-2/3}\, H_t = l^-\\
&\limsup_{t\to 0} t^{-1/3}(\ln\ln(1/t))^{-2/3}\, H_t = l_0^+\\
&\liminf_{t\to 0} t^{-1/3}(\ln\ln(1/t))^{-2/3}\, H_t = l_0^-.
\end{aligned}$$

Démonstration. Carefully adapting the proofs that we presented for X, we will at first simply prove bounds for the limsups/liminfs and then we will deduce the existence of a limit thanks to a 0-1 law.

Proof of the bounds : Using our tail estimates for the process H yields statements of the following type : There exists two positive finite constants $\tilde{l}$ and $\hat{l}$ such that almost surely

$$\hat{l} \leq \limsup_{t\to\infty} t^{-1/3}(\ln\ln(t))^{-2/3}\, H_t \leq \tilde{l}.$$

The upper bound is a direct consequence of the Borel-Cantelli Lemma, and the lower bound is obtained as in the case of X by considering events that are measurable with

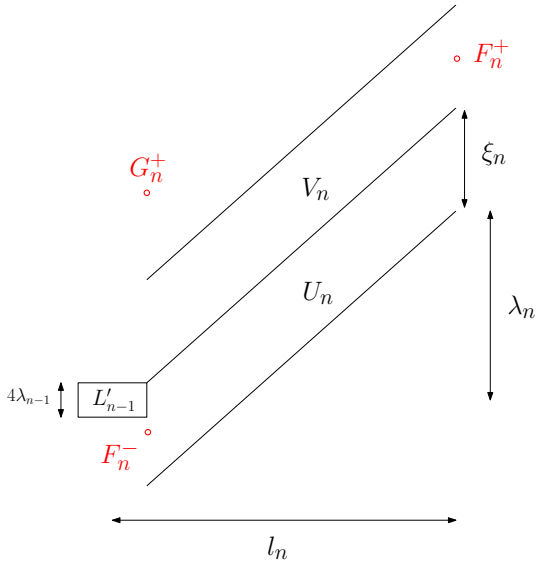

FIGURE III.10 – The three BW curves and the tubes

respect to the information provided by Brownian web restricted to disjoint domains. Let us briefly give the outline of the proof. As it is very similar to the fluctuations of X, we omit the details.

Let us choose a sequence (λ_n) increasing fast, but not too fast either (the sequence $\lambda_n := \lambda^{n(n-1)}$ with $\lambda > 1$ is suitable). It suffices to prove that there exists some absolute constant $c > 0$ such that almost surely, the process H reaches the height λ_n before time $c\,\lambda_n^3/(\ln(\lambda_n))^2$ for infinitely many values of n. For each given n, we will focus on the first time at which the TSRM X reaches the position $Y_{\lambda_n} := \inf\{y \geq 0 \,:\, \Gamma_0(y) = \lambda_n\}$. Clearly, at that random time $\sigma_{Y_{\lambda_n}}$, the height H is equal to λ_n.

Set $l_n := \lambda_n^2/\ln(n)$ and consider the boxes $L'_n := [-l_n, l_n] \times [-2\lambda_n, 2\lambda_n]$. It is easy to see via the Borel-Cantelli Lemma that almost surely, for all but finitely many n, the event

$$\mathcal{D}'_n := \{\Gamma_0[-l_n, l_n] \subset [-2\lambda_n, 2\lambda_n]\}$$

does hold.

We introduce also $\xi_n := \alpha\,\lambda_n/\ln(n)$. Similarly to the proof of the lower bound in III.5.2, we define two parallel upwards-going tubes U_n and V_n such that the bottom line of U_n is the segment joining the points $(l_{n-1}, -\xi_n + 2\lambda_{n-1})$ and (l_n, λ_n) and the vertical width of U_n is ξ_n. The tube V_n is simply the same tube as U_n but shifted vertically by ξ_n such that V_n lies just above U_n. We consider the following three BW-curves : F_n^- the BW-curve starting from $(l_{n-1}, -\xi_n/2)$, F_n^+ the backward BW-curve starting from $(l_n, \lambda_n + 3/2\xi_n)$ and G_n^+ the backward BW-curve starting at $(l_{n-1}, 2\xi_n)$ (see Fig. RéférencesLILH.).

We will now study $\mathcal{A}'_n$ that the following events occurs :

– F_n^- stays in the tube U_n and F_n^+ stays in the tube V_n.
– The integral of $G_n^+ - F_n^-$ over $(-\infty, l_{n-1}]$ is less than ξ_n^3 and G_n^+ and F_n^- do not enter in L'_{n-1}.

Notice that the events $\mathcal{A}'_n$ depend only on BW-curves in $L'_n \backslash L'_{n-1}$ and are therefore independent. Note also that the first event in $\mathcal{A}'_n$ is independent of the second one. The probability of the second event is bounded below by a constant. A similar computation to the proof of the lower bound in III.5.2 permits to deal with the first event and shows that the series $\sum \mathbb{P}(\mathcal{A}'_n)$ diverges. Thus almost surely $\mathcal{A}'_n$ holds infinitely often. Moreover, the values of the sequences ξ_n and l_n and BW monotonicity imply that $\mathcal{A}'_n \cap \mathcal{D}'_{n-1}$ is a sub-event of $\sigma_{Y_{\lambda_n}} \leq c\,\lambda_n^3/(\ln(\lambda_n))^2$ for some $c > 0$ which does not depend on n. It proves the desired bound.

0-1 law : Let us now describe how to use a $0-1$ type argument in order to conclude. We want for instance to show that

$$Z := \limsup_{t\to\infty} \frac{H_t}{t^{1/3}(\ln\ln t)^{2/3}}$$

is almost surely constant (the previous estimates then show that this constant is positive and finite).

Consider for any positive h, the curve $\Lambda_{(0,h)}$ started at height h on the vertical axis. It is the profile at the stopping time corresponding to the first time at which $L_t(0)$ reaches h. Let us denote this random time by ρ_h. We know that $\rho_h \to \infty$ almost surely as $h \to \infty$.

For all $h > 0$, we denote by $\mathcal{G}_h$ the σ-field that contains all the information about the Brownian web above the line $\Lambda_{(0,h)}$. In other words, it is the σ-field generated by this line and by $((X_{t+\rho_h}, H_{t+\rho_h}), t \geq 0)$. Note that Z is therefore $\mathcal{G}_h$ measurable (for all $h > 0$). As $\mathcal{G}_h$ is decreasing with h, it follows that Z is measurable with respect to $\mathcal{G}_\infty := \cap_h \mathcal{G}_h$.

For all positive N, let us now denote by $\mathcal{V}_N$ the σ-field generated by the process (X, H) up to the first time at which $\max(|X|, |H|)$ reaches N. Clearly, this stopping time is almost surely finite and when $N \to \infty$, it converges almost surely to ∞ because (X, H) is a continuous process. Furthermore, any event in $\mathcal{V}_N$ can be read off by looking at the Brownian web lines inside the square $A_N = [-N, N]^2$.

Suppose that N is fixed, that U is a $\sigma(Z)$-measurable event, and that V is $\mathcal{V}_N$ measurable. Suppose furthermore that $W_{h,N}$ is the event that the line $\Lambda_{(0,h)}$ does not intersect $[-N, N]^2$. Clearly, the events $W_{h,N} \cap U$ and V are independent as the former can be read off by looking only at the Brownian web outside of $[-N, N]^2$. On the other hand, we know that $P(W_{h,N}) \to 1$ as $h \to \infty$. Hence,

$$P(U \cap V) = \lim_{h\to\infty} P(U \cap V \cap W_{h,N}) = P(V) \lim_{h\to\infty} P(U \cap W_{h,N}) = P(U)P(V).$$

It follows that U is independent of the σ-field generated by $\cup_N \mathcal{V}_N$, that contains $\sigma(H_t, t \geq 0)$ and therefore also U. Hence, $P(U) = 0$ or $P(U) = 1$.

The proof of the fact that

$$Z' := \limsup_{t \to 0} \frac{H_t}{t^{1/3}(\ln \ln(1/t))^{2/3}}$$

is almost surely constant is similar. We know that almost surely $\rho_h \to 0$ as $h \to 0$, and that H is continuous. It follows that the process $(H_t, t \geq 0)$ is measurable with respect to $\sigma(\cup_h \mathcal{G}_h)$. But for any fixed $h_0 > 0$, the probability that $\Lambda_{(0,h_0)}$ intersects the box $[-1/N, 1/N]^2$ goes to 0 as $N \to \infty$, and on the other hand, we know that Z' is measurable with respect to each $\mathcal{V}_{1/N}$ (because $\rho_{1/N} > 0$). Hence, it follows readily that Z' is independent of $\mathcal{G}_{h_0}$, and then, letting $h_0 \to 0$ that the random variable Z' is independent of itself and therefore constant. □

CHAPITRE IV

Calculs explicites de lois marginales du TSRM

Les résultats de ce chapitre ont été obtenus en collaboration avec Bálint Tóth et ont été accepté pour publication dans le journal *Stochastic Processes and their applications*.

Let $X(t)$ be the *true self-repelling motion (TSRM)* constructed in [59], $L(t,x)$ its occupation time density (local time) and $H(t) := L(t, X(t))$ the height of the local time profile at the actual position of the motion. The joint distribution of $(X(t), H(t))$ was identified in [57] in somewhat implicit terms. Now we give explicit formulas for the densities of the marginal distributions of $X(t)$ and $H(t)$. The distribution of $X(t)$ has a particularly surprising shape (see Picture (IV.1) below): It has a sharp local *minimum* with discontinuous derivative at 0. As a consequence we also obtain a precise version of the large deviation estimate of [16].

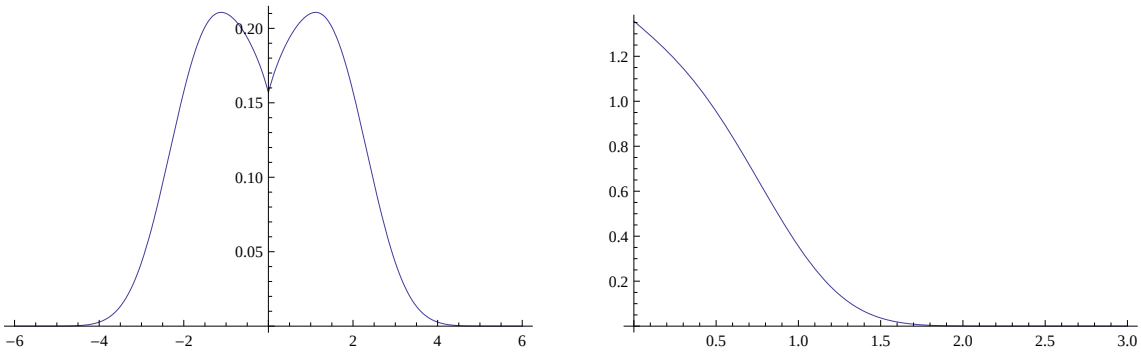

Figure IV.1: Density of $X(1)$ (on the right hand side) and of $H(1)$ (left hand side)

IV.1 Introduction and main results

IV.1.1 Introduction

In the present paper, we study some marginal densities of a self-interacting one dimensional process called the true self-repelling motion (TSRM), defined in [59]. The true self-repelling motion is a continuous real-valued process $(X(t),\ t \geq 0)$ that is locally self-interacting with its past occupation-time: It is pushed away from the places it has visited the most in its past. This process has a completely singular behavior compared to diffusions: For example, it has a finite variation of order 3/2, which contrasts with the finite quadratic variation of semi-martingales.

A crucial property of the TSRM is the existence of a continuous density for its occupation-time measure, denoted $L(t,x)$ and named again "local time" by analogy with semi-martingales (see Theorem 4.2 of [59]). This enables to prove that the TSRM is driven by the negative gradient of its own occupation time density $L(t,x)$. Written *formally*:

$$\partial_t X(t) = -\partial_x L(t, X(t)), \qquad \partial_t L(t,x) = \delta(x - X(t)) \tag{IV.1}$$

$$X(0) = 0, \qquad L(0,x) = 0. \tag{IV.2}$$

The driving mechanism (IV.1) is to be considered in a properly regularized form. Making proper mathematical sense of this mechanism is the main content of [59].

The local time at the current position of the TSRM is denoted by

$$H(t) := L(t, X(t))$$

and is called the *height process*. The processes $X(t)$, the local time $L(t,x)$ and the height $H(t)$ scale as follows:

$$X(at) \sim a^{2/3} X(t), \qquad L(at, a^{2/3}x) \sim a^{1/3} L(t,x), \qquad H(at) \sim a^{1/3} H(t).$$

We will examine in this paper the distributions of the marginals $X(t)$ and $H(t)$ at the fixed time t. It turns out that it is more convenient to work at first with an exponential random time of parameter s independent of the process instead of with a fixed time. With Feynman-Kac formulas applied for the Brownian motion, it is possible to deduce explicit expressions for its marginals (in terms of Airy function, confluent hypergeometric functions and Mittag-Leffler density). It leads to the Pictures IV.1 for $t = 1$. We found the shape of the of the density of the position $X(t)$ rather unusual and surprizing. Indeed, it has a *sharp wedge-like local minimum* at $x = 0$ with discontinuous derivative, and global maxima away from zero. It means that at any positive time, the process still remembers its starting point and it is strongly pushed away from it. These results are also confirmed by numerical simulations (see Figures IV.2. and IV.3.).

IV.1.2 Review of background and notations

The *true self-avoiding walk (TSAW)* is a nearest neighbor random walk with long memory on $\mathbb{Z}^d$ pushed by the negative gradient of its own occupation time measure (local time). For historical background see [3], [45], [46] or the introductions to [57] or [59]. In the present paper we are interested only in the one-dimensional case.

A discrete time version considered and analyzed in [57] is the following. Let $n \mapsto S(n) \in \mathbb{Z}$ be a nearest neighbor walk on $\mathbb{Z}$. The occupation time on lattice bonds, lattice sites, and the negative (discrete) gradient of bond occupation time are in turn:

$$\ell(n, j+1/2) := \#\{0 \le m < n : (S(m) + S(m+1))/2 = j + 1/2\},$$

$$\ell(n, j) := \Big(\ell(n, j-1/2) + \ell(n, j+1/2)\Big)/2,$$

$$\delta(n, j) := \ell(n, j-1/2) - \ell(n, j+1/2),$$

where $j \in \mathbb{Z}$ label lattice sites, $j \pm \frac{1}{2} \in \mathbb{Z} + \frac{1}{2}$ label lattice bonds and $n \in \mathbb{Z}_+$ is the (discrete) time of the process.

The TSAW (with bond repulsion) is defined by the law:

$$\mathbf{P}\Big(S(n+1) = j \pm 1 \;\Big|\; \mathcal{F}_n, S(n) = j\Big) = \frac{w(\pm\delta(n, j))}{w(\delta(n, j)) + w(-\delta(n, j))},$$

where $w : \mathbb{Z} \to (0, \infty)$ is a fixed rate function which is assumed nondecreasing and non-constant. In [57] limit theorem was proved for the distribution of the displacement of the TSAW, with time-to-the-two-thirds scaling. Later, the convergence was established for the whole process [59, 30]. In order to expose this and also prepare our present work we need some notation and preliminary concepts.

Let $\mathbb{R} \ni y \mapsto B(y) \in \mathbb{R}_+$ be a *two sided Brownian motion*, starting from level $h \ge 0$, and let ω' be the first hitting time of zero by the backward Brownian motion, ω_x the first one after time $x \ge 0$ of the forward Brownian motion:

$$\omega' := \sup\{y \le 0 : B(y) = 0\}, \tag{IV.3}$$

$$\omega_x := \inf\{y \ge x : B(y) = 0\}, \qquad x \ge 0, \tag{IV.4}$$

and denote:

$$T_x = \int_{\omega'}^{\omega_x} |B(t)| dt. \tag{IV.5}$$

The random variable T_x is a.s. positive and finite and has an absolutely continuous distribution with density

$$\varrho(t; x, h) := \partial_t \mathbf{P}\Big(T_x < t \;\Big|\; B(0) = h\Big), \qquad t \in \mathbb{R}_+,\ x \in \mathbb{R}_+,\ h \in \mathbb{R}_+.$$

The Laplace transform of this density with respect to the variable t is

$$\hat{\varrho}(s;x,h) := s\int_0^\infty e^{-st}\varrho(t;x,h)dt = s\mathbf{E}\Big(e^{-sT_x}\ \Big|\ B(0)=h\Big). \tag{IV.6}$$

We extend ϱ and $\hat{\varrho}$ to $x\in\mathbb{R}$ as *even* functions: $\varrho(t;x,h)=\varrho(t;|x|,h)$ and $\hat{\varrho}(s;x,h)=\hat{\varrho}(s;|x|,h)$ for all $x\in\mathbb{R}$, $h\geq 0$, $s\geq 0$ and $t\geq 0$. Let us introduce the following marginals:

$$\varrho_1(t;x) := \int_0^\infty \varrho(t;x,h)dh, \qquad \varrho_2(t;h) := \int_{-\infty}^\infty \varrho(t;x,h)dx,$$

$$\hat{\varrho}_1(s;x) := \int_0^\infty \hat{\varrho}(s;x,h)dh, \qquad \hat{\varrho}_2(s;h) := \int_{-\infty}^\infty \hat{\varrho}(s;x,h)dx.$$

Brownian scaling $\Big(B(a\cdot)\ \Big|\ B(0)=\sqrt{a}h\Big) \sim \Big(\sqrt{a}B(\cdot)\ \Big|\ B(0)=h\Big)$ implies the following scaling relations:

$$\varrho(t;x,h)=t^{-1}\nu(t^{-2/3}x,t^{-1/3}h),\quad \varrho_1(t;x)=t^{-2/3}\nu_1(t^{-2/3}x),\quad \varrho_2(t;h)=t^{-1/3}\nu_2(t^{-1/3}h), \tag{IV.7}$$

$$\hat{\varrho}(s;x,h)=s\nu(s^{2/3}x,s^{1/3}h),\qquad \hat{\varrho}_1(s;x)=s^{2/3}\hat{\nu}_1(s^{2/3}x),\qquad \hat{\varrho}_2(s;h)=s^{1/3}\hat{\nu}_2(s^{1/3}h),$$

where

$$\nu(x,h) := \varrho(1;x,h),\qquad \nu_1(x) := \varrho_1(1;x),\qquad \nu_2(h) := \varrho_2(1;h),$$

$$\hat{\nu}(x,h) := \hat{\varrho}(1;x,h),\qquad \hat{\nu}_1(x) := \hat{\varrho}_1(1;x),\qquad \hat{\nu}_2(h) := \hat{\varrho}_2(1;h).$$

We recall the main results of [57] and [59] and more recent large deviation estimates from [16] which are necessary background material for the present paper:

– Theorem 2 of [57]: $(x,h)\mapsto\nu(x,h)$ and $(x,h)\mapsto\hat{\nu}(x,h)$ are probability densities on $\mathbb{R}\times\mathbb{R}_+$:

$$\int_{-\infty}^\infty\int_0^\infty \nu(x,h)dhdx = 1 = \int_{-\infty}^\infty\int_0^\infty \hat{\nu}(x,h)dhdx. \tag{IV.8}$$

– Theorem 3 of [57]: Let $s>0$ be fixed and θ_n a sequence of geometrically distributed stopping times with $\mathbf{E}(\theta_n)=n/s$, independent of the TSAW $S(\cdot)$. The following limit theorem holds:

$$\Big((\alpha n)^{-2/3}S(\theta_n),(\alpha n)^{-1/3}\ell(\theta_n,S(\theta_n))\Big)\Rightarrow\Big(\hat{X}_s,\hat{H}_s\Big),$$

where the density of the joint distribution of $\Big(\hat{X}_s,\hat{H}_s\Big)$ is $\hat{\varrho}(s;x,h)$. The constant α in the norming factors on the left hand side depend only on the rate function $w(\cdot)$ and is given by formula (1.23) in [57].

Actually, in [57] only the case $w(z)=e^{-\beta z}$ was considered and only the limit theorem for the displacement was stated explicitly. However, the proofs implicitly contain these extensions.

– Remark after Theorem 3 of [57]: Assume that the sequence of random variables $\Big(n^{-2/3}S(n), n^{-1/3}\ell(n, S(n))\Big) \in \mathbb{R} \times \mathbb{R}_+$ is tight. Let $t > 0$ be fixed. Then

$$\Big((\alpha n)^{-2/3}S([nt]), (\alpha n)^{-1/3}\ell([nt], S([nt]))\Big) \Rightarrow \Big(X(t), H(t)\Big),$$

where the density of the joint distribution of $\Big(X(t), H(t)\Big)$ is $\varrho(t; x, h)$.

See also [58] for similar results for a continuous time version with on-site-repulsion.

– Finally, in [59] the *true self-repelling motion (TSRM)* introduced in the first paragraph of this paper,

$$t \mapsto X(t) \in \mathbb{R}$$

was constructed. This is the scaling limit of the properly rescaled TSAW, $t \mapsto (\alpha n)^{-2/3}S([nt])$, as $n \to \infty$. It implies that the density of the joint distribution of the position and height processes $(X(t), H(t))$ is exactly

$$\partial^2_{xh}\mathbf{P}\left(X(t) < x, H(t) < h\right) = \varrho(t; x, h).$$

Nevertheless, it is interesting to note that it can be proved directly in the continuous setting thanks to the local time properties established in [59]. Indeed, TSRM's construction immediately gives a strong "Ray-Knight" Theorem concerning its local times at certain random times (see Theorem 4.3 in [59]). Here is a weaker version: For every $(x, h) \in \mathbb{R} \times \mathbb{R}^+_*$, let us denote by $\tau_{x,h}$ the first hitting time of (x, h) by the process $(X(t), H(t))$. Then the local time at time $\tau_{x,h}$ has the distribution of a two sided Brownian motion starting at time x at the level h reflected above the x-line between 0 and x and absorbed by the x-line outside this interval. In particular, it implies that $\tau_{x,h}$ has the distribution of T_x conditionally on $B(0) = h$. Therefore, with the measure preserving change of variable $t = \tau_{x,h}$, we can write for every bounded Borel function f on $\mathbb{R} \times \mathbb{R}^+$,

$$\mathbf{E}\left(f\left(X(\theta_s), H(\theta_s)\right)\right) = s\int_{-\infty}^{+\infty}\int_0^{+\infty} f(x, h)\mathbf{E}\Big(e^{-sT_x} \;\Big|\; B(0) = h\Big)\, dh\, dx.$$

The scaling property readily gives that the density of $(X(t), H(t))$ at $(x, h) \in \mathbb{R} \times \mathbb{R}^+$ is equal to the density of $T_{x,h}$ at time t i.e. $\varrho(t; x, h)$.

– By choosing the initial conditions

$$X(0) = 0, \qquad\qquad L(0, x) = B(x),$$

where $x \mapsto B(x)$ is a two sided 1d Brownian motion, rather than (IV.2), we obtain a version of the TSRM *with stationary increments*. Denote this process

$X_{\rm st}(t)$, its local time $L_{\rm st}(t,x)$, and the height process $H_{\rm st}(t) := L_{\rm st}(t, X_{\rm st}(t))$. The scaling of the stationary version is similar to that of the TSRM starting from initial conditions (IV.2):

$$X_{\rm st}(at) \sim a^{2/3} X_{\rm st}(t), \quad L_{\rm st}(at, a^{2/3}x) \sim a^{1/3} L_{\rm st}(t,x), \quad H_{\rm st}(at) \sim a^{1/3} H_{\rm st}(t),$$

From the construction of TSRM it follows directly that

$$X_{\rm st}(1) \sim 2^{-1/3} X(1). \tag{IV.9}$$

But no distributional similarities of this sort hold for the 1d marginal $H_{\rm st}(1)$.

– In [16], using TSRM's construction, asymptotics for the tails of $X(1)$ and $H(1)$ are found. It is shown that:

$$\begin{aligned} \mathbf{P}\left(X(1) > x\right) &= \exp\left(-(4\delta_1'^3 x^3)/27 + O(\ln(x))\right), \\ \mathbf{P}\left(H(1) > h\right) &= \exp\left(-(8h^3)/9 + O(\ln(h))\right), \end{aligned} \tag{IV.10}$$

where δ_1' is the absolute value of the first negative zero of the derivative of a renormalized Airy function. It is precisely defined in paragraph IV.3.2.
In the stationary case, the tails of the distributions are also computed. In this case, due to (IV.9), the constant in front of the x^3 is multiplied by 2 for $X_{\rm st}(1)$. The height $H_{\rm st}(1)$ behaves differently as the initial local time helps to have large values of $|H_{\rm st}(1)|$. It is shown that there exists $\eta > 0$ such that for every large h:

$$\exp\left(-1/\eta\, h^{3/2}\right) \leq \mathbf{P}\left(\pm H_{\rm st}(1) > h\right) \leq \exp\left(-\eta\, h^{3/2}\right). \tag{IV.11}$$

IV.1.3 Main results

In the present paper, our main goal is to identify the marginal distributions, $\nu_1(x)$ and $\nu_2(h)$ more explicitly than it was done in [57]. Our main results are collected in the following theorem:

Theorem 4.1. *(i) The second marginal densities $\hat{\nu}_2(h)$ and $\nu_2(h)$ are*

$$\hat{\nu}_2(h) = -2u(h)u'(h) = -\partial_h\left(u^2\right)(h), \tag{IV.12}$$

$$\nu_2(h) = \frac{2 \cdot 6^{1/3}\sqrt{\pi}}{\Gamma(1/3)^2} e^{-(8h^3)/9} U(1/6, 2/3; (8h^3)/9), \tag{IV.13}$$

where $u : \mathbb{R}_+ \to \mathbb{R}$ is the (rescaled and normed) Airy function, as defined in subsection IV.3.2, (IV.42), (IV.43), and $U(1/2, 4/3; \cdot)$ is the confluent hypergeometric

function of the second kind (or Tricomi function), given by the integral representation (IV.52) *in subsection IV.3.4.*

(ii) The first marginal densities $\hat{\nu}_1(x)$ *and* $\nu_1(x)$ *are*

$$\hat{\nu}_1(x) = \sum_{k=1}^{\infty} p_k \frac{\delta'_k}{2} \exp(-\delta'_k |x|), \tag{IV.14}$$

$$\nu_1(x) = \sum_{k=1}^{\infty} p_k \frac{\delta'_k}{2} f_{2/3}(\delta'_k |x|), \tag{IV.15}$$

where $f_{2/3}$ *is the Mittag-Leffler density function as defined in subsection IV.3.3, the scaling factors* δ'_k *are the zeros of the derivative of the (rescaled and normed) Airy function* $u(\cdot)$*, and the coefficients* p_k *of the convex combinations are those given in subsection IV.3.2,* (IV.48).

It is worth to compare the computed graphs of these density functions with histograms of the empirical distributions on $X(1)$ and $H(1)$ (see Figures IV.2. and IV.3.).

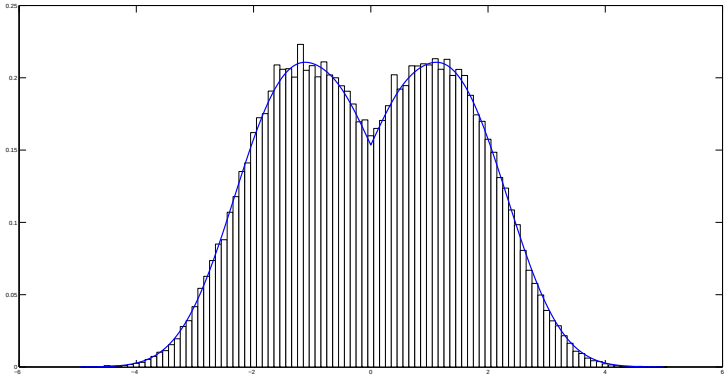

Figure IV.2: The histogram represents a numerical simulation of the TSRM at time one $X(1)$ with a sample of 10^5 independent realizations. Each realization is computed using the discrete "toy-model" introduced in [59] with a step of $2 \cdot 10^{-6}$. The plain blue line is the graph of the density of $X(1)$.

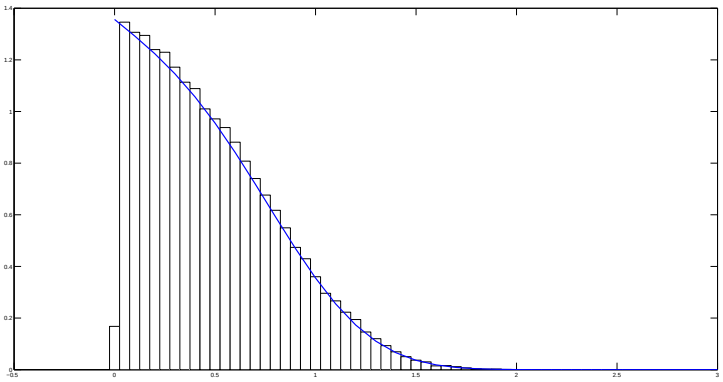

Figure IV.3: The histogram represents a numerical simulation of the height process at time one $H(1)$ (sample of 10^5 independent realizations using discrete "toy-model" with a step of $2 \cdot 10^{-6}$). The plain blue line is the graph of the density of $H(1)$.

The moments of the marginal distributions collected in Theorem 4.1 are as follows

$$\mathbf{E}\left(H(1)^n\right) = \int_0^\infty h^n \nu_2(h) dh = \Gamma(5/6) \frac{(2 \cdot 3^{1/3})^{-n}\, n!}{\Gamma(n/3+1)\Gamma(n/3+5/6)} \tag{IV.16}$$

$$\mathbf{E}\left(|X(1)|^n\right) = 2\int_0^\infty x^n \hat{\nu}_1(x) dx = \sum_{k=1}^\infty p_k \frac{n!}{(\delta_k')^n \Gamma(2n/3+1)}. \tag{IV.17}$$

As a direct consequence of (IV.13) and (IV.15) we also obtain the precise tail asymptotics of $\nu_2(h)$ and $\nu_1(x)$ as $h \gg 1$, respectively, as $|x| \gg 1$:

Corollary 4.2.

$$\lim_{h\to\infty} h^{-3} \log \mathbf{P}\left(H(1) > h\right) = -\frac{8}{9},$$

$$\lim_{x\to\infty} x^{-3} \log \mathbf{P}\left(X(1) > x\right) = -\frac{4}{27}\delta_1'. \tag{IV.18}$$

In view of (IV.9) the tail asymptotics (IV.18) also implies

$$\lim_{x\to\infty} x^{-3} \log \mathbf{P}\left(X_{\mathrm{st}}(1) > x\right) = -\frac{8}{27}\delta_1'.$$

Note that this is matching with the large deviation results of [16]. More precision in the asymptotics can be derived from the expression of the densities.

The structure of further parts of this note is as follows: In section IV.2 we present the proofs of the main statements. Section IV.3 is an Appendix which contains classical ingredients: the Feynman-Kac formulas used, and collections of facts about Airy function, Mittag-Leffler distributions and confluent hypergeometric functions. We do not prove the statements collected in the Appendix but give precise reference for all.

IV.2 Proofs

IV.2.1 Preliminaries

Recall the definitions of T_x, ω_x and ω' ($x \geq 0$) in IV.1.2, (IV.5), (IV.4), and (IV.3). We write

$$T_x = S + T_x^1 + T_x^2,$$

where

$$S := \int_{\omega'}^0 |B(y)|\, dy, \qquad T_x^1 := \int_0^x |B(y)|\, dy, \qquad T_x^2 := \int_x^{\omega_x} |B(y)|\, dy,$$

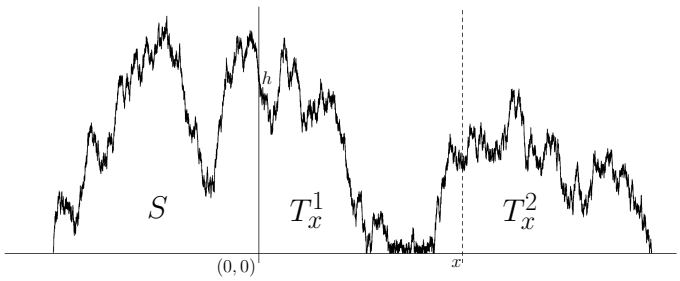

Figure IV.4: Representation of $T_x = S + T_x^1 + T_x^2$

(see Picture IV.4.)

The main ingredients of our investigations are the following three functions:

$$u(h) := \mathbf{E}\Big(e^{-S} \;\Big|\; B(0) = h\Big), \qquad h \geq 0, \tag{IV.19}$$

$$\varphi(x,h) := \mathbf{E}\Big(e^{-T_x^1 - T_x^2} \;\Big|\; B(0) = h\Big), \qquad x \geq 0,\ h \geq 0, \tag{IV.20}$$

$$w(x) := \varphi(x,0) = \mathbf{E}\Big(e^{-T_x^1 - T_x^2} \;\Big|\; B(0) = 0\Big) \qquad x \geq 0.$$

We also define the Laplace transforms (in the variable $x \geq 0$).

$$\tilde{\varphi}(\lambda,h) := \int_0^\infty e^{-\lambda x}\varphi(x,h)dx, \tag{IV.21}$$

$$\tilde{w}(\lambda) := \int_0^\infty e^{-\lambda x} w(x)dx.$$

Remark 4.3. *Note that this is a different type of Laplace transform than the one we used for the time variable. That is why we use different notations (hat for the time transform, tilde for this last one).*

In the following Proposition we collect the basic starting identities. All these follow from straightforward applications of infinitesimal conditioning and/or Feynman-Kac formula.

Proposition 4.4. *(i) The function $u : \mathbb{R}_+ \to [0,1]$ defined in (IV.19) is the unique bounded solution of the boundary value problem*

$$\partial_h^2 u(h) = 2hu(h), \qquad u(0) = 1. \tag{IV.22}$$

That is: It is exactly the normalized Airy function defined and treated in subsection IV.3.2, restricted to $h \in [0,\infty)$.

(ii) The function $\varphi : \mathbb{R}_+ \times \mathbb{R}_+ \to [0,1]$ *defined in* (IV.20) *is the unique bounded solution of the parabolic Cauchy problem*

$$\partial_x \varphi(x,h) = \frac{1}{2}\partial_h^2 \varphi(x,h) - h\varphi(x,h), \tag{IV.23}$$

with initial and boundary conditions

$$\text{IC}: \quad \varphi(0,h) = u(h), \qquad \text{BC}: \quad \partial_h \varphi(x,0) = 0, \quad \textit{for } x > 0. \tag{IV.24}$$

(iii) The function $\hat{\nu} : \mathbb{R}_+ \times \mathbb{R}_+ \to [0,1]$ *is the unique bounded solution of the parabolic Cauchy problem*

$$\partial_x \hat{\nu}(x,h) = \frac{1}{2}\partial_h \left(u(h)^2 \partial_h \left(u(h)^{-2} \hat{\nu}(x,h) \right) \right), \tag{IV.25}$$

with initial and boundary conditions

$$\text{IC}: \quad \hat{\nu}(0,h) = u(h)^2, \qquad \text{BC}: \quad \hat{\nu}(x,0) = w(x) \quad \textit{for } x > 0. \tag{IV.26}$$

Proof of Proposition 4.4.
(i) (IV.22) follows from usual "infinitesimal conditioning".
(ii) By strong Markov property of the Brownian motion

$$\varphi(x,h) = \mathbf{E}\Big(e^{-\int_0^x |B(y)| dy} u(|B(x)|) \;\Big|\; B(0) = h \Big),$$

and thus, we apply the Feynman-Kac formula from subsection IV.3.1, with $V(h) = |h|$ and $f(h) = u(|h|)$. Since for all $x > 0$, $h \mapsto \varphi(x,h)$ is even and smooth, the boundary condition in (IV.24) follows.
(iii) Note that

$$\hat{\nu}(x,h) = u(h)\varphi(x,h), \tag{IV.27}$$

and use (IV.22),(IV.23) and (IV.24).

□

IV.2.2 Computation of $\hat{\nu}_2$

Since

$$\hat{\nu}_2(h) = 2\int_0^\infty \hat{\nu}(x,h)dx,$$

from (IV.25) and (IV.26) we readily get

$$\Big(u(h)^2 \Big(u(h)^{-2} \hat{\nu}_2(h) \Big)' \Big)' = -4u(h)^2. \tag{IV.28}$$

Using the following identities (that directly come from integration by parts and the differential equation of u):

$$\int_0^h u(\chi)^2 d\chi = hu(h)^2 - u'(h)^2/2 + u'(0)^2/2,$$
$$\int_0^h u(\chi)^{-2} u'(\chi)^2 d\chi = -u'(h)/u(h) + u'(0) + h^2,$$

we deduce that the general solution of (IV.28) is

$$-2u(h)u'(h) + C_1 u(h)^2 + C_2 u(h)^2 \int_0^h u(\chi)^{-2} d\chi. \tag{IV.29}$$

From the asymptotics (IV.45) it follows that

$$u(h)^2 \int_0^h u(\chi)^{-2} d\chi \asymp h^{-1/2}, \quad \text{as } h \to \infty.$$

Since, by (IV.8),

$$\int_0^\infty \hat{\nu}_2(h) dh = 1, \tag{IV.30}$$

we must choose $C_2 = 0$. (Otherwise ν_2 wouldn't be integrable.) Finally, due to (IV.30) again, $C_1 = 0$, too. The proof of (IV.12) is completed.

Remark 4.5. *The interchange between integration and differentiation used to obtain* (IV.28) *is standard. One can justify it properly by taking the integral over a compact interval of the type* $[0, x]$ *first and deduce an expression for this function of a similar kind of* (IV.29)*. Taking the limit* $x \to \infty$ *gives the result.*

IV.2.3 Computation of ν_2

Due to (IV.6) and (IV.7) $\nu_2(h)$ and $\hat{\nu}_2(h)$ are related by

$$\hat{\nu}_2(h) = \int_0^\infty e^{-t} t^{-1/3} \nu_2(t^{-1/3} h) dt. \tag{IV.31}$$

The goal of the present subsection is inverting this integral transform.

By straightforward computations – performing a change of variables and an integration by parts – form (IV.12) and (IV.31) we obtain

$$u^2(z^{1/3}) = \frac{1}{3} \int_0^\infty e^{-sz} \nu_2(s^{-1/3}) s^{-4/3} ds,$$

and hence

$$\nu_2(h) = 3h^{-4} (f * f)(h^{-3}), \tag{IV.32}$$

where f is the inverse Laplace transform of the function $z \mapsto u(z^{1/3})$:

$$u(z^{1/3}) = \int_0^\infty e^{-hs} f(s) ds,$$

and $*$ stands for convolution on $[0, \infty)$.

In the following computations we denote generically by C a multiplicative constant. The value of this may change from line to line. These constants could be written explicitly in each step, but this wouldn't be much illuminating. The value of the norming constant in (IV.13) will be identified at the very end of the computations.

The function f is explicitly known, see [40]:

$$f(s) = C s^{-4/3} e^{-2/(9s)}.$$

Thus,

$$\begin{aligned} f * f(s) &= C \int_0^s \Big(t(s-t)\Big)^{-4/3} e^{-(2s)/(9t(s-t))} dt \\ &= C s^{-5/3} \int_0^1 \Big(t(1-t)\Big)^{-4/3} e^{-2/(9st(1-t))} dt \\ &= C s^{-5/3} e^{-8/(9s)} \int_0^\infty (1+z)^{-1/6} z^{-1/2} e^{-8z/(9s)} dz \\ &= C s^{-5/3} e^{-8/(9s)} U(1/2, 4/3; 8/(9s)). \\ &= C s^{-4/3} e^{-8/(9s)} U(1/6, 2/3; 8/(9s)). \end{aligned} \tag{IV.33}$$

In the third line we perform the change of integration variable $(t(1-t))^{-1} =: 4(1+z)$. Finally, in the last step we apply Kummer's identity (IV.53).

From (IV.32) and (IV.33) we readily get

$$\nu_2(h) = C e^{-(8h^3)/9} U(1/6, 2/3; (8h^3)/9).$$

Identification of the norming constant C in the last expression follows from (IV.12), (IV.44) and (IV.31):

$$\begin{aligned} 2^{4/3} 3^{1/3} \Gamma(2/3) \Gamma(1/3)^{-1} &= \hat{\nu}_2(0) = \Gamma(2/3) \nu_2(0) \\ &= C \Gamma(2/3) U(1/6, 2/3; 0) = C \Gamma(2/3) \Gamma(1/3) / \Gamma(1/2). \end{aligned}$$

Hence (IV.13).

IV.2.4 Computation of $\hat{\nu}_1$

Recall the definition of $\hat{\nu}_1$:

$$\hat{\nu}_1(x) = \int_0^\infty \hat{\nu}(x,h)dh.$$

Let us examine the case $x > 0$ (the function $\hat{\nu}_1$ is even). Using (IV.27) we readily obtain

$$\begin{aligned}\partial_x \hat{\nu}_1(x) &= \frac{1}{2}\int_0^\infty \partial_h \left(u(\chi)\partial_h\varphi(x,\chi) - u'(\chi)\varphi(x,\chi)\right) d\chi \\ &= \frac{1}{2}\left(u'(0)w(x) - u(0)\partial_h\varphi(x,0)\right). \end{aligned} \tag{IV.34}$$

Remark 4.6. *Again, the interchange between integration and differentiation is classical. Note first that for every $x \geq 0$, $\partial_h\varphi(x,h) \to 0$ when $h \to \infty$: It admits a finite or infinite limit (integrating (IV.23) with respect to h, one can see that the terms involved admits finite or infinite limits – recall $\partial_x\varphi(x,h)$ is negative) and its integral is finite. One can then integrate $\partial_x\hat{\nu}(x,h)$ first on $[0,h]$ and obtain an expression for $\int_0^h u(\chi)\varphi(x,\chi)d\chi$. Taking $h \to \infty$ and using $\lim_{h\to\infty}\partial_h\varphi(x,h) = 0$ rigorously prove (IV.34).*

Notice that we have $\partial_h\varphi(x,0) = 0$ for every x (see (IV.24)). The following lemma will serve to compute $w(x)$ on the right hand side of (IV.34).

Lemma 4.7. *The function $\tilde{\varphi} : \mathbb{R}_+ \times \mathbb{R}_+ \to \mathbb{R}$ defined in (IV.21) is expressed as*

$$\begin{aligned}\tilde{\varphi}(\lambda,h) = \frac{-1}{u(\lambda)u'(\lambda)}\Big\{ & u(\lambda+h)\int_0^\infty u(\lambda+\chi)u(\chi)d\chi \\ & + u(\lambda+h)\int_0^h v_\lambda(\lambda+\chi)u(\chi)d\chi \\ & + v_\lambda(\lambda+h)\int_h^\infty u(\lambda+\chi)u(\chi)d\chi \Big\},\end{aligned} \tag{IV.35}$$

where $v_\lambda : \mathbb{R} \to \mathbb{R}$ is the solution of the Airy equation (IV.42) with initial conditions

$$v_\lambda(\lambda) = u(\lambda), \qquad v'_\lambda(\lambda) = -u'(\lambda). \tag{IV.36}$$

Proof of Lemma 4.7. Let $v_\lambda : \mathbb{R} \to \mathbb{R}$ be the solution of (IV.42) with boundary conditions (IV.36) and

$$\begin{aligned}\phi_+(\lambda,h) &:= u(\lambda+h)\mathbf{1}h \geq 0 + v_\lambda(\lambda-h)\mathbf{1}h < 0, \\ \phi_-(\lambda,h) &:= \phi_+(\lambda,-h).\end{aligned}$$

Then $\phi_\pm(\lambda,\cdot)$ are exactly the unique solutions of (IV.40), with $V(h) = |h|$, such that $\lim_{h\to\pm\infty}\phi_\pm(\lambda,h) = 0$. Applying (IV.41) we readily obtain (IV.35). □

Using now (IV.35), we obtain

$$\begin{aligned}\tilde{w}(\lambda) = \tilde{\varphi}(\lambda, 0) &= \frac{-2}{u'(\lambda)} \int_0^\infty u(\lambda+\chi)u(\chi)d\chi \\ &= \frac{-1}{\lambda u'(\lambda)} \int_0^\infty \Big(u''(\lambda+\chi)u(\chi) - u(\lambda+\chi)u''(\chi)\Big)d\chi \\ &= \frac{-1}{\lambda u'(\lambda)} \int_0^\infty \Big(u'(\lambda+\chi)u(\chi) - u(\lambda+\chi)u'(\chi)\Big)'d\chi \\ &= \frac{u'(\lambda) - u'(0)u(\lambda)}{\lambda u'(\lambda)}. \end{aligned} \tag{IV.37}$$

In the first step we have used (IV.35), in the second step the Airy equation (IV.42). Now, using the key identity (IV.46) and the trace formula (IV.47), from (IV.37) we derive

$$\tilde{w}(\lambda) = \frac{|u'(0)|}{2} \sum_{k=1}^\infty (\delta_k')^{-2} \frac{1}{\delta_k' + \lambda},$$

and hence

$$w(x) = \frac{|u'(0)|}{2} \sum_{k=1}^\infty (\delta_k')^{-2} e^{-\delta_k' x}. \tag{IV.38}$$

Finally, (IV.34), (IV.26) and (IV.38) yield (IV.14).

IV.2.5 Computation of ν_1

Due to (IV.6) and (IV.7) $\nu_1(x)$ and $\hat{\nu}_1(x)$ are related by

$$\hat{\nu}_1(x) = \int_0^\infty e^{-t} t^{-2/3} \nu_1(t^{-2/3}x)dt.$$

The goal of the present subsection is inverting this integral transform. Since $\hat{\nu}_1(x)$ is convex combination of scaled exponentials, we only have to compute the inverse transform of the exponential density. Assume

$$e^{-x} = \int_0^\infty e^{-t} t^{-2/3} \phi(t^{-2/3}x)dt, \qquad x \geq 0.$$

Writing the integer moments of both sides, by elementary computations we obtain

$$\int_0^\infty \phi(x) x^n dx = \frac{n!}{\Gamma(2n/3+1)}.$$

This identifies ϕ as the Mittag-Leffler density $f_{2/3}$ from (IV.51) and (IV.54) thanks to (IV.50). Hence (IV.15).

IV.3 Appendix:

IV.3.1 Feynman-Kac formulas

According to the present context we formulate the Feynman-Kac formulas only for the one-dimensional Brownian motion. For the general theory of Feynman-Kac formulas see e.g. [38], [39], or [52].

Let $y \mapsto B(y)$ be a standard 1-dimensional Brownian motion which starts from level $B(0) = h \in \mathbb{R}$, and $V : \mathbb{R} \to \mathbb{R}_+$ and $f : \mathbb{R} \to \mathbb{R}$ be continuous functions. Assume that f is also bounded. Define

$$g(x,h) := \mathbf{E}\Big(e^{-\int_0^x V(B(y))dy} f(B(x)) \;\Big|\; B(0) = h\Big), \qquad x \geq 0,$$

$$\tilde{g}(\lambda,h) := \int_0^\infty e^{-\lambda x} g(x,h)dx, \qquad \lambda > 0.$$

Theorem 4.8. *[The Feynman-Kac formula for 1-d Brownian motion]*
(i) $(x,h) \mapsto g(t,x)$ is the unique bounded solution of the parabolic Cauchy problem

$$\partial_x g(x,h) = \frac{1}{2}\partial_h^2 g(x,h) - V(h)g(x,h), \qquad g(0,h) = f(h).$$

(ii) For $\lambda > 0$ fixed, $h \mapsto \tilde{g}(\lambda,h)$ is the unique bounded solution of the elliptic PDE

$$\frac{1}{2}\partial_h^2 \tilde{g}(\lambda,h) = \Big(V(h) + \lambda\Big)\tilde{g}(\lambda,h) - f(h). \tag{IV.39}$$

(iii) Fix $\lambda > 0$ and let $\phi_\pm(\lambda,\cdot) : \mathbb{R} \to \mathbb{R}$ be the unique solutions of the ODE

$$\frac{1}{2}\partial_h^2 \phi(h) = \Big(V(h) + \lambda\Big)\phi(h), \tag{IV.40}$$

for which which $\lim_{h\to\pm\infty} \phi_\pm(\lambda,h) = 0$. (The convergence is actually at least exponentially fast.) Then the unique bounded solution of (IV.39) is expressed as:

$$\begin{aligned}\tilde{g}(\lambda,h) =& 2\Big(\phi_+(\lambda,0)\phi'_-(\lambda,0) - \phi_-(\lambda,0)\phi'_+(\lambda,0)\Big)^{-1} \\ &\times \left\{\phi_+(\lambda,h)\int_{-\infty}^h \phi_-(\lambda,\chi)f(\chi)d\chi - \phi_-(\lambda,\chi)\int_h^\infty \phi_+(\lambda,\chi)f(\chi)d\chi\right\}.\end{aligned} \tag{IV.41}$$

For a full proof of these statements see e.g. [36].

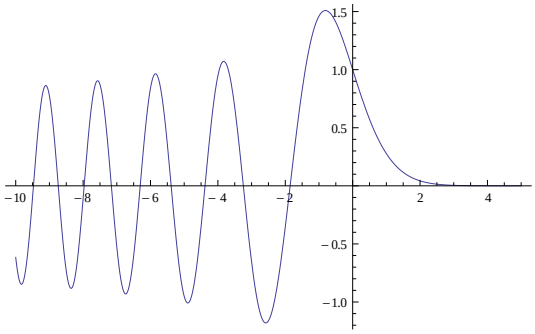

Figure IV.5: The normalized Airy function u

IV.3.2 Airy functions

In the present Appendix we collect the *necessary minimum* information about Airy function needed and used in this paper. For an exhaustive treatment of Airy functions see [1], [28], [40], [50].

Consider the second order linear ODE for $f : \mathbb{R} \to \mathbb{R}$:

$$f''(h) = 2hf(h), \tag{IV.42}$$

commonly called Airy's equation. We denote by $u : \mathbb{R} \to \mathbb{R}$ the unique solution of (IV.42) with boundary conditions

$$u(0) = 1, \qquad \lim_{h\to\infty} u(h) = 0. \tag{IV.43}$$

In terms of the conventionally defined Airy function of the first kind $\mathrm{Ai}(\cdot)$ we have

$$u(h) = 3^{2/3}\Gamma(2/3)\mathrm{Ai}(2^{1/3}h),$$

and we also have

$$u'(0) = -\frac{6^{1/3}\Gamma(2/3)}{\Gamma(1/3)}, \tag{IV.44}$$

$$u(h) \sim \frac{3^{2/3}\Gamma(2/3)}{2^{13/12}\sqrt{\pi}} h^{-1/4} \exp\left(-(2^{3/2}/3)h^{3/2}\right), \qquad \text{as } h \to \infty \tag{IV.45}$$

$$u(h) \sim \frac{3^{2/3}\Gamma(2/3)}{2^{1/12}\sqrt{\pi}} |h|^{-1/4} \sin\left((2^{3/2}/3)\,|h|^{3/2} + \pi/4\right), \qquad \text{as } h \to -\infty.$$

The function $u : \mathbb{R} \to \mathbb{R}$ is convex and decreasing on $[0, \infty)$ and oscillates indefinitely on $(-\infty, 0]$. The function u extends as an entire function to $\mathbb{C} \ni z \mapsto u(z) \in \mathbb{C}$.

We denote by δ'_k, $k = 1, 2, \ldots$ the consecutive zeros of $h \mapsto u'(-h)$. It is known that

$$0 < \delta'_1 < \delta'_2 < \cdots < \delta'_k < \ldots,$$

and their asymptotics, as $k \to \infty$, are

$$\delta'_k \sim \frac{1}{2}(3\pi k)^{2/3}.$$

(Finer asymptotics are also available but not needed for our purposes in this paper.)

The following key identity holds

$$\frac{u''(z)}{u'(z)} = -\sum_{k=1}^{\infty} \frac{1}{\delta'_k} \cdot \frac{z}{\delta'_k + z}, \qquad z \notin \{-\delta'_k : k = 1, 2 \ldots\}. \tag{IV.46}$$

It is easily seen that the sum on the right hand side is absolutely convergent and the two sides have simple poles at $-\delta'_k$, $k = 1, 2, \ldots$, with the same residues. Thus, the two sides can differ in an entire function only. For a full proof of this formula see [28].

From (IV.46) an infinite family of *trace formulas* for $\sum_{k=1}^{\infty}(\delta'_k)^{-n}$ $(n \geq 2)$ are expressed in terms of $u'(0)$. We will use only the first three of these:

$$\sum_{k=1}^{\infty}(\delta'_k)^{-2} = \frac{-2}{u'(0)}, \qquad \sum_{k=1}^{\infty}(\delta'_k)^{-3} = 2, \qquad \sum_{k=1}^{\infty}(\delta'_k)^{-4} = \frac{2}{u'(0)^2}. \tag{IV.47}$$

These are easily checked by differentiating both sides of (IV.47) at $z = 0$ and using (IV.42). We will denote

$$p_k := \frac{u'(0)^2}{2}(\delta'_k)^{-4}. \tag{IV.48}$$

Note that $\sum_{k=1}^{\infty} p_k = 1$.

IV.3.3 Mittag-Leffler distributions

Following the terminology of [25] and [15], we will call Mittag-Leffler distribution of index $\alpha \in [0, 1]$ the probability distribution $F_\alpha : \mathbb{R}_+ \to [0, 1]$ whose moment generating function (Laplace transform) is

$$\int_0^{\infty} e^{-yx} dF_\alpha(x) = \sum_{k=0}^{\infty} \frac{(-y)^k}{\Gamma(\alpha k + 1)} =: E_\alpha(-y). \tag{IV.49}$$

The function $y \mapsto E_\alpha(y)$ defined by the power series in (IV.49) is the Mittag-Leffler function of index $\alpha \in [0, 1]$. It is proved in [47] – where reference is also made to unpublished alternative proof of W. Feller – that, for $\alpha \in [0, 1]$, $[0, \infty) \ni y \mapsto E_\alpha(-y)$ is indeed completely monotone, and thus the Laplace transform of a probability density function on $\mathbb{R}_+$.

The moments of the Mittag-Leffler distributions are

$$\int_0^\infty x^m dF_\alpha(x) = \frac{m!}{\Gamma(\alpha m + 1)}. \tag{IV.50}$$

$\alpha = 0, \frac{1}{2}, 1$ are special cases:

$$F_0(x) = 1 - e^{-x}, \qquad F_{1/2}(x) = \sqrt{\frac{2}{\pi}} \int_0^x e^{-y^2/2} dy, \qquad F_1(x) = \mathbf{1}x > 1.$$

For $\alpha \in [0, 1)$ the distribution function F_α is smooth and the following power series expansion holds for the density function $f_\alpha(x) := F'_\alpha(x)$, see [47]:

$$f_\alpha(x) = \frac{1}{\pi} \sum_{k=0}^{\infty} \frac{\sin((k+1)\alpha\pi)\Gamma((k+1)\alpha)}{k!}(-x)^k \tag{IV.51}$$

This power series defines actually an entire function on $\mathbb{C}$. See the picture below for a representation of those functions with $\alpha = 0, 1/2$ and $2/3$.

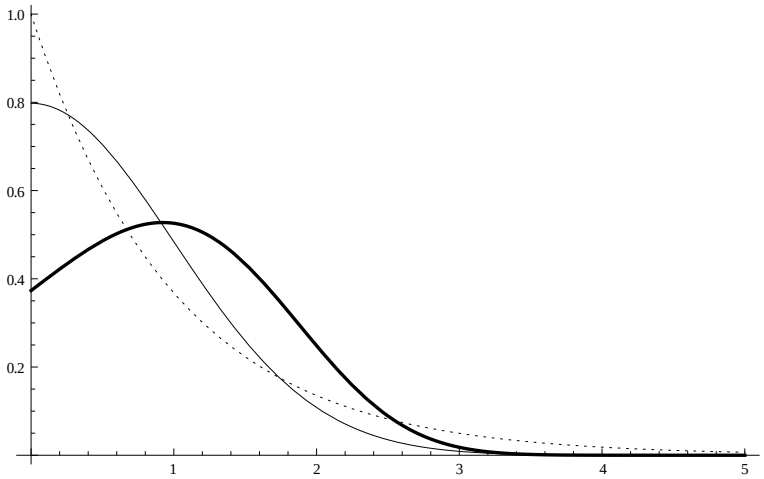

Figure IV.6: Mittag-Leffler density functions for $\alpha = 0$ (dotted), $\alpha = 1/2$ (plain) and $\alpha = 2/3$ (thick)

We are interested in the case $\alpha = 2/3$. This particular case is also expressed in terms of a confluent hypergeometric function, see (IV.54) below.

IV.3.4 Confluent hypergeometric functions

See [33], [1] for details on confluent hypergeometric functions. We collect here only a few facts needed for our purposes.

Let $a > 0$ and $b \in \mathbb{R}$ be fixed parameters. We define the *confluent hypergeometric functions of the second kind*, or *Tricomi functions*

$$U(a, b; \cdot) : \mathbb{R}_+ \mapsto \mathbb{R}$$

by the integrals

$$U(a,b;z)=\frac{1}{\Gamma(a)}\int_0^\infty e^{-zs}s^{a-1}(1+s)^{b-a-1}ds. \tag{IV.52}$$

(For more general definitions see [33], [1].) In our formulas the particular cases $U(1/6,2/3;\cdot)$, $U(1/2,4/3;\cdot)$, and $U(1/6,4/3;\cdot)$ will occur.

Kummer's identity

$$U(a,b;z)=z^{1-b}U(1+a-b,2-b,z) \tag{IV.53}$$

holds if $b>a+1$.

The Mittag-Leffler density function $f_{2/3}$, which appears in (IV.15) is also expressed in terms of $U(1/6,4/3;\cdot)$ as follows:

$$f_{2/3}(z)=\frac{2^{1/3}}{\sqrt{3\pi}}z\,e^{-(4z^3)/27}U(1/6,4/3;(4z^3)/27). \tag{IV.54}$$

Computing the moments of the right hand side of (IV.54) we obtain the expressions (IV.50).

Acknowledgements: The following grant supports are acknowledged: French-Hungarian Balaton/PHC grant 19482NA for mobility support; TÁMOP - 4.2.2.B-10/1–2010-0009 supporting research at the Graduate School of Mathematics TU Budapest; OTKA K100473 partially supporting BT's research.

CHAPTER V

Un voleur (auto-répulsif) astucieux

Les résultats de ce chapitre ont été publiés dans *Electronic Journal of Probability*.

We derive the following property of the "true self-repelling motion", a continuous real-valued self-interacting process $(X_t, t \geq 0)$ introduced by Bálint Tóth and Wendelin Werner. Conditionally on its occupation time measure at time one (which is the information about how much time it has spent where before time one), the law of X_1 is uniform in a certain admissible interval. This interval can be much shorter than the interval of its visited points but it has a positive probability (that we compute) to be this whole set. All this contrasts with the corresponding conditional distribution for Brownian motion that had been studied.

V.1 Introduction

The true self-repelling motion (TSRM) is a continuous real-valued process $(X_t, t \geq 0)$ constructed by Bálint Tóth and Wendelin Werner in [59], that is locally self-interacting with its past occupation-time measure. It can be understood as the scaling limit of certain discrete self-repelling integer-valued random walks.

One of the key-features of TSRM, that in fact enables its construction, is that almost surely, at any given time $t \geq 0$, its occupation time measure μ_t on $\mathbb{R}$ defined by

$$\mu_t(I) = \int_0^t 1_{X_s \in I} ds$$

for all intervals I, has a continuous density $\Lambda_t(x)$ with respect to the Lebesgue

measure:

$$\mu_t(I) = \int_I \Lambda_t(x)\, dx.$$

In other words, if the walker X walks with a bag that continuously loses sand, then after time t, the sand profile (given by $x \mapsto \Lambda_t(x)$) is a continuous function. Recall that such a property is true for Brownian motion, but that it fails to be true for smooth evolutions $t \mapsto X_t$ (as it would create a discontinuity of the sand profile – also referred to as the local time profile – at the point X_t).

The process $(X_t, t \geq 0)$ is interesting because its paths are of a very different type than Brownian motion (they do not have a finite quadratic variation for instance). It will turn out to be relevant for the present paper to note that X does almost surely have times of local increase: There almost surely exist (many) positive times s such that for some positive ϵ, one has $X_{s-v} < X_s < X_{s+v}$ for all $v \leq \epsilon$. Recall that this is almost surely never the case for Brownian motion (see [12] and the references therein). Hence, it follows easily that with positive probability, there will exist exceptional times $s \in (0, 1)$ such that

$$X_v < X_s < X_w$$

for all $0 \leq v < s < w \leq 1$. By symmetry, because X and $-X$ are identically distributed, the same holds for time of decrease.

The position X_s corresponding to such times s can be detected by looking at the local time profile at time 1. Indeed, they are exactly those points in the support S of the local time profile, for which $\Lambda_1(x) = 0$. Suppose that the local time profile Λ_1 is given and contains such points. They are exceptional (their Lebesgue measure is null) and a.s. the process cannot go fast two times through the same point (it is not possible to have $\Lambda_1(x) = 0$ for points x visited more than once by the process before time 1). Therefore, $X_0 = 0$ and X_1 have to be on different sides of each of these points x. Hence, it follows that necessarily, the position X_1 is located in the subinterval I of S that is separated from 0 by all these cut-points. When there are no cut-points (and this happens with a positive probability we will compute in Section V.4), we define I to be the entire support S. The observation of $\Lambda_1(\cdot)$ therefore limits the possible values of X_1 to I. The goal of the present paper is to prove that:

Theorem 5.1. *The conditional distribution of X_1 given $\Lambda_1(\cdot)$ is the uniform distribution in the interval I.*

This may at first seem quite surprising. Indeed, it for instance means that the conditional distribution depends only on I and not on the actual local time profile in I. On the other hand, we will see that this is a rather natural feature of TSRM, inherited from properties of a family of coalescing Brownian motions.

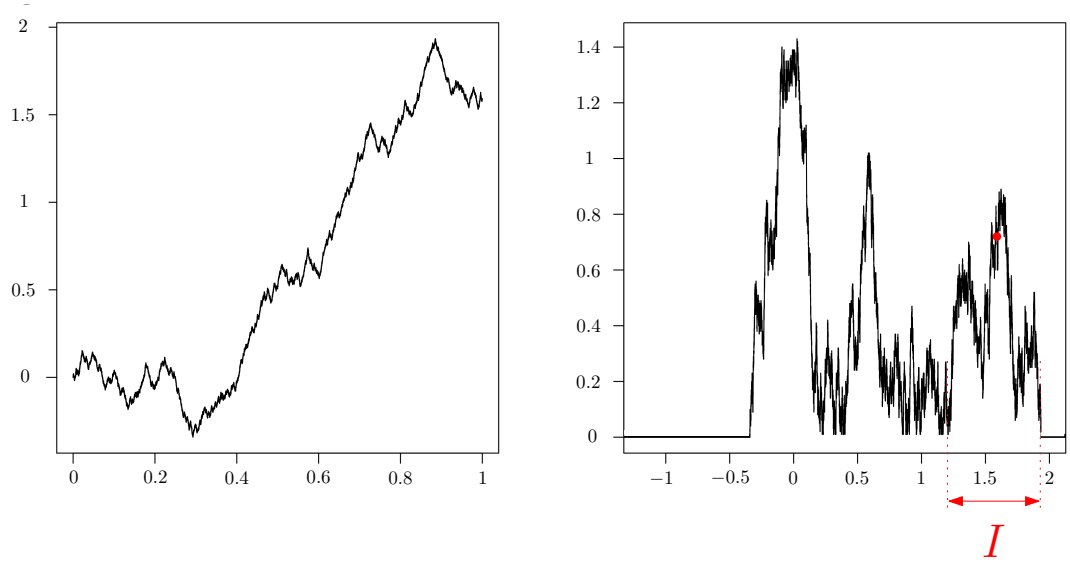

Figure V.1: Sample of the TSRM trajectory until $t = 1$ and of its local time profile at time 1.

This type of question was already studied in the case of Brownian motion by Warren and Yor in [65] and later also by Aldous in [2]. The resulting distribution (of the position of the Brownian motion given its local time) was called "Brownian burglar" because one can imagine that someone is trying to find a burglar moving like a Brownian motion and that the only piece of information one knows is the places he has previously robbed (or how many hotel bills he has paid etc.). We can keep here the same picture in mind except this self-repelling burglar is somehow more clever, because he manages to leave very little information behind. It is in fact a natural question to ask whether it is possible to find processes of a different kind with a similar property.

The TSRM is directly defined in the continuous setting without reference to a discrete model. It is in fact not so easy to prove that discrete self-repelling walks converge to the TSRM in strong topologies (see Newman and Ravinshankar [43]). But some of the properties related to TSRM are rather tricky to derive directly in the continuous setting, while their discrete counterparts are easy. A natural route to deriving them is therefore to control such a property in the scaling limit (when the discrete model tends to TSRM); See for instance [53] for a use of such invariance principles for the derivation of the joint law of local times measures at different stopping times. This is also the approach that we will use in the present paper.

However, as we will see, some minor complications pop up due to the fact that the result corresponding to Theorem 5.1 in the discrete setting fails to be exactly

true (it will hold only up to an error term that vanishes in the scaling limit). In view of this, it will be convenient to randomize time instead of considering the fixed time 1, and we will in fact establish the following variant of Theorem 5.1:

Theorem 5.2. *Suppose that τ is an exponential random variable with mean 1 that is independent of the TSRM X. Then, the conditional distribution of X_τ given $\Lambda_\tau(\cdot)$ is the uniform distribution in the interval I_τ.*

Here I_t is the obvious generalization at time t of I. The scaling property of TSRM i.e., the fact that for any positive A, $(X_{At}, t \geq 0)$ has the same law as $(A^{2/3}X_t, t \geq 0)$ together with the fact that τ can be read off from $\Lambda_\tau(\cdot)$ (it is the area under this curve) shows immediately that this statement is equivalent to Theorem 5.1.

V.2 The result in the discrete setting

Let us now describe a discrete self-repelling random walk $(\tilde{X}_n, n \geq 0)$ on the integers introduced in §11 of [59], that we will use in the present paper, and establish the discrete analog of Theorem 5.2 for this walk. Note that other self-repelling walks do also converge to the TSRM (e.g. the Amit-Parisi-Peliti true self-avoiding walk [3]) but this one turns out to be very convenient for our purposes because its "local times" form a simple discrete web. It can be defined in two equivalent ways that we now briefly review.

Self-interacting random walk definition. The first approach is to view $(\tilde{X}_n, n \geq 0)$ as a self-interacting random walk. Throughout the paper, we will view the set $E = \mathbb{Z} + 1/2$ as the set of edges that join two consecutive integers. For all $n \in \mathbb{N}$ and $e \in E$, let $l(n, e)$ denotes the number of jumps along the edge e before the n-th step:

$$l(n, e) = \#\left\{k \in \{0, \cdots, n-1\},\ \{\tilde{X}_k, \tilde{X}_{k+1}\} = \{e - 1/2, e + 1/2\}\right\}.$$

In fact, it is convenient to define a slight modification $\ell_n(e)$ of $l(n, e)$ by

$$\ell_n(e) = l(n, e) + a(e)$$

where $a(e)$ is equal to 0 or -1 depending on whether $|e| - 1/2$ is even or odd, respectively.

The law of the random walk $(\tilde{X}_n)$ is then defined inductively as follows: $\tilde{X}_0 = 0$ and for all $n \geq 0$, if we define

$$\ell_n^- := \ell_n(\tilde{X}_n - 1/2) \text{ and } \ell_n^+ := \ell_n(\tilde{X}_n + 1/2)$$

to be the slightly modified local times on the edges neighboring $\tilde{X}_n$, then

$$\mathbb{P}\left(\tilde{X}_{n+1} = \tilde{X}_n + 1 | \tilde{X}_0, \cdots, \tilde{X}_n\right) = 1 - \mathbb{P}\left(\tilde{X}_{n+1} = \tilde{X}_n - 1 | \tilde{X}_0, \cdots, \tilde{X}_n\right)$$
$$= \begin{cases} 1 & \text{if} \quad \ell_n^- > \ell_n^+ \\ 1/2 & \text{if} \quad \ell_n^- = \ell_n^+ \\ 0 & \text{if} \quad \ell_n^- < \ell_n^+ \end{cases}$$

In other words, at step n, the walk chooses to jump along the neighboring edge it has visited less often in the past (modulo the initializing term a), and in case $\ell_n^+ = \ell_n^-$, it tosses a fair coin to choose its direction.

It is important to remark that the initial state a is chosen in such a way that one has $|a(e) - a(e+1)| = 1$ for all $e \in E \setminus \{\tilde{X}_0 - 1/2\} (= E \setminus \{-1/2\})$ and $a(-1/2) = a(1/2)$, and this rule perpetuates: $|\ell(n,e) - \ell(n,e+1)| = 1$ for all $n \in \mathbb{N}$ and all $e \in E$ except one, which is the edge $e = \tilde{X}_n - 1/2$. At this point, we have $\ell(n,e) - \ell(n,e+1) \in \{-2, 0, 2\}$. Thus, with such an initial condition, $\tilde{X}$ can be read off from ℓ (therefore, ℓ is Markov). The initial condition a is the "flattest" condition one can define which follows those rules. This particular type of initial condition avoids some artificial deterministic behavior such as the one we would obtain by making the initial local time null everywhere (in this case the walk would go deterministically in the direction of its first choice). Note that one can consider other natural initializations a (such as the i.i.d. case, when $(a(k+1/2), k \in \mathbb{N})$ and $(a(-k-1/2), k \in \mathbb{N})$ are random and follow independent simple random walks starting at 0, which also observes the ± 1 rule with one spot where the gradient is -2, 0, or 2), that will converge to TSRM with another initial condition (the i.i.d case converges towards the "stationary" TSRM defined in §10 of [59]).

Second approach. It turns out (and this is very simple to check, see §11 of [59]) that this walk can also be interpreted in terms of a path that walks through a simple two-dimensional labyrinth in the upper half-plane. Let us write $\mathbb{N}^\# := \mathbb{N} \cup \{-1\}$ and let F and B be the lattices:

$$F := \{(x - 1/2, h) \in (\mathbb{Z} - 1/2) \times \mathbb{N}^\# \ : \ x + h \text{ is odd}\},$$
$$B := ((\mathbb{Z} - 1/2) \times \mathbb{N}^\#) \setminus F.$$

We divide the upper half-plane into 1×2 rectangles of the type $(x-1/2, x+1/2) \times (h-1, h+1)$ for $(x-1/2, h) \in F$. In each rectangle associated with $(x-1/2, h) \in F$ such that $h \notin \{-1, 0\}$, we toss independently a fair coin in order to choose between the two fillings depicted in Figure V.2: Either we draw two diagonally upwards parallel lines from $(x-1/2, h) \in F$ to $(x+1/2, h+1) \in F$ and from $(x-1/2, h-1) \in B$ to $(x+1/2, h) \in B$ or we draw two diagonally downwards lines from $(x-1/2, h) \in F$ to $(x+1/2, h-1) \in F$ and from $(x-1/2, h+1) \in B$ to $(x+1/2, h) \in B$.

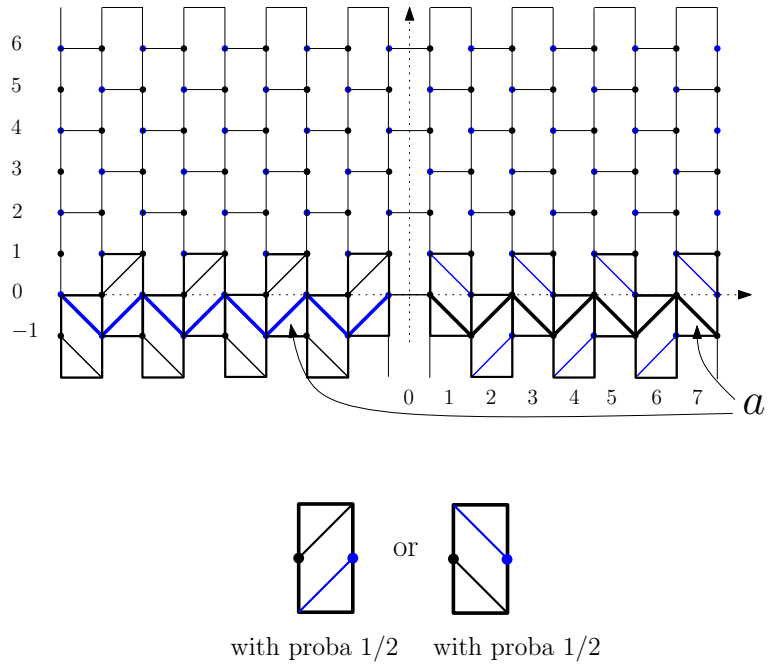

Figure V.2: The lattice with the initial conditions and the possible configurations in a rectangle

If $h \in \{-1, 0\}$, the lines are determined by the initial condition a defined above: For all $e \in E \setminus \{-1/2\}$, we draw the line from $(e, a(e))$ to $(e+1, a(e+1))$ and its parallel line located in the same rectangle (see Figure V.2 where the initial lines are drawn). When $e = -1/2$ we do not draw any line.

Note that in this way, the lines going through the lattice F are a family of independent coalescing simple random walks going forward (i.e. to the right) starting from each point of F and reflected at 0 on the left side of the origin and absorbed at 0 on the right side of the origin. Similarly, the lines going through B create coalescing backwards random walks, that do never cross the forward lines (see Fig. V.3). Those families correspond to the discrete counterpart of the "Brownian web", a family of coalescing independent Brownian motions (see §V.3 of this paper and [59] for more details) and using this analogy, we call it the discrete web.

The two families of forward and backward lines create a random maze, with one single connected component (this is a simple consequence of the coalescing property). The path starting at $(0, 0)$ that explores this maze (see Fig. V.4) can be viewed as a discrete path we denote $(\tilde{X}_n, \tilde{H}_n) \in \mathbb{Z} \times \mathbb{N}$. As shown in [59], its first coordinate has the same distribution as the $\mathbb{Z}$-valued random walk defined above and its second coordinate corresponds to the average of the slightly modified local times at time n on the two edges adjacent to $\tilde{X}_n$, i.e., $\tilde{H}_n = (\ell_n^+ + \ell_n^-)/2$.

For each $(e_0, h) \in F$ with $h \geq 1$, and each $e \in E$ with $e \geq e_0$, we denote by

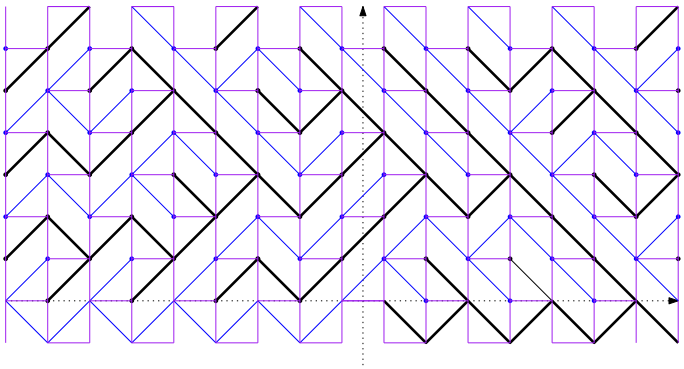

Figure V.3: A sample of the coalescing random walks

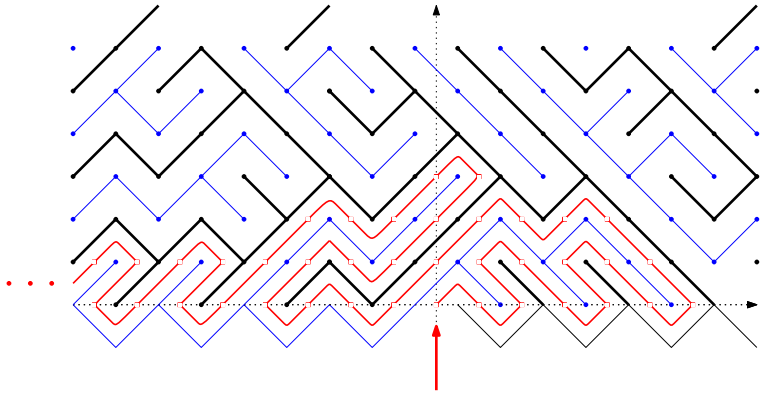

Figure V.4: Sample of the 39 first steps of $(\tilde{X}_n, \tilde{H}_n)$

$\tilde{\Lambda}_{e_0,h}(e)$ the value at e of the *forward* line in the web that starts at (e_0, h) (it is a simple random walk indexed by E and absorbed at 0) When $(e, h) \in B$, we use the same notation $\tilde{\Lambda}_{e,h}(e')$ to define the backward line starting in the left direction from (e, h) (defined for $e' \leq e$). Then, at time n, if the walker is at the position x, the local time profile $e \mapsto \ell_n(e)$ is equal to the lines $\tilde{\Lambda}_{x+1/2,\ell_n^+}(e)$ and $\tilde{\Lambda}_{x-1/2,\ell_n^-}(e)$ respectively for $e > x$ and $e < x$. Each time the walk is at the bottom line of a rectangle (i.e. when $\tilde{X}_n + \tilde{H}_n \in 2\mathbb{N}$), it discovers the status of the rectangle (meaning that it reveals if the lines are diagonally upwards or downwards lines in the rectangle) and this corresponds to moments for which $\ell_n^+ = \ell_n^-$. The position at time $n+1$ will be $\tilde{X}_n \pm 1$ depending on whether the rectangle contains upwards/downwards lines (respectively). When the walk is in the middle of a (revealed) rectangle (when $\tilde{X}_n + \tilde{H}_n \in 2\mathbb{N}+1$) i.e. when $\ell_n^+ \neq \ell_n^-$, it follows the direction given by the lines in the rectangle: It goes to the right/left depending on whether the lines are downwards/upwards lines, respectively.

Modified local time. Suppose now that a time n is given, and that we observe the discrete local time profile at time n, i.e., the function $e \mapsto \ell_n(e)$. What can one

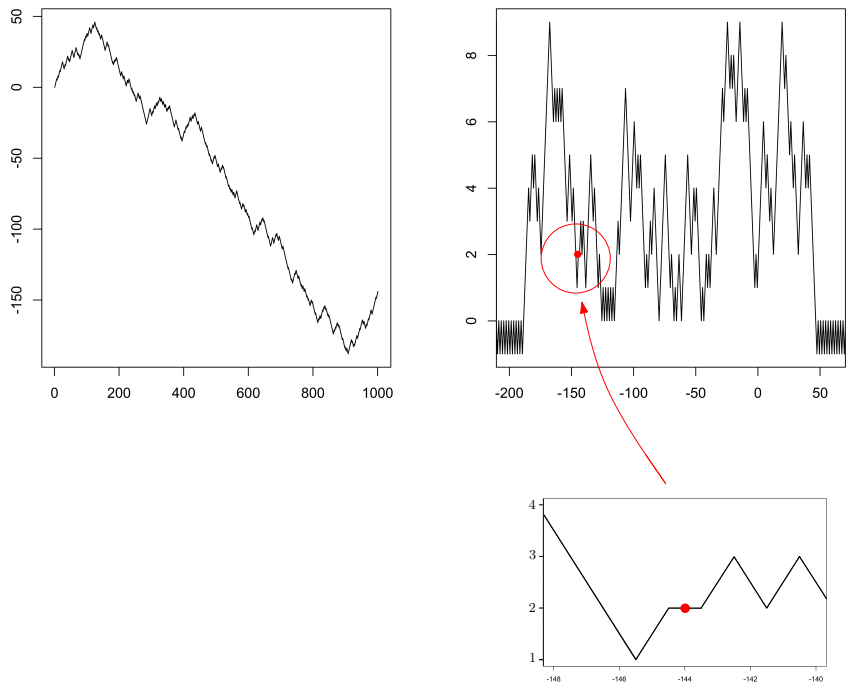

Figure V.5: Sample of the discrete model until time $n = 1000$. On the left, $k \mapsto \tilde{X}_k$; on the right, the local time at time n and a dot at the position of $(\tilde{X}_n, \tilde{H}_n)$. A zoom is made around the position at time n

say about the conditional law of $\tilde{X}_n$? A first observation is that one can immediately recover the location of $\tilde{X}_n$ by just looking at the local time profile, because as already noticed in the first definition, it is the only integer x such that $|\ell_n(x+1/2) - \ell_n(x-1/2)| \neq 1$ (see the zoom in Fig. V.5).

So, in order to "erase" this information, it is natural to slightly modify ℓ_n locally in the neighborhood of $\tilde{X}_n$. There are in fact several ways to proceed. The one that we choose to work with in the present paper is to simply concatenate the part of ℓ to the left of $x - 1/2$ directly to the part to the right of $x + 1/2$. However, then one may still be able to detect where such a surgery took place if $|\ell_n^- - \ell_n^+| = 2$. To avoid this problem, we will restrict our observations to the times at which $\ell_n^- = \ell_n^+$.

We therefore denote by $(N(k), k \in \mathbb{N})$ the times at which one really tosses a coin: $N(0) = 0$, and for every $k \geq 0$, $N(k+1) := \inf\{n > N(k) \,:\, \ell_n^+ = \ell_n^-\} = \inf\{n > N(k) \,:\, \tilde{X}_n + \tilde{H}_n \in 2\mathbb{N}\}$. As one can somehow expect (half of the space-time points correspond to times $N(k)$ while the other half not, see Fig. V.6), $N(k)$ almost surely behave like $2k$ up to lower order terms when $k \to \infty$ (this will be proved later, see (V.3)). In fact, we have an exact formula which links $N(k)$ to k.

Lemma 5.3. *For all $k \geq 0$,*

$$k = \frac{N(k) + \tilde{H}_{N(k)}}{2}. \tag{V.1}$$

There are various possible proofs of this simple combinatorial identity. We give a short one that uses our "random walk" interpretation:

Proof. Indeed, the identity clearly holds for $k = 0$ because $N(0) = \tilde{H}_0 = 0$. Suppose it holds for k. Then, if $N(k+1) = N(k) + 1$, this means that $\tilde{H}_{N(k+1)} = 1 + \tilde{H}_{N(k)}$, and therefore the identity for $k+1$ follows from that for k. If $N(k+1) = N(k) + j$ with $j \geq 2$, then it means that the TSRM has made $j-1$ forced moves, i.e. $(\tilde{X}_n, \tilde{H}_n)$ did "slide down" a slope. Therefore $\tilde{H}_{N(k+1)} = \tilde{H}_{N(k)} - (j-1) + 1 = \tilde{H}_{N(k)} - j + 2$ from which (V.1) follows. □

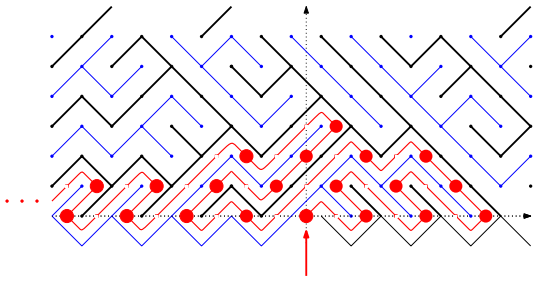

Figure V.6: Dots correspond to the times $N(k)$

We will now mainly restrict ourselves to the set of times at which $\ell_n^+ = \ell_n^-$ i.e. to the case where $n \in N(\mathbb{N})$ and we construct the curve $x \mapsto \tilde{\ell}_n(x)$ for all integer x as follows:

$$\tilde{\ell}_n(x) := \ell_n(x - 1/2)1_{x \leq \tilde{X}_n} + \ell_n(x + 1/2)1_{x > \tilde{X}_n}.$$

In plain words, we shift the graph of ℓ_n horizontally by $1/2$ in the direction of $\tilde{X}_n$ on both sides of $\tilde{X}_n$. Note that for large enough $|x|$, the function $\tilde{\ell}_n$ coincides with the shifted function initial line $\tilde{\ell}_0$ i.e. with $\tilde{a}(x) = -1_{x \in (2\mathbb{Z}+1)}$.

To sum up the previous few paragraphs: We have defined the function $x \mapsto \tilde{\ell}_n(x)$ which is a slightly modified local time, where we lost some information about the position of $\tilde{X}_n$ in the case where $\ell_n^+ = \ell_n^-$. In the rest of the paper, we shall refer to this modified curve $\tilde{\ell}$ as the "modified local time".

Properties of modified local times. In the remaining of this section, $f : \mathbb{Z} \mapsto \mathbb{N}$ will always denote a function that has a positive probability of being realized by some $\tilde{\ell}_{N(k)}$ for some $k \geq 0$, i.e. such that

$$\mathbb{P}(\exists k \ : \ f = \tilde{\ell}_{N(k)}) > 0.$$

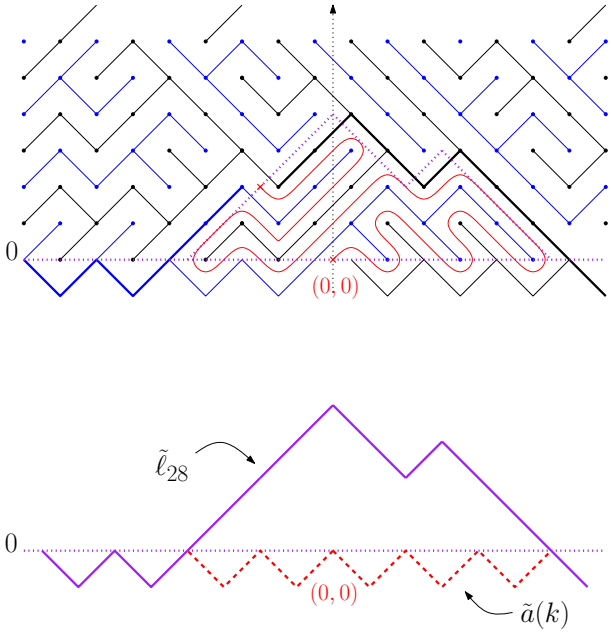

Figure V.7: The self-repelling walk until $n = 28$ and its modified local time

We denote by $\mathcal{C}$ this set of functions. Note that being in $\mathcal{C}$ implies certain necessary conditions for f: It is a function $f : \mathbb{Z} \to \mathbb{N}^{\#}$ such that $|f(x+1) - f(x)| = 1$ for all x, and if we define $m_- = m_-(f) := 1 + \max\{x \in -\mathbb{N} : f(x) = -1\}$ and $m_+ = m_+(f) := -1 + \min\{x \in \mathbb{N} : f(x) = -1\}$, then $f = \tilde{a}$ on $(-\infty, m_-] \cup [m_+, \infty)$. Furthermore, we can note that $f(0)$ is necessarily even (this is just because if $\tilde{X}_n \leq 0$, then $\tilde{X}$ has jumped an even number of times along the edge $1/2$, and if $\tilde{X}_n > 0$, then it has jumped an even number of times on $-1/2$).

Note that it can happen that $f(x)$ is equal to 0 for some integer values of x in (m_-, m_+) (but it can never be equal to -1 on this interval). Let $O(f)$ denotes the number of zeroes of f in this open interval. We define an excursion-interval to be a maximal interval on which f is positive. Then (m_-, m_+) can be split into $O(f) + 1$ excursion-intervals.

Note that 0 necessarily belongs to the left-most or to the right-most excursion interval: Indeed, suppose for instance that $f = \tilde{\ell}_N$ and $\tilde{X}_N \geq 0$ (the case $\tilde{X}_N \leq 0$ can be treated similarly), then every edge to the left of the origin is visited an even number of times (because $\tilde{X}$ has to jump equally often in both directions along that edge, as it starts to its right and ends up to its right), from which it follows that 0 is in the left-most excursion interval of f. Exactly the same argument shows that $\tilde{X}_N$ also belongs to the left-most or to the right-most interval which is at the opposite side of the 0-interval, and also that $\tilde{X}_N$ cannot be one of the $O(f)$ internal zeros of f.

Hence, let us define $I(f)$ to be equal to $[m_-, m_+]$ if $O(f) = 0$, and if $O(f) \geq 1$,

then

$$I(f) = (o_+, m_+] \text{ or } [m_-, o_-)$$

depending on whether $o_+ := \max\{x < m_+ : \ f(x) = 0\}$ is positive or $o_- := \min\{x > m_- : \ f(x) = 0\}$ is negative. In the special case where $f = \tilde{a}$, we set $I(f) = \{0\}$.

Then necessarily, if $\tilde{\ell}_{N(k)} = f$ for some k, then this implies that $\tilde{X}_{N(k)} \in I(f)$.

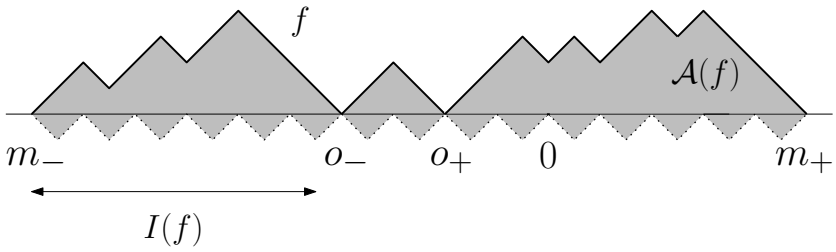

Figure V.8: A modified local time and some notations

Behavior of the walk given a modified local time curve f and a position x. Conversely, if $f \in \mathcal{C}$ is given and if $x \in I(f)$, we denote by $E_{x,f}$ the event that f is a modified local time for which the surgery took place at position x i.e. that for some k, $f = \tilde{\ell}_{N(k)}$ and $\tilde{X}_{N(k)} = x$. This means exactly that $\tilde{\Lambda}_{x+1/2,f(x)}(e)$ and $\tilde{\Lambda}_{x-1/2,f(x)}(e)$ are equal to $f(e + 1/2)$ or $f(e - 1/2)$ depending on $e < x$ or $e > x$.

But, for a given f and x, the point $(x, f(x))$ is fixed and the forward curve $\tilde{\Lambda}_{x+1/2,f(x)}$ and the backward one $\tilde{\Lambda}_{x-1/2,f(x)}$ are distributed as independent random walks reflected at 0 during the time-interval between x and the origin and absorbed at 0 outside this interval. It therefore follows that

$$\mathbb{P}(E_{x,f}) = \left(\frac{1}{2}\right)^{(m_+ - m_-) - O(f)}.$$

We crucially see that $\mathbb{P}(E_{x,f})$ is the same for all x in $I(f)$.

Let us now suppose that $E_{x,f}$ holds, and study the value of n and k at which $(\tilde{X}_n, \tilde{H}_n) = (\tilde{X}_{N(k)}, \tilde{H}_{N(k)}) = (x, f(x))$. Clearly both n and k are determined by x and f. This is the content of the following Lemma:

Lemma 5.4. *Let us fix $f \in \mathcal{C}$ and $x \in I(f)$. We denote by $\mathcal{A}(f)$ the area between f and $\tilde{a}$ i.e. $\mathcal{A}(f) = \sum_y (f(y) - \tilde{a}(y))$. If $E_{x,f}$ holds, then the time $n(x, f) = N(k(x, f))$ at which $(\tilde{X}_n, \tilde{H}_n) = (x, f(x))$ satisfies:*

$$n(x, f) = \mathcal{A}(f) + f(x).$$

Consequently, using formula (V.1),

$$k(x, f) = (n(x, f) + f(x))/2 = \mathcal{A}(f)/2 + f(x). \tag{V.2}$$

Proof. The time $n = n(x, f)$ is equal to the area between the non modified local time associated to the pair (x, f) and the initial local time a. Let us denote here the non modified function by g. For all $e \in E$ such that $e \leq x - 1/2$, $g(e) := f(e + 1/2)$ and when $e \geq x - 1/2$, $g(e) := f(e - 1/2)$. Therefore, the time n is equal to $\mathcal{A}(f)$, to which one has to add $f(x)$, because of the additional column of height $f(x)$ that one has removed in order to obtain $\tilde{\ell}$ out of ℓ (see Figure V.7). More precisely,

$$\begin{aligned} n &= \sum_{e \in E} g(e) - a(e) \\ &= \sum_{\substack{e \in E \\ e \in [m_- - \frac{1}{2}, x - \frac{1}{2}]}} f(e + \frac{1}{2}) + \sum_{\substack{e \in E \\ e \in [x + \frac{1}{2}, m_+ + \frac{1}{2}]}} f(e - \frac{1}{2}) - \sum_{\substack{e \in E \\ e \in [m_- - \frac{1}{2}, -\frac{1}{2}]}} \tilde{a}(e + \frac{1}{2}) - \sum_{\substack{e \in E \\ e \in [\frac{1}{2}, m_+ + \frac{1}{2}]}} \tilde{a}(e - \frac{1}{2}) \\ &= f(x) - \tilde{a}(0) + \sum_{y \in \mathbb{Z}} f(y) - \tilde{a}(y) \\ &= f(x) + \mathcal{A}(f). \end{aligned}$$

The first equality in (V.2) follows from (V.1). □

In particular, we see that for a given f, the time $k(x, f)$ depends on the position of x in $I(f)$. However, we will see that this dependency is mild: because the slope of f is never larger than one, it follows that for any x, the area underneath f is at least $|f(x)|^2$. With equality (V.2), this implies that

$$\frac{\mathcal{A}(f)}{2} \leq k(x, f) \leq \frac{\mathcal{A}(f)}{2} + \sqrt{\mathcal{A}(f)}. \tag{V.3}$$

Randomization of the observation. For each A, let us define a geometric random variable q_A with mean $A/2$. We want to describe the joint distribution of

$$(x_A, \gamma_A(\cdot)) := (\tilde{X}_{N(q_A)}, \tilde{\ell}_{N(q_A)}(\cdot)).$$

Suppose we only observe $\gamma_A(\cdot)$. As we have already indicated, the point x_A is necessarily in the interval $I(\gamma_A)$. Let us sample uniformly an integer u_A in this interval. We now show that the law of (u_A, γ_A) is close to that of (x_A, γ_A) when A is large. More precisely:

Lemma 5.5. *The total variation distance between the distributions of (u_A, γ_A) and (x_A, γ_A) tends to 0 as $A \to \infty$.*

Proof. In order to prove the Lemma, we have to see that the probabilities that $x_A = x$ and $\gamma_A = f$ are almost the same for all $x \in I(f)$. The reason for this result is that $f(x)$ will tend to be much smaller than $\mathcal{A}(f)$ in the limit when A tends to

∞ for a proportion of f's that goes to 1. Clearly, this probability (for a given $f \in \mathcal{C}$ and $x \in I(f)$) is equal to

$$\mathbb{P}\left(E_{x,f},\ q_A = k(x,f)\right) = \mathbb{P}(E_{x,f})\mathbb{P}(q_A = k(x,f)) = \left(\frac{1}{2}\right)^{(m_+-m_-)-O(f)} \left(1-\frac{2}{A}\right)^{k(x,f)-1} \frac{2}{A}.$$

When $A \to \infty$, the time q_A will typically be large so that $\sqrt{\mathcal{A}(\gamma_A)}$ will become negligible compared to $\mathcal{A}(\gamma_A)$. For every $f \in \mathcal{C}$, let us define

$$p(f) = \left(\frac{1}{2}\right)^{(m_+-m_-)-O(f)} \left(1-\frac{2}{A}\right)^{\mathcal{A}(f)/2-1} \frac{2}{A}.$$

Thanks to (V.3), for every $f \in \mathcal{C}$ and $x \in I(f)$, we can write:

$$\left(1-\frac{2}{A}\right)^{\sqrt{\mathcal{A}(f)}} \leq \frac{\mathbb{P}((x_A,\gamma_A)=(x,f))}{p(f)} \leq 1.$$

Taking the mean over x in $I(f)$, we get that

$$\left(1-\frac{2}{A}\right)^{\sqrt{\mathcal{A}(f)}} \leq \frac{\mathbb{P}(\gamma_A = f)}{p(f)\times \#I(f)} = \frac{\mathbb{P}((u_A,\gamma_A)=(x,f))}{p(f)} \leq 1.$$

Hence,

$$\left(1-\frac{2}{A}\right)^{\sqrt{\mathcal{A}(f)}} \leq \frac{\mathbb{P}((x_A,\gamma_A)=(x,f))}{\mathbb{P}((u_A,\gamma_A)=(x,f))} \leq \left(1-\frac{2}{A}\right)^{-\sqrt{\mathcal{A}(f)}}.$$

It therefore suffices to prove that

$$\mathbb{E}\left(\left(1-\frac{2}{A}\right)^{\sqrt{\mathcal{A}(\gamma_A)}}\right) \to 1 \text{ and } \mathbb{E}\left(\left(1-\frac{2}{A}\right)^{-\sqrt{\mathcal{A}(\gamma_A)}}\right) \to 1$$

as $A \to \infty$. This is straightforward because

$$\frac{\mathcal{A}(\gamma_A)}{2} \leq q_A \leq \frac{\mathcal{A}(\gamma_A)}{2} + \sqrt{\mathcal{A}(\gamma_A)}$$

keeping in mind also that q_A is a geometric random variable with mean $A/2$. □

V.3 Convergence from discrete to continuous

The definition of the continuous TSRM by Tóth and Werner uses a continuous analogue of the definition of $\tilde{X}_n$ via the maze that $(\tilde{X}_n, \tilde{H}_n)$ has to go through. One starts with a family of coalescing Brownian motions (instead of coalescing random walks) $(\Lambda_{x,h},\ (x,h) \in \mathbb{R}\times\mathbb{R}_+^*)$ starting from all points in the upper half-plane. Such families had been constructed by Arratia in [4], and were further studied in

[59, 53, 30, 43] and are called Brownian web (BW) in the latter papers (note that in the most recent papers, this is a family of curves starting from the whole plane). This is shown to define a continuous half-plane-filling maze. For each (x, h) in the upper half plane, $\Lambda_{x,h}$ has the distribution of a (one dimensional) two-sided Brownian motion with initial condition $\Lambda_{x,h}(x) = h$ reflected at 0 in the time-interval between 0 and x and absorbed at 0 outside this interval. One of the main properties of the BW is that almost surely its curves do not cross. The interaction between the BW-curves can be understood as follows: We first define the BW-curves starting from points belonging to a countable dense subset of the upper half plane $Q = (x_i, h_i)_{i\in\mathbb{N}^*}$. We also take $(x_0, h_0) := (0, 0)$ and let Λ_{x_0,h_0} be the function identically equal to 0. We then construct the curves recursively. Given $(\Lambda_{x_i,h_i}, 0 \leq i < k)$, the *forward* process $(\Lambda_{x_k,h_k}(x), x \geq x_k)$ has the law of an independent Brownian motion starting at h_k at time x_k coalescing with the *forward* previously drawn curves $(\Lambda_{x_i,h_i}(x), x \geq x_i;\ 0 \leq i < k)$ and reflected at the *backward* curves $(\Lambda_{x_i,h_i}(x), x \leq x_i;\ i < k)$. The *backward* process $(\Lambda_{x_k,h_k}(x), x \leq x_k)$ is then an independent Brownian motion coalescing with the *backward* previously drawn curves and reflected at the *forward* ones. In this way, we defined the "skeleton" of the BW. One can extend this definition to the whole half plane by continuity (there is some freedom left for the construction of the other curves, we do not enter into the details here). An alternative construction (which is the original one) is to construct all the forward BW-curves at first and then to define the backward BW-curves with the help of the non-crossing property.

The intuitive link between TSRM and BW goes as follows: Let us consider the process (X_t, H_t) started at $(0, 0)$ which traces the contour of the "tree" of these coalescing Brownian motions, then one obtains a space-filling curve that can be parametrized by the area it has swept. For every (x, h) in the upper half plane, the process (X_t, H_t) visits the point (x, h) at the random time $t = T_{x,h} := \int \Lambda_{x,h}$. There is a difficulty here because the set of times given by the family $(T_{x,h},\ (x, h) \in \mathbb{R}\times\mathbb{R}^*_+)$ is not the entire set of times $\mathbb{R}_+$. Nevertheless, it has good enough properties (such as density in $\mathbb{R}^+$, see Proposition 4.1 in [59]) to enable one to define the process (X, H). Its first coordinate X will be the TSRM, while the second coordinate H_t will turn out to be equal to its occupation time density (defined in the introduction) at its current position i.e. $H_t = \Lambda_t(X_t)$. Moreover, the distribution (and even the joint distribution) of the occupation time density is known at the random times $T_{x,h}$. By construction, we have: a.s., for all $(x, h) \in \mathbb{R} \times \mathbb{R}^*_+$, $\Lambda_{T_{x,h}} = \Lambda_{x,h}$. We refer to [59] for more details.

Newman and Ravishankar [43] have shown that the (properly renormalized version of the) process $(\tilde{X}_n, \tilde{H}_n)$ converges to the continuous process (X_t, H_t). We could try to extend this proof in order to also have convergence of the corresponding in-

tervals I, but as we only need the convergence at the independent random time τ, we will follow a more direct method. Let $\mathbb{R}$ and $\mathbb{R}^2$ be equipped with the Euclidean topology and let us denote by C the set of continuous functions with compact support from $\mathbb{R}$ to $\mathbb{R}^+$ admitting a left-most and a right-most excursion such that 0 belongs to the right-most or the left-most excursion, equipped with the uniform topology.

The goal is to establish the following convergence (where an interval (x_-, x_+) in $\mathbb{R}$ is identified with a point $(x_-, x_+) \in \mathbb{R}^2$):

Proposition 5.6. *The triplet*

$$(A^{-2/3}x_A, A^{-1/3}\gamma_A(A^{2/3}\cdot), A^{-2/3}I(\gamma_A)) = \left(A^{-2/3}\tilde{X}_{N(q_A)},\ A^{-1/3}\tilde{\ell}_{N(q_A)}(A^{2/3}\cdot),\ A^{-2/3}I\left(\ell_{N(q_A)}\right)\right) \tag{V.4}$$

converges in distribution towards

$$(X_\tau,\ \Lambda_\tau(\cdot),\ I_\tau) \qquad \text{as } A \to \infty.$$

(recall that I_τ is the opposite excursion from the 0*-excursion in the continuous process Λ_τ).*

Proof. The trick will be to express the expectation of continuous bounded functionals of the triplet in terms of just one simple random walk/Brownian motion thanks to a simple change of variables from $\mathbb{R}_+$ into the upper half-space using the time-parametrization of the TSRM $t = T_{x,h}$. Indeed, the law of the occupation time is very easy to describe at the (random) first hitting times of (x, h) both in the discrete and continuous models: In the discrete model, for $(x, h) \in \mathbb{Z} \times \mathbb{N}$ with $x + h$ even, it is a two-sided simple random walk properly reflected/absorbed and starting at $(x+1/2, h)$ for the forward one, $(x-1/2, h)$ for the backward one; in the continuous model, we have just seen that $\Lambda_{T_{x,h}} = \Lambda_{x,h}$.

Let us take a continuous and bounded function $\varphi : \mathbb{R} \times C \times \mathbb{R}^2 \to \mathbb{R}$. For each positive A, we define the rescaled functional φ^A as

$$\varphi^A(x, \ell(\cdot), I) := \varphi(A^{-2/3}x, A^{-1/3}\ell(A^{2/3}\cdot), A^{-2/3}I).$$

For every $(x, h) \in \mathbb{Z} \times \mathbb{N}$ such that $x + h$ is even (we call $\mathcal{F}$ this set of pairs), we define $f_{x,h} \in \mathcal{C}$ to be the random continuous polygonal curve which shifts and concatenates the forward discrete BW-curve starting from $(x+1/2, h)$ and the backward one from $(x - 1/2, h)$. In other words, for every $(x, h) \in \mathcal{F}$ and $f \in \mathcal{C}$ such that $x \in I(f)$ and $f(x) = h$, we have $f_{x,h} := f$ on the integers if $E_{x,f}$ holds (and $f_{x,h}$ is then naturally extended to a polygonal curve).

Using (V.2), we get:

$$\begin{aligned}
&\mathbb{E}\left(\varphi^A\left(\tilde{X}_{N(q_A)}, \tilde{\ell}_{N(q_A)}(\cdot), I(\ell_{N(q_A)})\right)\right)\\
&= \sum_{k=0}^{\infty} \sum_{(x,h)\in\mathcal{F}} \mathbb{E}\left(\varphi^A(x, f_{x,h}(\cdot), I(f_{x,h}))1_{\{\mathcal{A}(f_{x,h})+2h=2k\}}\right)\mathbb{P}(q_A = k)\\
&= \frac{2}{A}\sum_{(x,h)\in\mathcal{F}} \mathbb{E}\left(\varphi^A(x, f_{x,h}(\cdot), I(f_{x,h})) \times (1-2/A)^{(\mathcal{A}(f_{x,h})+2h)/2-1}\right)
\end{aligned}$$

For all (x,h) in the *upper half-plane* $\mathbb{R}\times\mathbb{R}_+$, we now define the point $(x^A, h^A) \in \mathcal{F}$ such that $A^{2/3}x \in [x^A, x^A+1)$ and $A^{1/3}h \in [h^A, h^A+1)$ or $[h^A-1, h^A)$ depending on whether x_A is even or odd, and define f^A to be the rescaled function f_{x^A,h^A} i.e.

$$f^A(\cdot) := A^{-1/3} f_{x^A,h^A}(A^{2/3}\cdot)$$

and we let $\mathcal{A}^A(f^A)$ denote the area between f^A and the rescaled bottom line. Then, we can rewrite this last expression as

$$\int_{-\infty}^{\infty}\int_0^{\infty} \mathbb{E}\left(\varphi(A^{-2/3}x^A, f^A(\cdot), I(f^A)) \times (1-2/A)^{(A\mathcal{A}^A(f^A)+2h^A)/2-1}\right) dx\ dh. \quad \text{(V.5)}$$

In the continuous setting, recall the definition of $T_{x,h} := \int \Lambda_{x,h}$ where $\Lambda_{x,h}$ is the BW-curve starting at $\Lambda_{x,h}(x) = h$. Using the (measure-preserving) change of variables $t = T_{x,h}$ (see Proposition 4.1 in [59]) and Fubini's Theorem,

$$\begin{aligned}
\mathbb{E}(\varphi(X_\tau, \Lambda_\tau, I_\tau)) &= \mathbb{E}\left(\int_0^{\infty} e^{-t}\varphi(X_t, \Lambda_{X_t,\Lambda_t(X_t)}, I_{X_t,\Lambda_t(X_t)})dt\right)\\
&= \mathbb{E}\left(\int_{-\infty}^{+\infty}\int_0^{\infty} e^{-T_{x,h}}\varphi(x, \Lambda_{x,h}, I_{x,h})dhdx\right)\\
&= \int_{-\infty}^{+\infty}\int_0^{\infty} \mathbb{E}\left(e^{-T_{x,h}}\varphi(x, \Lambda_{x,h}, I_{x,h})\right)dhdx. \quad \text{(V.6)}
\end{aligned}$$

where $I_{x,h}$ is the excursion of $\Lambda_{x,h}$ furthest from the origin.

Now, the convergence of (V.5) towards this last expression boils down to a simple random walk/Brownian motion matter. Indeed, f_{x^A,h^A} is the concatenation of two simple random walks and $\Lambda_{x,h}$ is a two-sided Brownian motion. A little care is needed here as $\Lambda_{x,h}$ is not a continuity point of the function which associates to $f \in C$ the opposite excursion from the 0-excursion (see Billigsley [7] for background). Nevertheless, the convergence holds thanks to the following classical argument:

Let $h > 0$ and let (for each n), $(S^n_k)_{k\in\mathbb{N}}$ denote a simple random walk starting at $[n^{1/3}h]$ and define $S^{(n)}(\cdot) := n^{-1/3}S^n_{[n^{2/3}\cdot]}$ its renormalization. By Skorohod's representation Theorem, it is possible to couple all these walks $S^{(n)}$ with a one dimensional Brownian motion B started at h in such a way that $S^{(n)}$ almost-surely converges towards B for the uniform topology on any compact time-interval. With continuity

of B and the fact that the Brownian motion almost surely becomes negative immediately after its first hitting time of the origin, it follows that the first hitting time of the x-axis by $S^{(n)}$ converges also almost-surely towards the first hitting time of the x-axis by B.

It follows that for every $(x,h) \in \mathbb{R} \times \mathbb{R}_+^*$,

$$\mathbb{E}\left(\varphi(A^{-2/3}x^A, f^A(\cdot), I(f^A)) \times (1-2/A)^{(A\,\mathcal{A}^A(f^A)+2h^A)/2-1}\right) \longrightarrow \mathbb{E}\left(e^{-T_{x,h}}\varphi(x, \Lambda_{x,h}, I_{x,h})\right)$$

as $A \to \infty$. In order to deduce the convergence of (V.5) to (V.6), it remains to apply the dominated convergence theorem (it is easy to see that the expectation (V.5) admits the rough upper bound $\|\varphi\|_\infty \exp(-c([x]+[h]))$ for all A large enough and for some constant $c > 0$ and all large x and h thanks to Markov property applied $[x]$ and $[h]$ times); this concludes the proof of Proposition 5.6. □

Combining Lemma 5.5. and Proposition 5.6. now also concludes the proof of our Theorem 5.2.

V.4 Probability to be perfectly hidden

We have seen that the burglar is well hidden in the interval I. It can however happen that the interval I is much shorter than the whole support of the local time (in particular when the burglar is close to its past maximum). It is natural to wonder what is the probability that I_1 is equal to the whole support $\mathrm{supp}(\Lambda_1)$ (when this is the case, the burglar's strategy turned out to be particularly efficient...). This question is answered by the following statement:

Proposition 5.7. *The probability that I_1 is equal to the entire support of the local time is equal to*

$$1 - 9\sqrt{3}\,\Gamma(2/3)^6/(4\pi^3) \approx 0.225.$$

Proof. Let us notice at first that with the scaling property, we have:

$$\mathbb{P}(\mathrm{supp}(\Lambda_1) = I_1) = \mathbb{P}(\mathrm{supp}(\Lambda_\tau) = I_\tau),$$

where τ is an independent exponential variable with mean 1, just as before. Recall that for a point (x,h) in the upper half-plane, the probability that $\Lambda_{x,h}$ has only one excursion corresponds to the event that the Brownian motion that starts from the point (x,h) in the direction of 0 does hit 0 "on the other side" of 0. Using the

measure preserving change of variable $t = T_{x,h}$ from $\mathbb{R}_+$ onto the upper half-plane,

$$\begin{aligned}\mathbb{P}(\mathrm{supp}(\Lambda_\tau) = I_\tau) &= \int_0^\infty e^{-t}\mathbb{P}\left(\mathrm{supp}(\Lambda_t) = I_t\right) dt \\ &= \int_0^\infty \int_{-\infty}^\infty \mathbb{E}\left(e^{-T_{x,h}} 1_{\mathrm{supp}(\Lambda_{x,h})=I_{x,h}}\right) dxdh \\ &= \int_0^\infty \int_{-\infty}^\infty \mathbb{E}_h\left(\exp\left(-\int_{\xi'}^\xi B_t dt\right) 1_{\xi'<x<\xi}\right) dxdh\end{aligned}$$

where $(B, \mathbb{P}_h)$ is a two-sided Brownian motion started at level h at time 0, and $\xi := \inf\{t \geq 0,\ B_t = 0\}$ and $\xi' := \sup\{t \leq 0,\ B_t = 0\}$. With Fubini's theorem, we can now swap the expectation and the integral with respect to x, this shows that

$$\begin{aligned}\mathbb{P}(\mathrm{supp}(\Lambda_\tau) = I_\tau) &= \int_0^\infty \mathbb{E}_h\left((\xi - \xi')\exp\left(-\int_{\xi'}^\xi B_t dt\right)\right) dh \\ &= 2\int_0^\infty \mathbb{E}_h\left(\xi \exp\left(-\int_{\xi'}^\xi B_t dt\right)\right) dh. \qquad \text{(V.7)}\end{aligned}$$

Note that with the scaling property of Brownian motion (ξ and ξ' scale like h^2 and the integral like h^3),

$$\begin{aligned}\mathbb{E}_h\left(\xi \exp\left(-\int_{\xi'}^\xi B_t dt\right)\right) &= \mathbb{E}_1\left(h^2\xi \exp\left(-h^3\int_{\xi'}^\xi B_t dt\right)\right) \\ &= -\frac{d}{dh}\left[\mathbb{E}_1\left(\frac{\xi}{3\int_{\xi'}^\xi B_t dt}\exp\left(-h^3\int_{\xi'}^\xi B_t dt\right)\right)\right]\end{aligned}$$

(we can exchange the expectation $\mathbb{E}_1$ and the differentiation with respect to h because the function $h \mapsto h^2\xi\exp\left(-h^3\int_{\xi'}^\xi B_t dt\right)$ is bounded from above by $(2/(3e))^{2/3}\xi/(\int_{\xi'}^\xi B_t dt)^{2/3}$ whose expectation is finite). Therefore, the integral (V.7) is equal to $2/3 \times \mathbb{E}_1\left(\xi/\int_{\xi'}^\xi B_t dt\right)$, which seems however difficult to compute directly.

Let us compute (V.7) with a different method. Independence between the two-sides of the Brownian motion shows that

$$\mathbb{E}_h\left(\xi\ \exp\left(-\int_{\xi'}^\xi B_t dt\right)\right) = u(h)\, v(h) \qquad \text{(V.8)}$$

where

$$u(h) := \mathbb{E}_h\left(\exp\left(-\int_0^\xi B_t dt\right)\right)$$

and

$$v(h) := \mathbb{E}_h\left(\xi\ \exp\left(-\int_0^\xi B_t dt\right)\right).$$

It is not difficult to see (and has been used in several papers, see for instance formula 2.8.1 p. 167 in [9] or [40]) that the function u solves the differential equation:

$$u''(x) = 2x\, u(x) \tag{V.9}$$

with initial condition $u(0) = 1$ (and is bounded on $\mathbb{R}^+$) which implies that it can be expressed in terms of the airy function Ai: $u(\cdot) = \mathrm{Ai}(2^{1/3}\cdot)/\mathrm{Ai}(0)$.
Let us now show that

$$v(h) = u(h)u'(0) - u'(h). \tag{V.10}$$

We fix $h > 0$, $\varepsilon > 0$ and define $\tilde{\xi}$ to be the first time at which a Brownian motion B started at $h + \varepsilon$ hits ε. The strong Markov property shows that

$$\begin{aligned} u(h+\varepsilon) &= \mathbb{E}_{h+\varepsilon}\left(\exp\left(-\int_0^{\tilde{\xi}} B_t dt\right)\right) u(\varepsilon) \\ &= u(\varepsilon)\mathbb{E}_h\left(\exp\left(-\int_0^{\xi}(B_t+\varepsilon)dt\right)\right) \\ &= u(\varepsilon)\mathbb{E}_h\left(\exp(-\varepsilon\xi)\times\exp\left(-\int_0^{\xi} B_t dt\right)\right) \end{aligned}$$

so that

$$\begin{aligned} u(h+\varepsilon) - u(h) = u(\varepsilon)\mathbb{E}_h&\left((\exp(-\varepsilon\xi)-1)\times\exp\left(-\int_0^{\xi} B_t dt\right)\right) \\ &+ (u(\varepsilon)-1)\mathbb{E}_h\left(\exp\left(-\int_0^{\xi} B_t dt\right)\right). \end{aligned}$$

Letting ε to 0, using the fact that we know that u is C^1, we get (V.10) by bounded convergence.

Notice also that with an integration by parts and the differential equation (V.9), we get that:

$$\int_0^{\infty} u^2(y)dy = u'(0)^2/2 \tag{V.11}$$

We are now ready to conclude: The relations (V.7), (V.8), (V.10) and (V.11) lead to:

$$\begin{aligned} \mathbb{P}(\mathrm{supp}(\Lambda_1) = I_1) &= 2\int_0^{\infty} dh u(h)v(h) \\ &= 2\int_0^{\infty} u(h)^2 u'(0)dh - 2\int_0^{\infty} u'(h)u(h)dh \\ &= u'(0)^3 + 1. \end{aligned}$$

By 10.4.4 and 10.4.5 [1], we have $u'(0) = -6^{1/3}\Gamma(2/3)/\Gamma(1/3)$ and the studied probability is equal to $1 - (6\,\Gamma(2/3)^3/\Gamma(1/3)^3) = 1 - 9\sqrt{3}\Gamma(2/3)^6/(4\pi^3)$. □

Acknowledgements: I warmly thank my supervisor Wendelin Werner for his precious help and advices throughout this work and for his careful reading of this paper. I am also grateful to the anonymous referee for his/her useful comments.

La loi de Tracy-Widom-β

CHAPITRE VI

L'exposant de l'asymptotique de la queue droite de la loi de Tracy-Widom-β

Les résultats de ce chapitre ont été obtenus en collaboration avec Bálint Virág et ont été acceptés pour publication dans *Annales de l'IHP*.

The Tracy-Widom β distribution is the large dimensional limit of the top eigenvalue of β random matrix ensembles. We use the stochastic Airy operator representation to show that as $a \to \infty$ the tail of the Tracy Widom distribution satisfies

$$P\left(TW_\beta > a\right) = a^{-\frac{3}{4}\beta + o(1)} \exp\left(-\frac{2}{3}\beta a^{3/2}\right).$$

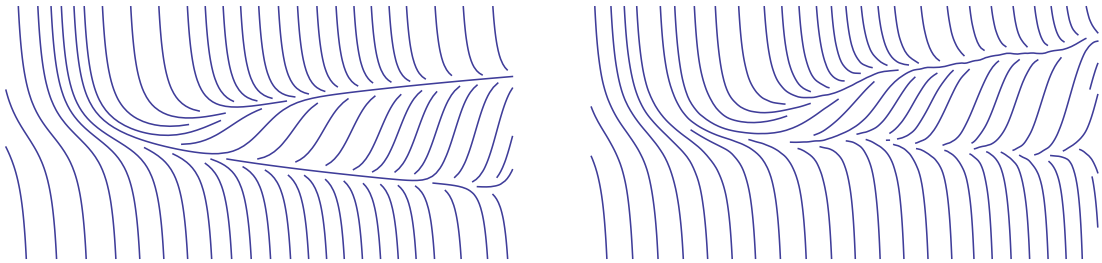

Flowlines for the ODE of $X - \frac{2}{\sqrt{\beta}}B$

VI.1 Introduction

For $\beta > 0$ fixed, we examine the probability density of $\lambda_1 \geq \lambda_2 \geq \ldots \geq \lambda_n \in \mathbb{R}$ given by :

$$\mathbb{P}_\beta(\lambda_1, \lambda_2, \ldots, \lambda_n) = \frac{1}{Z_{n,\beta}} e^{-\beta \sum_{k=1}^n \lambda_k^2/4} \prod_{j<k} |\lambda_j - \lambda_k|^\beta, \tag{VI.1}$$

in which $Z_{n,\beta}$ is a normalizing constant. This family of distribution is called the β-ensemble. When $\beta = 1, 2$ or 4, this is the joint density of eigenvalues for respectively the Gaussian orthogonal, unitary, or symplectic ensembles of random matrix theory. But the law (VI.1) has a physical sense for all the β as it describes a one-dimensional Coulomb gas at inverse temperature β (see e.g. Chapter 1. Section 1.4 of [31]). Dumitriu and Edelman [20] discovered that (VI.1) is the eigenvalue distribution for the tridiagonal matrix

$$H_n^\beta = \frac{1}{\sqrt{\beta}} \begin{bmatrix} g_1 & \chi_{(n-1)\beta} & & & \\ \chi_{(n-1)\beta} & g_2 & \chi_{(n-2)\beta} & & \\ & \ddots & \ddots & \ddots & \\ & & \chi_{2\beta} & g_{n-1} & \chi_\beta \\ & & & \chi_\beta & g_n \end{bmatrix},$$

where the random variables $g_1, g_2, \cdots, g_n$ are independent Gaussians with mean 0 and variance 2 and $\chi_\beta, \chi_{2\beta}, \cdots, \chi_{(n-1)\beta}$ are independents χ random variables indexed by the shape parameter.

When $n \uparrow \infty$, the largest eigenvalue centered by $2\sqrt{n}$ and scaled by $n^{1/6}$ converges in law to the Tracy-Widom(β) distribution. This was first shown in [61] and [62] for the cases $\beta = 1, 2$ or 4, where exact formulae are available. Ramírez, Rider and Virág [48] extended this result for all the β. They show that the rescaled operator:

$$\tilde{H}_n^\beta := n^{1/6}(2\sqrt{n}I - H_n^\beta)$$

converges to the stochastic Airy operator (SAE_β) :

$$\mathcal{H}_\beta = -\frac{d^2}{dx^2} + x + \frac{2}{\sqrt{\beta}} B'_x \tag{VI.2}$$

in the appropriate sense (here B' is a white noise). In particular, the low-lying eigenvalues of $\tilde{H}_n^\beta$ converge in law to those of $\mathcal{H}_\beta$. Thanks to the Ricatti transform, the eigenvalues of SAE_β can be reinterpreted in terms of the explosion probabilities of a one-dimensional diffusion. In particular, Ramírez et al. [48] show that

$$\mathbb{P}(TW_\beta > a) \quad = \quad \mathbb{P}_{+\infty}(X \text{ blows up in a finite time}), \tag{VI.3}$$

where X is the diffusion

$$\begin{cases} dX(t) = (t + a - X^2(t))dt + \frac{2}{\sqrt{\beta}} dB(t), \\ X(0) = \infty. \end{cases} \tag{VI.4}$$

Note also that $X - \frac{2}{\sqrt{\beta}} B$ satisfies an ODE, simulated on the front page with $\beta = \infty$ and 2. The starting time of the separatrix is distributed as $-\mathrm{TW}_\beta$.

Asymptotic expansions of beta-ensembles are of active interest in the literature, see for example [13], [64], [22] and [14].

In this article, we study the diffusion (VI.4) in order to obtain the right tail of the Tracy-Widom law. Our main tool will be the Cameron-Martin-Girsanov theorem: it permits us to change the drift coefficient of the diffusion and evaluate the probability of explosion using the new process.

Using the variational characterization of the eigenvalues of SAE_β (VI.2) and an analysis of the SDE (VI.4) Ramírez et al. [48] show that as $a \to \infty$ we have

$$\begin{aligned} P\left(TW_\beta < -a\right) &= \exp\left(-\tfrac{1}{24}\beta a^3(1 + o(1))\right), \quad \text{and} \\ P\left(TW_\beta > a\right) &= \exp\left(-\tfrac{2}{3}\beta a^{3/2}(1 + o(1))\right). \end{aligned} \tag{VI.5}$$

While we were finishing this article, Borot, Eynard, Majumdar and Nadal [10], in a physics paper, using completely different methods, calculated more precise asymptotics for the *left tail* of the Tracy-Widom distribution.

In this paper we evaluate the exponent of the polynomial factor in the asymptotics of the right tail.

Theorem 6.1. *When $a \to +\infty$, we have*

$$P\left(TW_\beta > a\right) = a^{-3\beta/4} \exp\left(-\frac{2}{3}\beta a^{3/2} + O\left(\sqrt{\ln a}\right)\right). \tag{VI.6}$$

This generalizes, in a less precise form, a result that follows from Painlevé asymptotics for the case $\beta = 2$ (see the slide 3 of the presentation [5]).

$$P(TW_2 > a) = \frac{a^{-3/2}}{16\pi} \exp\left(-\frac{4}{3}a^{3/2} + O\left(a^{-3/2}\right)\right).$$

The structure of the proof of Theorem 6.1 is contained in Section VI.2.

Preliminaries and notation. For every initial condition in $[-\infty, +\infty]$, the SDE (VI.4) admits a unique solution, and this solution is increasing in a for each time t (see Fact 3.1 in [48]). From now on, we denote by $(\Omega, \mathcal{F}, \mathbb{P}_{(t,x)})$ the probability space on which the solution of this SDE X begins at time t with the value $X_t = x$

almost surely, and $\mathbb{E}_{(t,x)}$ its corresponding expectation ($x \in [-\infty, +\infty]$). When the starting time is $t = 0$, we simply write $\mathbb{P}_x$ and $\mathbb{E}_x$.

The first passage time to a level $x \in [-\infty, \infty]$ for the diffusion X will be denoted $T_x := \inf\{s \geq 0,\ X_s = x\}$.

Throughout this paper, we study many solutions of stochastic differential equations by comparing them to expressions involving Brownian motion. The letter B will denote a standard Brownian motion on the probability space $(\Omega, \mathcal{F}, P)$. We will use the following easy estimates. For the upper bounds, these inequalities hold for every $x \geq 0$:

$$\begin{cases} P(B_1 > x) & \leq e^{-\frac{1}{2}x^2} \\ P\left(\sup_{t\in[0,1]} |B_t| > x\right) & \leq 4e^{-\frac{1}{2}x^2}. \end{cases} \tag{VI.7}$$

For the lower bounds, there exists $c_{bm} > 0$ such that for every $\varepsilon \in (0, 1)$:

$$P\left(\sup_{t\in[0,1]} |B_t| < \varepsilon\right) \geq \exp\left(-c_{bm}\,\frac{1}{\varepsilon^2}\right). \tag{VI.8}$$

In the sequel, asymptotic notation always refers to $a \to \infty$ unless stated otherwise. Inequalities are meant to hold for all large enough a.

VI.2 Proof of the main Theorem

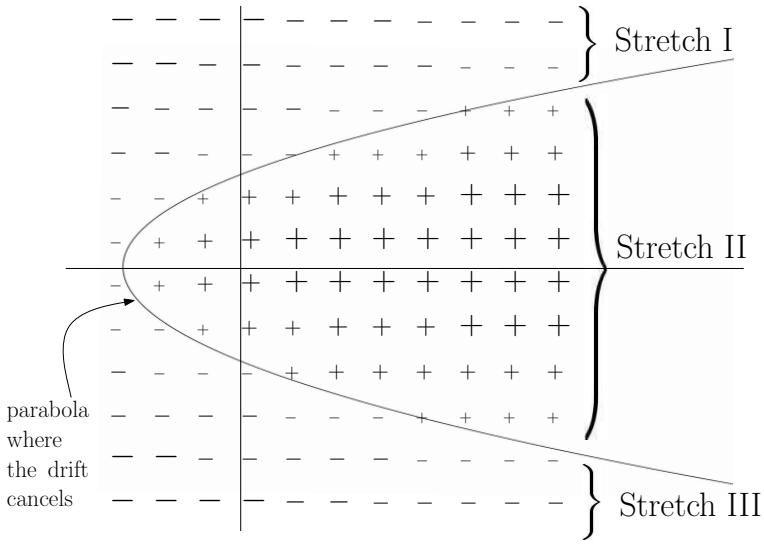

Figure VI.2: The critical parabola $\{(t, x) : t + a - x^2 = 0\}$

This section gives the structure of proof of the Theorem 6.1. The proof of technical points will be treated in the following sections in chronological order.

We rely on the characterization (VI.3), and separate our study of the diffusion (VI.4) into three distinguished parts demarcated by the **critical parabola**

$$\{(t,x) : t + a - x^2 = 0\}$$

where the drift vanishes (see Figure VI.2). The exponential leading term of the asymptotic (VI.6) comes from the part inside the parabola (Stretch II): the drift is positive and makes it difficult for the particle to go down. One part of the logarithmic term comes from the time it takes to reach the upper part of the parabola (Stretch I): the t-term of the drift adds this cost.

VI.2.1 Upper bound, above the parabola

At first, let us approximate the critical parabola by the two horizontal lines $\sqrt{a}$ and $-\sqrt{a}$ (as the blow-down times will be typically very small). Moreover, the part below the parabola gives no contribution for the upper bound, and we use

$$\mathbb{P}_\infty(T_{-\infty} < +\infty) \leq \mathbb{P}_\infty(T_{-\sqrt{a}} < +\infty).$$

The first step is to control the time it takes to reach $\sqrt{a}$. Indeed, as the cost for crossing the interval $[-\sqrt{a}, \sqrt{a}]$ increases with time, we need to find a good lower bound for this time. A comparison with the solution of an ODE linked to our SDE enables us to have a quite precise information: its typical value is $3/8 \ln a/\sqrt{a}$, which does not depend on the factor β. It is very unlikely to happen in time faster than

$$\tau_- = (3/8 - 1/\sqrt{\ln a}) \ln a/\sqrt{a}.$$

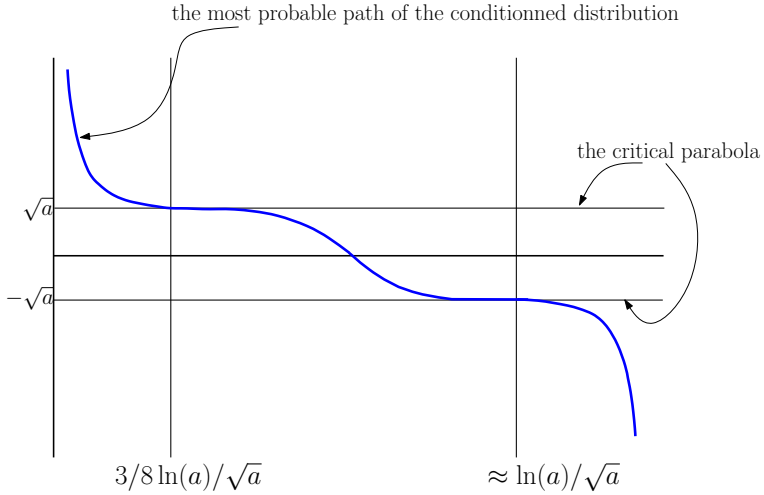

Figure VI.3: The most probable path of the conditioned diffusion for $a = 100$

This is the content of Proposition 6.2. Therefore, using this proposition, the decreasing property in t and the Markov property, we can write:

$$\mathbb{P}_\infty\left(T_{\sqrt{a}} < \tau_-,\ T_{-\sqrt{a}} < \infty\right) \leq \exp\left(-\frac{4}{3}\beta e^{2\sqrt{\ln a}}\right) \mathbb{P}_{\sqrt{a}}(T_{-\sqrt{a}} < \infty). \tag{VI.9}$$

The asymptotic formula (VI.15) given by Lemma 6.6 will highlight the fact that even if the process is considered to start immediately at $\sqrt{a}$ in line (VI.9), the award is small (of the order $\exp(O(\ln a))$ compared to the cost it takes to go down quickly. Consequently, with a much more significant probability, it will take a longer time than the one considered in (VI.9) to reach $\sqrt{a}$. Let us find an upper bound for this case:

$$\mathbb{P}_\infty\left(T_{-\sqrt{a}} < \infty,\ T_{\sqrt{a}} \geq \tau_-\right) \leq \mathbb{P}_{\tau_-,\sqrt{a}}(T_{-\sqrt{a}} < \infty)$$

Thanks to the Markov property, the process X under the probability measure $\mathbb{P}_{\tau_-,\sqrt{a}}$ is identically distributed with $\tilde{X}$ defined with the same SDE (VI.4) where the variable a is replaced by $\tilde{a} := a + \tau_-$ with the initial condition $\tilde{X}(0) = \sqrt{a}$. Observe now $\sqrt{a} < \sqrt{\tilde{a}}$, but it does not matter as we will be allowed to reduce the interval $[-\sqrt{a}, \sqrt{a}]$ a bit without affecting the relevant terms in our asymptotics. More precisely, the interval we will study for the middle is $[-\sqrt{a} + \delta, \sqrt{a} - \delta]$, where $\delta := \sqrt[4]{\ln a/a}$.
Let $\tilde{T}_x$ denote the first passage times of $\tilde{X}$. The inequality $\sqrt{\tilde{a}} - \tilde{\delta} \leq \sqrt{a}$ gives:

$$\mathbb{P}_{\tau_-,\sqrt{a}}(T_{-\sqrt{a}} < \infty) = \mathbb{P}_{\sqrt{a}}(\tilde{T}_{-\sqrt{a}} < \infty) \leq \mathbb{P}_{\sqrt{\tilde{a}}-\tilde{\delta}}(\tilde{T}_{-\sqrt{\tilde{a}}+\tilde{\delta}} < \infty). \tag{VI.10}$$

VI.2.2 Preliminary upper bound inside the parabola

Recall $\delta := \sqrt[4]{\ln a/a}$ we would like to find the asymptotic of:

$$\mathbb{P}_{\sqrt{a}-\delta}\left(T_{-\sqrt{a}+\delta} < \infty\right) \geq \mathbb{P}_{\sqrt{a}}\left(T_{-\sqrt{a}} < \infty\right). \tag{VI.11}$$

The key is Girsanov formula.

Girsanov formula. To evaluate the cost inside the parabola, we use the Cameron-Martin-Girsanov formula which allows us to change the drift coefficient of X and evaluate the relevant probability by analyzing the new process. The issue is to find a suitable new drift. The best would be to have the one corresponding to the conditional distribution of the diffusion X under the event it crosses the critical parabola in a finite time: this would lead to an exact formula. As we are not able to do that, we use an approximation of the conditional diffusion. In this direction,

we introduce a new SDE in which the drift of X is reversed with a correction term given by a function φ:

$$dY_t = \left(-a + Y_t^2 - t + \varphi(Y_t)\right) dt + \frac{2}{\sqrt{\beta}} dB_t.$$

Let T'_x denote the first passage time of the process Y to the level x.

With this diffusion and under some mild assumptions, the Cameron-Martin Girsanov formula gives for every non negative measurable function f and every fixed time $t > 0$ and level $l \in [0, 1]$:

$$\mathbb{E}_{\sqrt{a}-l}\left(f\left(X_u, u \le T_{-\sqrt{a}+l} \wedge t\right)\right) = \mathbb{E}_{\sqrt{a}-l}\left(f\left(Y_u, u \le T'_{-\sqrt{a}+l} \wedge t\right) \exp\left(G_{T'_{-\sqrt{a}+l} \wedge t}(Y)\right)\right). \tag{VI.12}$$

More details about this and the application of the Girsanov formula can be found in Section VI.4.2. The exact expression of $G_{T'_{-\sqrt{a}+l}}(Y)$ contains $\beta/4$ times

$$-\frac{8}{3}a^{3/2} - \frac{4}{3}l^3 + 4\sqrt{a}\, l^2 + 2l\, T'_{-\sqrt{a}+l} - 2\sqrt{a}\, T'_{-\sqrt{a}+l} + \left(\frac{8}{\beta} - 2\right) \int_0^{T'_{-\sqrt{a}+l}} Y_t dt. \tag{VI.13}$$

plus terms involving the function φ.

Notice that we can already see the correct coefficient in front of the main term. We are now confronted with an expectation over the paths of the diffusion Y. To find a good estimate of the exponential martingale, we need to control the first passage time to the level $-\sqrt{a} + l$ and check that the diffusion do not go far above $\sqrt{a}$ when this time is finite (in order to control the last integral in (VI.13)). We will at first focus on a preliminary bound, for which we do not need any result about the first passage time. The price of this approach is that it uses a finer control of the paths which go down.

Control of the paths. To have a good control of the paths, we examine at first a smaller interval than $[\sqrt{a} - \delta, -\sqrt{a} + \delta]$. On this new interval, the diffusion will go down without hitting $\sqrt{a}$ with a sufficiently large probability. Indeed, we show that for $\varepsilon := \frac{4}{\sqrt{\beta}} \sqrt{\ln a} / \sqrt[4]{a}$ we have

$$\mathbb{P}_{\sqrt{a}-\varepsilon}(T_{-\sqrt{a}+\varepsilon} < \infty) = (1 - o(1))\mathbb{P}_{\sqrt{a}-\varepsilon}\left(T_{-\sqrt{a}+\varepsilon} < \infty, T_{-\sqrt{a}+\varepsilon} < T_{\sqrt{a}-\varepsilon/2}\right). \tag{VI.14}$$

This is accomplished by two applications of the strong Markov property. From now on, we denote $T_+ = T_{\sqrt{a}-\varepsilon/2}$, $T_- = T_{-\sqrt{a}+\varepsilon}$ and $\mathcal{A} = \{T_+ > T_-\}$, and have:

$$\mathbb{P}_{\sqrt{a}-\varepsilon}\left(T_- < \infty, \mathcal{A}^c\right) \le \mathbb{P}_{\sqrt{a}-\frac{\varepsilon}{2}}\left(T_- < \infty\right) \le \mathbb{P}_{\sqrt{a}-\frac{\varepsilon}{2}}\left(T_{\sqrt{a}-\varepsilon} < \infty\right) \mathbb{P}_{\sqrt{a}-\varepsilon}\left(T_- < \infty\right).$$

Both inequalities use the fact that the hitting probability of any level below the starting place is decreasing in the starting time of the diffusion X. Rearranging this formula we get

$$\mathbb{P}_{\sqrt{a}-\varepsilon}(T_- < \infty) \leq \frac{\mathbb{P}_{\sqrt{a}-\varepsilon}(T_- < \infty, \mathcal{A})}{\mathbb{P}_{\sqrt{a}-\frac{\varepsilon}{2}}(T_{\sqrt{a}-\varepsilon} = \infty)} .$$

Lemma 6.4 shows that as $a \to \infty$ the denominator converges to 1.

Application of the Girsanov formula. We will now study the right hand side of (VI.14) $\mathbb{P}_{\sqrt{a}-\varepsilon}(T_- < \infty, \mathcal{A})$ which is the probability of an event under which the absolute value of the diffusion is bounded by $\sqrt{a}$.

In order to find an upper bound for the term (VI.13) with $l = \varepsilon$, it would be useful to have a bound on the time T_-. As we do not have any information about that yet, one idea is to choose the function φ such that the coefficient appearing in front of the $\sqrt{a}\,T_-$ term becomes negative. The function φ_1 of Section VI.4.3 works and it gives an upper bound that is sharp up to, but not including, the exponent of the polynomial factor. This is the content of Lemma 6.6. As $a \to \infty$ we conclude

$$\mathbb{P}_{\sqrt{a}-\varepsilon}(T_- < \infty) \leq \exp\left(-\frac{2}{3}\beta a^{3/2} + O(\ln a)\right), \qquad \varepsilon = \tfrac{4}{\sqrt{\beta}}\sqrt{\ln a}/\sqrt[4]{a}. \tag{VI.15}$$

In addition, Lemma 6.6 also shows that with $\xi = c_3 \ln a/\sqrt{a}$ we have

$$\mathbb{P}_{\sqrt{a}-\delta}(\xi \leq T_{-\sqrt{a}+\delta} < \infty) \leq \exp\left(-\frac{2}{3}\beta a^{3/2} - \beta \ln a\right), \qquad \delta = \sqrt[4]{\ln a/a} \tag{VI.16}$$

i.e. long times have polynomially smaller probability than what we expect for normal times.

VI.2.3 Final upper bound inside the parabola

Decomposition according to the time the process spends near $\sqrt{a}$. Let us introduce the last passage time to the level $\sqrt{a} - \delta$:

$$L := \sup\{t \geq 0 \ : \ X_t = \sqrt{a} - \delta\}, \qquad \delta = \sqrt[4]{\ln a/a}.$$

and use the temporary notation $\tau = c \ln a/\sqrt{a}$. We can use the less precise result and, similarly to the part above the parabola, make a change of variable $\hat{a} := a + \tau$. The strong Markov property and the monotonicity gives

$$\mathbb{P}_{\sqrt{a}-\delta}\left(T_{-\sqrt{a}+\delta} < \infty, L > \tau\right) \leq \mathbb{P}_{(\tau,\sqrt{a}-\delta)}\left(T_{-\sqrt{a}+\delta} < \infty\right). \tag{VI.17}$$

Since $\sqrt{a}-\delta \geq \sqrt{\hat{a}}-\hat{\varepsilon}$ we get the upper bound

$$\mathbb{P}_{(0,\sqrt{\hat{a}}-\hat{\varepsilon})}\left(\tilde{T}_{-\sqrt{\hat{a}}+\hat{\varepsilon}}<\infty\right) \leq \exp\left(-2/3\beta a^{3/2}-\beta\ln a\right)$$

as long as c (depending on β) is large enough. The last inequality for some constant $c>0$ follows from the preliminary bound (VI.15). This again is polynomially smaller than the probability we expect for the main event.

For finer information about the last passage time, one can divide the paths according to the value of this last passage time to formalize the idea the process does not earn a lot when it stays near $\sqrt{a}-\delta$.

$$\mathbb{P}_{\sqrt{a}-\delta}(T_{-\sqrt{a}+\delta}<\infty,\ L<\tau) \leq \sum_{k=0}^{\lfloor c\ln a\rfloor} \mathbb{P}\left(L\in[\frac{k}{\sqrt{a}},\frac{k+1}{\sqrt{a}}),\ T_{-\sqrt{a}+\delta}<+\infty\right)$$

The event in the sum implies that X visits $\sqrt{a}-\delta$ in the time interval but not later. By the strong Markov property for the first visit after time $k/\sqrt{a}$ in that time interval and monotonicity, the sum can be bounded above by

$$\lfloor 1+c\ln a\rfloor\, \mathbb{P}_{\sqrt{a}-\delta}\left(L<\frac{1}{\sqrt{a}},\ T_{-\sqrt{a}+\delta}<\infty\right).$$

To complete the picture, we find an upper bound of the process between the times 0 and $1/\sqrt{a}$. This will be possible thanks to a comparison with reflected Brownian motion. Indeed, the drift is non-positive above the critical parabola, and so up to time $1/\sqrt{a}$ the process X_t started at $\sqrt{a+1/\sqrt{a}}$ is stochastically dominated by $\sqrt{a+1/\sqrt{a}}$ plus reflected Brownian motion. This leads to the very rough estimate:

$$\begin{aligned}\mathbb{P}_{\sqrt{a+1/\sqrt{a}}}\left(\sup_{t\in[0,1/\sqrt{a}]} X_t > c_2\sqrt{a}\right) &\leq P\left(\sup_{s\in[0,1/\sqrt{a}]}|B_s|>(c_2-2)\sqrt{a}\right)\\ &\leq \exp\left(-\frac{1}{2}(c_2-2)^2a^{3/2}\right).\end{aligned}$$

If c_2 is large enough (precisely if $c_2>2/\sqrt{3}\sqrt{\beta}+2$), this event becomes negligible compared to the probability to cross the whole parabola. Therefore, we can examine the studied probability under the event that X_t is bounded from above by $c_2\sqrt{a}$ for $t\leq 1/\sqrt{a}$.

We denote by $\mathcal{C}$ the event under which the above conditions are satisfied

$$\mathcal{C}:=\left\{L<1/\sqrt{a},\ \sup_{t\in[0,1/\sqrt{a}]} X_t<c_2\sqrt{a}\right\}.$$

We have just seen that

$$\mathbb{P}_{\sqrt{a}-\delta}\left(T_{-\sqrt{a}+\delta}<\infty\right) \leq (2c\ln a)\mathbb{P}_{\sqrt{a}-\delta}\left(T_{-\sqrt{a}+\delta}<\infty,\ \mathcal{C}\right)+O\left(\exp(-2/3\beta a^{3/2}-\beta\ln a)\right). \tag{VI.18}$$

Application of the Girsanov formula. We will apply the Girsanov formula with a function $\varphi = \varphi_2$ such that it compensates exactly the integral

$$\int_0^{T'_{-\sqrt{a}+\delta}} \left(\frac{8}{\beta} - 2\right) Y_t - 2\sqrt{a}\, dt.$$

The suitable function φ_2 blows up at $-\sqrt{a}$ and $\sqrt{a}$. Therefore we only use it in the interval $[-\sqrt{a}+\delta, \sqrt{a}-\delta]$ and set $\varphi_2 := 0$ outside $[-\sqrt{a}, \sqrt{a}]$. Partially because of those blowups, this function creates error terms involving the first passage time to the level $-\sqrt{a}+\delta$, which, if finite, by (VI.16) can be assumed to satisfy $T_{-\sqrt{a}+\delta} < \xi$. Girsanov's formula applied to the event $\left\{T_{\sqrt{a}+\delta} < \xi,\ \mathcal{C}\right\}$ with (VI.18) leads to the fundamental upper bound of Proposition 6.8:

$$\mathbb{P}_{\sqrt{a}-\delta}\left(T_{-\sqrt{a}+\delta} < \xi\right) \leq \exp\left(-\frac{2}{3}\beta a^{3/2} - \frac{3}{8}\beta \ln a + O(\sqrt{\ln a})\right). \tag{VI.19}$$

Conclusion for the upper bound. Using (VI.19) with $\tilde{a}$ as in the inequality (VI.10) of the part above the parabola, we deduce the upper bound part of (VI.6).

VI.2.4 Outline of the lower bound

The lower bound, as often in the literature, is easier. It suffices to consider the most probable paths. For the part above the parabola, we can write the inequality

$$\mathbb{P}_\infty(T_{-\infty} < \infty) \geq \mathbb{P}_\infty\left(T_{\sqrt{a}} \leq \frac{3}{8}\frac{\ln a}{\sqrt{a}}\right) \mathbb{P}_{\left(\frac{3}{8}\frac{\ln a}{\sqrt{a}}, \sqrt{a}\right)}(T_{-\infty} < \infty)$$

and use Proposition 6.2 to bound the first factor. The second factor can be bounded below by the following:

$$\mathbb{P}_{\left(\frac{3}{8}\frac{\ln a}{\sqrt{a}}, \sqrt{a}\right)}\left(T_{\sqrt{\tilde{a}}-\tilde{\delta}} < \frac{1}{\sqrt{a}}\right) \times \mathbb{P}_{\sqrt{\tilde{a}}-\tilde{\delta}}\left(T_{-\sqrt{\tilde{a}}+\tilde{\delta}} < \tilde{\xi}\right) \times \mathbb{P}_{(\tilde{\xi}, -\sqrt{\tilde{a}}+\tilde{\delta})}(T_{-\infty} < \infty). \tag{VI.20}$$

where $\tilde{a} := 3/8 \ln a/\sqrt{a} + 1/\sqrt{a}$.

A domination by a Brownian motion with drift permits to deal with the first term of (VI.20) which is of the order $\exp(-O(\sqrt{\ln a}))$. The middle term can be controlled with the same event $\tilde{\mathcal{C}}$ introduced for the upper bound with a replaced by $\tilde{a}$. We apply Girsanov formula directly with the SDE used for the precise result of the upper bound to obtain Proposition 6.8:

$$\mathbb{P}_{\sqrt{\tilde{a}}-\tilde{\delta}}\left(T_{-\sqrt{\tilde{a}}+\tilde{\delta}} < \tilde{\xi},\, \tilde{\mathcal{C}}\right) \geq \exp\left(-\frac{2}{3}\beta\tilde{a}^{3/2} - \frac{3}{8}\beta \ln \tilde{a} + o(\ln \tilde{a})\right) \mathbb{P}_{\sqrt{\tilde{a}}-\tilde{\delta}}\left(T'_{-\sqrt{\tilde{a}}+\tilde{\delta}} < \tilde{\xi},\, \tilde{\mathcal{C}}'\right)$$

(recall the "prime" notation deals with the "new" diffusion Y).

A comparison with the solution of a simple differential equation will show that the solution of the new SDE indeed has a "large" probability to go down to $-\sqrt{\tilde{a}}+\tilde{\delta}$ before the time $\tilde{\xi}$. This is the content of Lemma 6.9.

We conclude the proof of the lower bound by checking that the last term of (VI.20) is also negligible: the proof is similar to the study above the parabola and can be found in Proposition 6.10. □

VI.3 Above the parabola

We show at first that we need a certain amount of time to reach the level $\sqrt{a}$, typically a time $\tau := 3/8 \ln a/\sqrt{a}$. The following Proposition proves indeed that the probability the process hits $\sqrt{a}$ significantly before τ is small, but becomes quite large if this hitting happens around the time τ.

Proposition 6.2. *The following upper bound holds for all sufficiently large a:*

$$\mathbb{P}_\infty\left(T_{\sqrt{a}} \leq \left(\frac{3}{8}-\frac{1}{\ln a}\right)\frac{\ln a}{\sqrt{a}}\right) \leq \exp\left(-\frac{4}{3}\beta e^{2\sqrt{\ln a}}\right). \tag{VI.21}$$

There exists $c_0 > 0$ depending only on β such that we also have the lower bound:

$$\mathbb{P}_\infty\left(T_{\sqrt{a}} \leq \frac{3}{8}\frac{\ln a}{\sqrt{a}}\right) \geq c_0\frac{1}{\sqrt{\ln a}}. \tag{VI.22}$$

Proof. **First part.** Fix $\sigma \in (0, 1/8)$ and let

$$\tau' := \left(\frac{3}{8}-\sigma\right)\frac{\ln a}{\sqrt{a}}.$$

It helps to remove the time dependence from the drift coefficient of (VI.4). In this direction, consider the SDE:

$$\begin{cases} dY_t &= (a - Y_t^2)dt + \frac{2}{\sqrt{\beta}}dB_t \\ Y_0 &= +\infty. \end{cases} \tag{VI.23}$$

The process X stochastically dominates Y. Therefore, if $T^Y_{\sqrt{a}}$ is the first passage time to $\sqrt{a}$ for the diffusion Y, we have:

$$\mathbb{P}_\infty\left(T_{\sqrt{a}} \leq \tau'\right) \leq \mathbb{P}\left(T^Y_{\sqrt{a}} \leq \tau'\right).$$

Now, we study the difference $Z_t := Y_t - \frac{2}{\sqrt{\beta}} B_t$ where B is the Brownian motion driving Y in (VI.23). It satisfies the (random) ODE:

$$dZ_t = \left[a - Z_t^2 \left(1 + \frac{2}{\sqrt{\beta}} \frac{B_t}{Z_t} \right)^2 \right] dt. \tag{VI.24}$$

Define $M := \sup\{|B_t|, t \in [0, \tau']\}$ and notice that thanks to the Brownian tail (VI.7),

$$\mathbb{P}(M \geq 1) \leq 4 \exp\left(-\frac{1}{2(3/8 - \sigma)} \frac{\sqrt{a}}{\ln a} \right).$$

By definition, for all $t \in [0, \tau' \wedge T^Y_{\sqrt{a}}]$, the process Z_t is above $\sqrt{a} - 2/\sqrt{\beta} M$ and consequently above the (random) solution of the differential equation:

$$\begin{cases} F'(t) = a - C f^2(t) \\ F(0) = +\infty \end{cases}$$

where C has the following expression:

$$C := \left(1 + \frac{4}{\sqrt{\beta}} \frac{M}{\sqrt{a} - \frac{2}{\sqrt{\beta}} M} \right)^2.$$

This differential equation admits almost surely the unique solution

$$\forall t \geq 0, \ F(t) = \sqrt{\frac{a}{C}} \coth(\sqrt{aC}\, t).$$

Hence,

$$\begin{aligned} \mathbb{P}\left(T^Y_{\sqrt{a}} \leq \tau' \right) &\leq \mathbb{P}\left(\inf_{t \in [0, \tau']} \left(F(t) + \frac{2}{\sqrt{\beta}} B_t \right) \leq \sqrt{a} \right) \\ &\leq \mathbb{P}\left(F(\tau') - \sqrt{a} \leq -\frac{2}{\sqrt{\beta}} \inf_{t \in [0, \tau']} B_t \right). \end{aligned} \tag{VI.25}$$

Let us compute $F(\tau')$:

$$F(\tau') = \sqrt{\frac{a}{C}} \frac{1 + e^{-2\tau' \sqrt{aC}}}{1 - e^{-2\tau' \sqrt{aC}}} = \sqrt{\frac{a}{C}} \left(1 + 2e^{-2\tau' \sqrt{aC}} + O\left(e^{-4\tau' \sqrt{aC}} \right) \right).$$

Under the event $\{M \leq 1\}$,

$$\sqrt{C} = 1 + \frac{2}{\sqrt{\beta}} \frac{M}{\sqrt{a}} + O\left(\frac{1}{a} \right).$$

This implies:

$$\sqrt{\frac{a}{C}} = \sqrt{a} - \frac{2}{\sqrt{\beta}}M + O\left(\frac{1}{\sqrt{a}}\right), \tag{VI.26}$$

and

$$\begin{aligned}\exp\left(-2\tau'\sqrt{aC}\right) &= \exp\left(-2(3/8-\sigma)\ln a\left(1+O\left(\frac{1}{\sqrt{a}}\right)\right)\right)\\ &= \frac{1}{a^{\frac{3}{4}-2\sigma}} + O\left(\frac{\ln a}{a^{\frac{5}{4}-2\sigma}}\right).\end{aligned} \tag{VI.27}$$

Taylor expansions (VI.26) and (VI.27) give:

$$\begin{aligned}F(\tau') &= \left(\sqrt{a} - \frac{2}{\sqrt{\beta}}M + O\left(\frac{1}{\sqrt{a}}\right)\right)\left(1 + \frac{2}{a^{3/4-2\sigma}} + O\left(\frac{\ln a}{a^{5/4-2\sigma}}\right)\right)\\ &= \sqrt{a} - \frac{2}{\sqrt{\beta}}M + \frac{2}{a^{1/4-2\sigma}} + O\left(\frac{1}{\sqrt{a}}\right).\end{aligned} \tag{VI.28}$$

Inequality (VI.25) becomes:

$$\begin{aligned}\mathbb{P}_\infty\left(T_{\sqrt{a}} \le \tau'\right) &\le \mathbb{P}\left(F(\tau') - \sqrt{a} \le \frac{2}{\sqrt{\beta}}M,\ M \le 1\right) + \mathbb{P}(M > 1)\\ &\le \mathbb{P}\left(\sqrt{\beta}\frac{1}{a^{1/4-2\sigma}} + O\left(\frac{1}{\sqrt{a}}\right) \le M,\ M \le 1\right) + \mathbb{P}(M > 1)\\ &\le 4\exp\left(-\frac{4}{3}\beta\frac{a^{4\sigma}}{\ln a} + o\left(\frac{a^{4\sigma}}{\ln a}\right)\right).\end{aligned}$$

If we take $\sigma = \frac{1}{\sqrt{\ln a}}$, we have:

$$\mathbb{P}_\infty\left(T_{\sqrt{a}} \le \left(\frac{3}{8} - \frac{1}{\sqrt{\ln a}}\right)\frac{\ln a}{\sqrt{a}}\right) \le 4\exp\left(-\frac{4}{3}\beta e^{4\sqrt{\ln a} - \ln\ln a}\right),$$

and so inequality (VI.21) holds.

Second part. The proof is similar. Let us check the main lines. At first, we have:

$$\mathbb{P}_\infty\left(T_{\sqrt{a}} \le \tau\right) \ge \mathbb{P}_\infty\left(T_{\sqrt{a}+\frac{15}{\sqrt[4]{a}}} \le \tau - \frac{1}{\sqrt{a}}\right) \times \mathbb{P}_{\sqrt{a}+\frac{15}{\sqrt[4]{a}}}\left(T_{\sqrt{a}} \le \frac{1}{\sqrt{a}}\right).$$

Now the process $(X_t,\ t \in [0, T_{\sqrt{a}}])$ starting at a value above $\sqrt{a}$ has a non-positive drift and is therefore stochastically dominated by Brownian motion. Thus the second factor can be bounded below by

$$P\left(B_{\frac{1}{\sqrt{a}}} \ge \frac{15}{\sqrt[4]{a}}\right) = P(B_1 \ge 15).$$

For the first factor, instead of the SDE (VI.23) we choose:

$$\begin{cases} dY_t &= (a+\tau-Y_t^2)dt + \frac{2}{\sqrt{\beta}}dB_t \\ Y_0 &= +\infty \end{cases} \tag{VI.29}$$

and study the difference

$$Z_t := Y_t - \frac{2}{\sqrt{\beta}}B_t.$$

Set $M' := \sup\{B_t,\ t \in [0, \tau - 1/\sqrt{a}]\}$. For every $t \in [0, (\tau - 1/\sqrt{a}) \wedge T^Y_{\sqrt{a}}]$, the process Z_t is below

$$F(t) := \sqrt{\frac{a+\tau}{C}}\coth\left(\sqrt{(a+\tau)C}\,t\right)$$

where

$$C := 1 - \frac{4}{\sqrt{\beta}}\frac{M'}{\sqrt{a} - \frac{2}{\sqrt{\beta}}M'}.$$

The Taylor expansion of $F(\tau - 1/\sqrt{a})$ under $\{M' \leq 1\}$ gives:

$$F\left(\tau - \frac{1}{\sqrt{a}}\right) = \sqrt{a} + \frac{2e^2}{a^{1/4}} + \frac{2}{\sqrt{\beta}}M' + O\left(\frac{1}{\sqrt{a}}\right).$$

Therefore

$$\mathbb{P}_\infty\left(T_{\sqrt{a}+\frac{15}{\sqrt[4]{a}}} \leq \tau - \frac{1}{\sqrt{a}}\right) \geq P\left(F(\tau - \frac{1}{\sqrt{a}}) - \frac{2}{\sqrt{\beta}}B\left(\tau - \frac{1}{\sqrt{a}}\right) \leq \sqrt{a} + \frac{15}{\sqrt[4]{a}}\right).$$

Since $M' - B(\tau - 1/\sqrt{a})$ has the same law as the reflected Brownian motion at time $\tau - 1/\sqrt{a}$ and $15 - 2e^2 > 0$, we get the lower bound

$$P\left(\frac{2}{\sqrt{\beta}}\left|B\left(\tau - \frac{1}{\sqrt{a}}\right)\right| \leq \frac{15-2e^2}{\sqrt[4]{a}}\right) \geq c_0\frac{1}{\sqrt{\ln a}}. \tag{VI.30}$$

Here c_0 in represents an adequate constant depending only on β. □

VI.4 Inside the parabola

The exponential cost comes from this stretch. This section will be devoted to the proof of the following Proposition:

Proposition 6.3. *Recall $\delta := \sqrt[4]{\ln a}/\sqrt[4]{a}$, we have:*

$$\mathbb{P}_{\sqrt{a}-\delta}(T_{-\sqrt{a}+\delta} < \infty) = \exp\left(-\frac{2}{3}\beta a^{3/2} - \frac{3}{8}\beta\ln a + O(\sqrt{\ln a})\right).$$

VI.4.1 Control of the path behavior

Here we show a lemma about the return to $-\sqrt{a}+\varepsilon$.

Lemma 6.4. *For* $\varepsilon := \frac{4}{\sqrt{\beta}}\sqrt{\ln a}/\sqrt[4]{a}$ *as* $a \to \infty$ *we have* $\mathbb{P}_{\sqrt{a}-\varepsilon/2}(T_{\sqrt{a}-\varepsilon} = \infty) \to 1$.

Proof. Certainly, the probability that X begun at $\sqrt{a}-\varepsilon/2$ never reaches $\sqrt{a}-\varepsilon$ is bounded below by the same probability where X is replaced by its reflected (downward) at $\sqrt{a}-\varepsilon/2$ version. Further, when restricted to the space interval $[\sqrt{a}-\varepsilon, \sqrt{a}-\varepsilon/2]$, the X-diffusion has drift everywhere bounded below by $t + 1/2\sqrt{a}\,\varepsilon$. Thus, we may consider instead the same probability for the appropriate reflected Brownian motion with quadratic drift.

To formalize this, it is convenient to shift orientation. Let now

$$\bar{X} := \frac{2}{\sqrt{\beta}}B(t) - \frac{1}{2}t^2 - q\,t, \qquad q := \frac{1}{2}\sqrt{a}\,\varepsilon.$$

Let X^* denote reflected (upward) at the origin. Namely,

$$X^*(t) = \bar{X}(t) - \inf_{s\le t}\bar{X}(s). \tag{VI.31}$$

If we can show that $P(X^*$ never reaches $\varepsilon/2)$ tends to 1 when $a \to \infty$, then it will also be the case for the X-probability in question.

We need to introduce the first hitting time of level y for the new process $\bar{X}$: $\tau_y := \inf\{t \ge 0 \,:\, \bar{X}(t) = y\}$. For each $n \in \mathbb{N}$, define the event:

$$D_n = \left\{\bar{X}(t) \text{ hits } -(n-1)\varepsilon/4 \text{ for some } t \text{ between } \tau_{-n\varepsilon/4} \text{ and } \tau_{-(n+1)\varepsilon/4}\right\}.$$

From the representation (VI.31), one can see that $\{\sup_{t\ge0} X^*(t) > \varepsilon/2\}$ implies that some D_n must occur. Indeed, for this $\bar{X}$ must go above its past minimum by at least $\varepsilon/2$, so in this case it would have to retreat at least one level before establishing reaching a new minimum level among multiples of $\varepsilon/4$. Define the event

$$\mathcal{E} = \left\{\bar{X}(t) \ge -\frac{1}{2}t^2 - 2qt - 1\right\},$$

The event $\mathcal{E}^c$ is equivalent to the Brownian motion $\frac{2}{\sqrt{\beta}}B(t)$ hitting a line of slope $-q$ starting at -1. Since $|B(t)|$ is sublinear, this will not happen for large enough q. So

$$P(\mathcal{E}^c) \to 0 \quad \text{when } a \to +\infty. \tag{VI.32}$$

On $\mathcal{E}$, when the following term under the square root is positive, we have

$$\tau_{-x} \geq \sqrt{2}\sqrt{2q^2 + x - 1} - 2q$$

Assume that $q \geq 1$. A calculation shows that if $q \leq \sqrt{x}/2$ then the above inequality implies $\tau_{-x} \geq \sqrt{x}/2$. So on $\mathcal{E}$ for all $x \geq 0$ we have

$$\tau_{-x} + q \geq q \vee \sqrt{x}/2,$$

and so for all $t \geq 0$

$$\bar{X}(\tau_{-x} + t) - \bar{X}(\tau_{-x}) \leq \frac{2}{\sqrt{\beta}} B(\tau_{-x} + t) - (q \vee \sqrt{x}/2)t. \tag{VI.33}$$

Setting $x = \varepsilon n/4$ we see that for all $n \geq 0$

$$P\left(D_n \cap \mathcal{E} \,|\, \mathcal{F}_{\tau_{-n\varepsilon/4}}\right) \leq P\left(\text{the process on the right of (VI.33) hits } \varepsilon/4 \text{ before } -\varepsilon/4\right).$$

The distribution of that process is just Brownian motion with drift. By a stopping time argument for the exponential martingale $\exp(\gamma \hat{B}_t - t\gamma^2/2)$ with $\gamma = (q \vee \sqrt{n\varepsilon}/4)\sqrt{\beta}$ the above probability equals $1/(1 + e^{\gamma\varepsilon\sqrt{\beta}/8}) \leq e^{-\gamma\varepsilon/\sqrt{\beta}/8}$. We get

$$P(D_n \cap \mathcal{E}) \leq \exp\left(-(q \vee \sqrt{n\varepsilon}/4)\beta\varepsilon/8\right).$$

Recall that

$$P\left(\sup_{t\geq 0} X^*(t) > \varepsilon/2\right) \leq P(\mathcal{E}^c) + \sum_{n\geq 0} P(\mathcal{E} \cap D_n).$$

The sum of terms where $n\varepsilon \leq (4q)^2$ is bounded above by $(1 + (4q)^2\varepsilon^{-1})e^{-\varepsilon q\beta/8}$. The sum of the rest is not more than

$$\sum_{n\geq (4q)^2/\varepsilon} \exp\left(-\varepsilon^{3/2}\beta\sqrt{n}/32\right) \leq c_1 \frac{q}{\varepsilon^2} \exp\left(-\varepsilon q\beta/8\right),$$

where c_1 depends on β only. Replacing ε and q by their expressions in terms of a, and using (VI.32) we obtain:

$$P\left(\sup_{t\geq 0} X^*(t) > \varepsilon/2\right) \leq P(\mathcal{E}^c) + a^{3/4+o(1)} e^{-(\beta/16)(16/\beta)\ln a} = o(1). \qquad \square$$

VI.4.2 Application of the Girsanov formula

For every $\varphi \in C^2(\mathbb{R}, \mathbb{R})$ such that $\sup_{x\in\mathbb{R}} |\varphi(x)| \leq \sqrt{a}$ (the function φ is in fact small compared to the other terms, and it will be chosen after), we would like to consider the following SDE (defined on the same probability spaces as (VI.4)):

$$dY_t = \left(-a + Y_t^2 - t + \varphi(Y_t)\right) dt + \frac{2}{\sqrt{\beta}} dB_t \tag{VI.34}$$

Remark 6.5. *The drift of this SDE is the reversal of the drift in the initial SDE (VI.4). The solution of the new SDE starting around $\sqrt{a}$ is a good candidate for the process X conditioned to blow up to $-\infty$ when a goes to $+\infty$. Its expression comes from minimizing (approximately) the potential:*

$$\int_0^s (g'(u) - (u + a - g^2(u))^2) du.$$

over the set of functions g such that $g(0) = \sqrt{a}$ and $g(s) = -\sqrt{a}$.

If we look at events under which the diffusion is bounded, it is easy to modify the drift of the new diffusion outside the studied domain and prove that the Novikov condition is satisfied as long as the examined events are in the space $\mathcal{F}_t$ for a fixed $t > 0$. Let us fix a time $t > 0$, a level $l \in (0, 1)$ and denote by $T_\pm := T_{\pm(\sqrt{a}-l)}$ the first passage times to $\pm(\sqrt{a} - l)$ for the diffusion X (respectively $T'_\pm := T'_{\pm(\sqrt{a}-\delta)}$ for Y). We take an event $E \in \mathcal{F}_t \cap \mathcal{F}_{T'_-}$ under which the paths of the diffusion are bounded by a deterministic value, which can depend on a and β. Since E is $\mathcal{F}_t$-measurable, Girsanov's theorem gives

$$\mathbb{P}_{\sqrt{a}-l}(E) = \mathbb{E}_{\sqrt{a}-l}\left(1_E \exp(G_t(Y))\right).$$

The Radon Nikodym density $\exp(G_{\cdot\wedge t\wedge T'_-}(Y))$ is a bounded martingale, and E is $\mathcal{F}_{T'_-}$-measurable, so by the optional stopping theorem the above quantity equals

$$\mathbb{E}_{\sqrt{a}-l}\left(\mathbb{E}_{\sqrt{a}-l}\left(1_E \exp(G_t(Y))\middle|\mathcal{F}_{T'_-}\right)\right) = \mathbb{E}_{\sqrt{a}-l}\left(1_E \ \exp\left(G_{T'_-\wedge t}(Y)\right)\right). \tag{VI.35}$$

In the following, we consider E of the form $E = \{T_- < \infty\} \cap E_1$. The assumption on E requires E_1 being an event under which the diffusion is bounded from above. Taking the limit $t \to +\infty$ leads to the fundamental formula:

$$\mathbb{P}_{\sqrt{a}-l}(T_- < \infty, E_1) = \mathbb{E}_{\sqrt{a}-l}\left(1_{T'_-<\infty,\, E'_1} \ \exp\left(G_{T'_-}(Y)\right)\right). \tag{VI.36}$$

Thanks to Itô's formula we can write the exponential martingale $\frac{4}{\beta}G_{T'_-}(Y)$ as

$$2\int_0^{T'_-} (t + a - Y_t^2)\, dY_t \tag{VI.37}$$
$$+ \phi(Y_0) - \phi(Y_{T'_-})$$
$$+ \int_0^{T'_-} \frac{2}{\beta}\varphi'(Y_t) + \frac{1}{2}\varphi(Y_t)^2 + \varphi(Y_t)(Y_t^2 - a - t)\, dt, \tag{VI.38}$$

where φ' denotes the derivative of φ and ϕ the indefinite integral. Again by Itô's formula, we can compute the first term (VI.37) above.

$$\text{(VI.37)} = 2a(Y_{T'_-} - Y_0) - \frac{2}{3}(Y_{T'_-}^3 - Y_0^3) + \left(\frac{8}{\beta} - 2\right)\int_0^{T'_-} Y_t dt + 2T'_- Y_{T'_-}.$$

Replacing $Y_{T'_-}$ by its value, we obtain the expression (valid under E):

$$(\text{VI.37}) = -\frac{8}{3}a^{3/2} - \frac{4}{3}l^3 + 4\sqrt{a}\,l^2 + 2\,l\,T'_- - 2\sqrt{a}T'_- + \left(\frac{8}{\beta} - 2\right)\int_0^{T'_-} Y_t dt. \quad \text{(VI.39)}$$

VI.4.3 The preliminary upper bound

Let c_1 be a constant such that $c_1 > (|8/\beta - 2| - 2) \vee 0$. Recall that

$$\delta := \sqrt[4]{\ln a/a}, \qquad \varepsilon = \frac{4}{\sqrt{\beta}}\sqrt{\ln a}/\sqrt[4]{a}$$

and take the function φ_1 defined by

$$\varphi_1 : x \mapsto \begin{cases} \frac{c_1\sqrt{a}}{a-x^2} & \text{if } x \in (-\sqrt{a}+\delta, \sqrt{a}-\delta) \\ 0 & \text{if } x \notin (-\sqrt{a}, \sqrt{a}) \end{cases} \quad \text{(VI.40)}$$

and extend this function on the entire real line such that φ_1 remains a smooth function supported on $[-\sqrt{a}, \sqrt{a}]$ (this is possible for all large enough "a"). Of course, there are many functions satisfying the above conditions but we just need to fix one. Let ϕ_1 be an antiderivative of φ_1.

A first step is to prove a less precise upper bound which does not give us the constant in front of the logarithm term of (VI.6). In this subsection, the notations Y, T'_-, $\mathcal{A}'$ will always refer to the definitions using this particular φ_1. We have the events

$$\mathcal{A} = \{T_{\varepsilon-\sqrt{a}} < T_{\sqrt{a}-\varepsilon/2}\}, \qquad \mathcal{C} = \{T_{\delta-\sqrt{a}} < T_{c_2\sqrt{a}}, L \le \frac{1}{\sqrt{a}}\}.$$

Lemma 6.6. *(a) The following inequality holds:*

$$\mathbb{P}_{\sqrt{a}-\varepsilon}(T_{\varepsilon-\sqrt{a}} < \infty,\ \mathcal{A}) \le \exp\left(-\frac{2}{3}\beta a^{3/2} + O(\ln a)\right). \quad \text{(VI.41)}$$

(b) for some $c_3 \ge 1$ we also have

$$\mathbb{P}_{\sqrt{a}-\delta}\Big(c_3 \ln a/\sqrt{a} \le T_{\delta-\sqrt{a}} < \infty,\ \mathcal{C}\Big) \le \exp\left(-\frac{2}{3}\beta a^{3/2} - \beta \ln a\right). \quad \text{(VI.42)}$$

Part (a) with Lemma 6.4 immediately give the following.

Corollary 6.7. *The following upper bound holds:*

$$\mathbb{P}_{\sqrt{a}-\varepsilon}(T_- < \infty) \le \exp\left(-\frac{2}{3}\beta a^{3/2} + O(\ln a)\right).$$

Proof. **Part (a).** First let $T_- = T_{\sqrt{a}-\varepsilon}$. Consider the process Y defined with the function φ_1. The equality (VI.35) gives:

$$\mathbb{P}_{\sqrt{a}-\varepsilon}\Big(T_- < \infty,\ \mathcal{A}\Big) = E_{\sqrt{a}-\varepsilon}\Big(1_{\{T'_-<\infty\ \mathcal{A}'\}}\ \exp\Big(G_{T'_-}(Y)\Big)\Big)$$

with $G_{T'_-}(Y)$ given by (VI.37-VI.38).

To find an upper bound of the last term (VI.38) in G, we remark that the chosen function φ_1 on $[-\sqrt{a}+\varepsilon, \sqrt{a}-\varepsilon/2]$ attains its maximum at time $\sqrt{a}-\varepsilon/2$. Under the event $\mathcal{A}'$, it gives:

$$(\text{VI.38}) \le \left(\frac{2c_1^2 + 8/\beta c_1}{\varepsilon^2} - c_1\sqrt{a}\right) T'_-. \tag{VI.43}$$

Moreover:

$$\phi_1(Y_0) - \phi_1(Y_{T'_-}) = c_1\ \ln\left(2\frac{\sqrt{a}}{\varepsilon} + 1\right). \tag{VI.44}$$

Thanks to (VI.39), (VI.43) and (VI.44), we deduce:

$$\begin{aligned}\frac{4}{\beta}G_{T'_-}(Y) + \frac{8}{3}a^{3/2} \le 4\sqrt{a}\,\varepsilon^2 + 2\varepsilon T'_- + \left(\left|\frac{8}{\beta} - 2\right| - 2 - c_1\right)\sqrt{a}T'_- \\ + \left(\frac{8}{\beta}c_1 + 2c_1^2\right)\frac{1}{\varepsilon^2}T'_- + c_1\ \ln\left(2\frac{\sqrt{a}}{\varepsilon} + 1\right).\end{aligned}$$

We now take c_1 such that $|8/\beta - 2| - 2 - c_1 < 0$ and the coefficient in front of $\sqrt{a}T'_-$ becomes negative and dominates the terms involving T'_-. The last one creates the logarithmic error, and (VI.41) follows from

$$G_{T'_-}(Y) \le -\frac{2}{3}\beta a^{3/2} + \left(\frac{3}{16}c_1\beta + 16\right)\ln a + o(\ln a).$$

Part (b). Now let $T_- = T_{\sqrt{a}-\delta}$. Just as in part (a), we need to bound the Girsanov terms. To find an upper bound of the last term (VI.38), namely

$$\int_0^{T'_-} \frac{2}{\beta}\varphi'(Y_t) + \frac{1}{2}\varphi(Y_t)^2 + \varphi(Y_t)(Y_t^2 - a - t)\,dt$$

note that φ^2 and φ' are both uniformly $o(\sqrt{a})$. On the other hand, we have $\varphi(Y_t)(a - Y^2)$ is nonnegative. Moreover, it is greater than $c_1\sqrt{a} + o(\sqrt{a})$ as long as $L' \le t \le T'_-$. So on $\mathcal{C}'$ we have the lower bound

$$(\text{VI.38}) \le o(\sqrt{a})T'_- - c_1\sqrt{a}(T'_- - L'). \tag{VI.45}$$

The other inequalities are similar to part (a) with δ replaced by ε, except the last term in (VI.39) gives an extra term due to the fact that Y is only bounded by $c_2\sqrt{a}$ up to time L'.
Thanks to (VI.39), (VI.45) and (VI.44), we deduce:

$$\frac{4}{\beta}G_{T'_-}(Y)+\frac{8}{3}a^{3/2}\le 4\sqrt{a}\,\delta^2+2\delta T'_-+\left(\left|\frac{8}{\beta}-2\right|-2-c_1\right)\sqrt{a}T'_- \\ +(c_1+c_2)\sqrt{a}L'+o(\sqrt{a})T'_-+c_1\,\ln\left(2\frac{\sqrt{a}}{\delta}+1\right).$$

From part (a), we have $c:=|8/\beta-2|-2-c_1<0$. We chose $c_3\ge 1$ large enough so that the terms involving $T'_-\ge c_3\ln a/a$ together with the $\ln a$ term coming from the antiderivative are less than $-\beta\ln a$, i.e. $\frac{\beta}{4}c_3c+\frac{3}{16}c_1\beta<-\beta$. This completes the proof of (VI.42) since

$$G_{T'_-}(Y)\le -\frac{2}{3}\beta a^{3/2}-\beta\ln a+o(\ln a).$$ □

VI.4.4 Precise asymptotics for the exponent

Recall $\delta:=\sqrt[4]{\ln a/a}$, L the last passage time to $\sqrt{a}-\delta$, and the event introduced for technical reasons:

$$\mathcal{C}:=\left\{L<1/\sqrt{a},\ \sup_{t\in[0,1/\sqrt{a}]}X_t<c_2\sqrt{a}\right\}$$

defined in the outline of the proof. We will study in this section $\mathbb{P}_{\sqrt{a}-\delta}\left(T_{-\sqrt{a}+\delta}<\infty,\ \mathcal{C}\right)$.

In order to obtain the coefficient in front of the logarithm term, we need to be more precise in our analysis and we will look more carefully at T_-, the first passage time to $-\sqrt{a}+\delta$ of X.

Our tool is again the Cameron-Martin-Girsanov formula with a drift containing a different function φ. Let us define φ_2 in the following way:

$$\varphi_2:x\mapsto\begin{cases}\frac{(8/\beta-2)x-2\sqrt{a}}{a-x^2} & \text{if } x\in(-\sqrt{a}+\delta/2,\sqrt{a}-\delta)\\ 0 & \text{if } x\notin(-\sqrt{a},\sqrt{a})\end{cases} \tag{VI.46}$$

and extend it such that it remains a smooth function on $\mathbb{R}$ satisfying: $\sup|\varphi|\le\sqrt[4]{a}$ and $\sup|\varphi'|\le\sqrt{a}$ (this is possible for a large enough "a"). Similarly to the previous subsection, the notations Y, T'_-, $\mathcal{C}'$ etc. refers to definitions with this chosen function.

Proposition 6.8. *We have*

$$\mathbb{P}_{\sqrt{a}-\delta}\left(T_-<c_3\ln a/\sqrt{a},\ \mathcal{C}\right) \\ =\exp\left(-\frac{2}{3}\beta a^{3/2}-\frac{3}{8}\beta\ln a+O\left(\sqrt{\ln a}\right)\right)\mathbb{P}_{\sqrt{a}-\delta}\left(T'_-<c_3\ln a/\sqrt{a},\ \mathcal{C}'\right)$$

Proof. Let us compute the new Radon-Nikodym derivative according to the position of Y using the relations (VI.37-VI.38) and (VI.13).

At first, the term $\phi(Y_0) - \phi(Y_{T'_-})$ is equal to $-3/2 \ln a$. Moreover,

$$\forall y \in \left[-\sqrt{a}+\delta, \sqrt{a}-\delta\right], \quad -2\sqrt{a} + \left(\frac{8}{\beta} - 2\right) y + (y^2 - a)\varphi(y) = 0.$$

Consequently, there exists a constant $c' > 0$, depending only on β, such that for every $y \in [-\sqrt{a}+\delta, \sqrt{a}-\delta]$,

$$\left| -2\sqrt{a} + \left(\frac{8}{\beta} - 2\right) y + (y^2 - a)\varphi(y) + \frac{2}{\beta}\varphi'(y) + \frac{1}{2}\varphi(y)^2 \right| \leq \frac{c'a}{(a-y^2)^2} \leq \frac{2c'}{\delta^2}.$$

There is another constant $c'' > 0$ such that

$$\left| \int_0^{T'_-} u\, \varphi(Y_u) du \right| \leq \frac{c''}{\delta} T'^2_-.$$

For every $y \geq \sqrt{a} - \delta$,

$$\left| \frac{2}{\beta}\varphi'(y) + \frac{1}{2}\varphi(y)^2 + \varphi(y)(y^2 - a - t) \right| \leq \left(\frac{2}{\beta} + 1\right)\sqrt{a}$$

Putting all together and using the upper bound on the last passage time to $\sqrt{a} - \delta$ contained in $\mathcal{C}$, we obtain:

$$\left| \frac{4}{\beta} G_{T'_-}(Y) + \frac{8}{3}a^{3/2} + \frac{3}{2}\ln a \right| \leq 4\sqrt{a}\delta^2 + \frac{2c'}{\delta^2} T'_- + \frac{c''}{\delta} T'^2_- + 2\delta T'_- + \frac{4}{3}\delta^3 + \left(\frac{2}{\beta} + 1\right).$$

If $\{T'_- \leq c_3 \ln a/\sqrt{a}\}$ holds,

$$\frac{2c'}{\delta^2} T'_- + \frac{c''}{\delta} T'^2_- + 2\delta T'_- + \frac{4}{3}\delta^3 \leq 2c'\sqrt{\ln a} + O(1).$$

Under $\{T'_- < c_3 \ln a/\sqrt{a}\} \cap \mathcal{C}'$, we conclude

$$G_{T'_-}(Y) = -\frac{2}{3}\beta a^{3/2} - \frac{3}{8}\beta \ln a + O\left(\sqrt{\ln a}\right) \qquad \square$$

To complete the study inside the parabola for the lower bound, we prove:

Lemma 6.9. *There exists $c_4 > 0$ depending only on β such that with $\xi = c_3 \ln a/\sqrt{a}$*

$$\mathbb{P}_{\sqrt{a}-\delta}(T'_- < \xi,\ \mathcal{C}') \geq \exp\left(-c_4\sqrt{\ln a}\right).$$

Proof. For the lower bound we can replace the event C' by the event that $T'_+ = T'_{\sqrt{a}-\delta/2}$ is infinite, i.e. the corresponding level is never hit. We will show that this events happens as long as

$$M := \sup\{|B_t|,\ t \in [0,\xi]\} \leq \delta\sqrt{\beta}/5,$$

which by the Brownian motion estimate (VI.8) has the right probability.

Let $\xi = c_3 \ln a/\sqrt{a}$. Again, we compare our equation to an ODE. The quantity $Z = X - B$ on $[0,\xi]$ satisfies

$$Z' = -(Z-B)^2 + t - a \leq Z^2 + a + \tfrac{4}{\sqrt{\beta}} MZ + \xi,$$

so let H be the solution of the (random) ODE:

$$\begin{cases} H'(t) = H^2(t) - C, \\ H(0) = \sqrt{a} - \delta, \end{cases} \tag{VI.47}$$

where the random constant satisfies

$$C = a - \frac{4}{\sqrt{\beta}}\sqrt{a}M + O(1).$$

By the same argument of comparison as in the Section VI.3, when $M \leq c\delta$ the diffusion Y is under $t \mapsto H(t) + 2/\sqrt{\beta}B_t$ up to the minimum of ξ and the exit time from $[-\sqrt{a}-1, \sqrt{a}]$. Therefore we will have $T'_- < \xi, T'_- < T'_+$ as long as

$$H(\xi) + \frac{2}{\sqrt{\beta}}B_\xi \leq -\sqrt{a} + \delta, \quad \text{and} \qquad \sup_{s\in[0,\xi]}\left(H(s) + \frac{2}{\sqrt{\beta}}B_s\right) < \sqrt{a} - \delta/2.$$

Since $H(s)$ is decreasing in s, the second event is implied by our assumption on M.

The solution H takes the form:

$$H(t) = -\sqrt{C}\tanh\left(\sqrt{C}t - \operatorname{arctanh}(b)\right) = \frac{\sqrt{C}\left(\tanh\left(\sqrt{C}t\right) - b\right)}{b\tanh\left(\sqrt{C}t\right) - 1}, \qquad b = \frac{\sqrt{a}-\delta}{\sqrt{C}}.$$

When $c_3 \geq 1$ we have $\tanh(\sqrt{C}t) = 1 + O(a^{-2})$. So we get the asymptotics

$$H(\xi) = -\sqrt{a} + 2M/\sqrt{\beta} + o(\delta),$$

and we indeed have

$$H(\xi) + \frac{2}{\sqrt{\beta}}B_\xi \leq -\sqrt{a} + \frac{4M}{\sqrt{\beta}} \leq \frac{4}{5}\delta + o(\delta). \qquad \square$$

VI.5 Under the parabola, lower bound

We will prove:

Proposition 6.10. *There exists $c_5 > 0$ depending only on β such that,*

$$\mathbb{P}_{-\sqrt{a}+\delta}(T_{-\infty} < \infty) \geq \exp\left(-c_5\sqrt{\ln a}\right).$$

Proof. Using the strong Markov property and the increasing property, we can lower bound the left hand side by

$$\mathbb{P}_{-\sqrt{a}+\delta}\left(T_{-\sqrt{a}-\delta} < \frac{1}{\sqrt{a}} \wedge T_{-\sqrt{a}+2\delta}\right) \times \mathbb{P}_{(\frac{1}{\sqrt{a}},-\sqrt{a}-\varepsilon)}\left(T_{-\sqrt{a}-\frac{\sqrt{\ln a}}{\sqrt[4]{a}}} < \frac{\ln a}{2\sqrt{a}} \wedge T_{-\sqrt{a}}\right) \times \mathbb{P}_{\left(\frac{\ln a}{\sqrt{a}},-\sqrt{a}-\frac{\sqrt{\ln a}}{\sqrt[4]{a}}\right)}(T_{-\infty} < \infty).$$

• The first probability gives the main cost. Under this event, the process X is stochastically dominated by the drifted Brownian motion:

$$t \mapsto -\sqrt{a} + \delta + 2\sqrt{a}\,\delta t + \frac{2}{\sqrt{\beta}}B_t.$$

Thus,

$$\mathbb{P}_{-\sqrt{a}+\varepsilon}\left(T_{-\sqrt{a}-\varepsilon} < \frac{1}{\sqrt{a}} \wedge T_{-\sqrt{a}+2\varepsilon}\right) \geq \mathbb{P}\left(B_1 < -\frac{3}{2}\sqrt{\beta}\sqrt[4]{a}\,\varepsilon,\ \sup_{s\in[0,1]} B_s \leq \frac{1}{2}\sqrt{\beta}\sqrt[4]{a}\varepsilon\right).$$

By the reflection principle, this equals

$$\mathbb{P}\left(\frac{5}{2}\sqrt{\beta}\sqrt[4]{a}\varepsilon \geq B_1 \geq \frac{3}{2}\sqrt{\beta}\sqrt[4]{a}\,\varepsilon\right) \geq \sqrt{\beta}\sqrt[4]{\ln a}\,\exp\left(-\frac{25}{4}\beta\sqrt{\ln a}\right).$$

• For the second part, under the studied event, the diffusion $(X_t,\ t \geq 1/\sqrt{a})$ is stochastically dominated by

$$\frac{1}{4\sqrt{a}} + t + \frac{2}{\sqrt{\beta}}B_t - \sqrt{a} - \varepsilon.$$

Thus the studied probability is bounded from below by a constant depending only on β.

• For the last part, we need to compare the diffusion with the solution of a simple differential equation. Similarly to the previous comparisons, under the event $\{X(\ln a/\sqrt{a}) = -\sqrt{a} - \sqrt{\ln a}/\sqrt[4]{a},\ T_{-\infty} < T_{-\sqrt{a}} \wedge (3/8\ln a/\sqrt{a})\}$, the diffusion X is

stochastically dominated by $G(t)+2/\sqrt{\beta}B_t$ where G is the solution of the differential equation:

$$\begin{cases} G'(t) = a + \frac{11}{8}\frac{\ln a}{\sqrt{a}} - \left(1 - \frac{4}{\sqrt{\beta}}\frac{M}{\sqrt{a}}\right) G^2(t) \\ G(0) = -\sqrt{a} - \frac{\sqrt{\ln a}}{\sqrt[4]{a}}. \end{cases}$$

and

$$M = \sup_{s\in[0,\frac{3}{8}\frac{\ln a}{\sqrt{a}}]} |B_s|.$$

Whenever we have

$$\left\{ M \leq \frac{2}{2\sqrt{\beta}} \frac{\sqrt{\ln a}}{\sqrt[4]{a}} \right\},$$

the function G blows up to $-\infty$ at a time smaller than $3/8 \ln a/\sqrt{a}$ and the diffusion $(X_t,\ t \in [0, 3/8 \ln a/\sqrt{a}])$ stays under $-\sqrt{a}$. Therefore:

$$\mathbb{P}_{\left(\frac{\ln a}{\sqrt{a}}, -\sqrt{a} - \frac{\sqrt{\ln a}}{\sqrt[4]{a}}\right)} (T_{-\infty} < \infty) \geq P\left(M \leq \frac{2}{2\sqrt{\beta}} \frac{\sqrt{\ln a}}{\sqrt[4]{a}} \right)$$

which is greater than a constant depending only on β. It leads to the result. □

Acknowledgement: The authors would like to thank the BME of Budapest for its kind hospitality while we finished this article. L.D. is also grateful to the mathematics department of the University of Toronto for its welcome during her visits. L.D. acknowledges support from the Balaton/PHC grant #19482NA and B. V. Canada Research Chair program and the NSERC DAS program.

Bibliographie

[1] Milton Abramowitz and Irene Stegun. *Handbook of Mathematical Functions with Formulas, Graphs, and Mathematical Tables*. Dover Publications, 1964.

[2] David J. Aldous. Brownian excursion conditioned on its local time. *Electron. Comm. Probab.*, 3 :79–90 (electronic), 1998.

[3] Daniel J. Amit, G. Parisi, and L. Peliti. Asymptotic behavior of the "true" self-avoiding walk. *Phys. Rev. B (3)*, 27(3) :1635–1645, 1983.

[4] Richard Alejandro Arratia. *Coalescing Brownian motion on the line*. ProQuest LLC, Ann Arbor, MI, 1979. Thesis (Ph.D.)–The University of Wisconsin - Madison.

[5] Jinho Baik. Asymptotics of tracy-widom distribution functions. 2006.

[6] Jinho Baik, Percy Deift, and Kurt Johansson. On the distribution of the length of the longest increasing subsequence of random permutations. *J. Amer. Math. Soc.*, 12(4) :1119–1178, 1999.

[7] Patrick Billingsley. *Convergence of probability measures*. Wiley Series in Probability and Statistics : Probability and Statistics. John Wiley & Sons Inc., New York, second edition, 1999. A Wiley-Interscience Publication.

[8] A. Bloemendal and B. Virág. Limits of spiked random matrices i. *ArXiv e-prints*, 2010.

[9] Andrei N. Borodin and Paavo Salminen. *Handbook of Brownian motion—facts and formulae*. Probability and its Applications. Birkhäuser Verlag, Basel, second edition, 2002.

[10] G Borot, B Eynard, S N Majumdar, and C Nadal. Large deviations of the maximal eigenvalue of random matrices. *Journal of Statistical Mechanics : Theory and Experiment*, 2011(11) :P11024, 2011.

[11] Gaëtan Borot and Céline Nadal. Right tail asymptotic expansion of tracy–widom beta laws. *Random Matrices : Theory and Applications*, 01(03) :1250006, 2012.

[12] Krzysztof Burdzy. On nonincrease of Brownian motion. *Ann. Probab.*, 18(3) :978–980, 1990.

[13] L. O. Chekhov, B. Eynard, and O. Marchal. Topological expansion of beta-ensemble model and quantum algebraic geometry in the sectorwise approach. *ArXiv e-prints*, September 2010.

[14] Y. Chen and S. M. Manning. Some eigenvalue distribution functions of the Laguerre ensemble. *J. Phys. A*, 29(23) :7561–7579, 1996.

[15] D. A. Darling and M. Kac. On occupation times for Markoff processes. *Trans. Amer. Math. Soc.*, 84 :444–458, 1957.

[16] Laure Dumaz. Large deviations and path properties of the true self-repelling motion. *ArXiv e-prints*, 2011.

[17] Laure Dumaz. A clever (self-repelling) burglar. *Elec. Journal of Probab.*, 17(61) :1–17, 2012.

[18] Laure Dumaz and Bálint Tóth. Marginal densities of the "true" self-repelling motion. *ArXiv e-prints*, 2012.

[19] Laure Dumaz and Bálint Virág. The right tail exponent of the tracy-widom-beta distribution. *ArXiv e-prints*, 2011.

[20] Ioana Dumitriu and Alan Edelman. Matrix models for beta ensembles. *J. Math. Phys.*, 43(11) :5830–5847, 2002.

[21] R. T. Durrett and L. C. G. Rogers. Asymptotic behavior of brownian polymers. *Probab. Theory Related Fields*, 92(3) :337–349, 1992.

[22] Freeman J. Dyson. Statistical theory of the energy levels of complex systems. II. *J. Mathematical Phys.*, 3 :157–165, 1962.

[23] Alan Edelman and Brian D. Sutton. From random matrices to stochastic operators. *J. Stat. Phys.*, 127(6) :1121–1165, 2007.

[24] Anna Erschler, Bálint Tóth, and Wendelin Werner. Some locally self-interacting walks on the integers. *ArXiv e-prints*, 2010.

[25] William Feller. Fluctuation theory of recurrent events. *Trans. Amer. Math. Soc.*, 67 :98–119, 1949.

[26] P. A. Ferrari, L. R. G. Fontes, and Xian-Yuan Wu. Two-dimensional Poisson trees converge to the Brownian web. *Ann. Inst. H. Poincaré Probab. Statist.*, 41(5) :851–858, 2005.

[27] P. A. Ferrari, C. Landim, and H. Thorisson. Poisson trees, succession lines and coalescing random walks. *Ann. Inst. H. Poincaré Probab. Statist.*, 40(2) :141–152, 2004.

[28] P. Flajolet and G. Louchard. Analytic variations on the Airy distribution. *Algorithmica*, 31(3) :361–377, 2001. Mathematical analysis of algorithms.

[29] L. R. Fontes, M. Isopi, C. M. Newman, and D. L. Stein. Aging in 1d discrete spin models and equivalent systems. *Phys. Rev. Lett.*, 87(11), 2001.

[30] L. R. G. Fontes, M. Isopi, C. M. Newman, and K. Ravishankar. The Brownian web : characterization and convergence. *Ann. Probab.*, 32(4) :2857–2883, 2004.

[31] P. J. Forrester. *Log-gases and random matrices*, volume 34 of *London Mathematical Society Monographs Series*. Princeton University Press, Princeton, NJ, 2010.

[32] Sreela Gangopadhyay, Rahul Roy, and Anish Sarkar. Random oriented trees : a model of drainage networks. *Ann. Appl. Probab.*, 14(3) :1242–1266, 2004.

[33] I. S. Gradshteyn and I. M. Ryzhik. *Table of integrals, series, and products*. Elsevier/Academic Press, Amsterdam, seventh edition, 2007. Translated from the Russian, Translation edited and with a preface by Alan Jeffrey and Daniel Zwillinger, With one CD-ROM (Windows, Macintosh and UNIX).

[34] Chris Howitt and Jon Warren. Consistent families of brownian motions and stochastic flows of kernels. *Ann. Probab.*, 37(4) :1237–1272, 2009.

[35] Chris Howitt and Jon Warren. Dynamics for the brownian web and the erosion flow. *Stochastic Processes and their Applications*, 119(6) :2028–2051, 2009.

[36] Svante Janson. Brownian excursion area, Wright's constants in graph enumeration, and other Brownian areas. *Probab. Surv.*, 4 :80–145 (electronic), 2007.

[37] K. Johansson. Shape Fluctuations and Random Matrices. *Communications in Mathematical Physics*, 209 :437–476, 2000.

[38] M. Kac. On distributions of certain Wiener functionals. *Trans. Amer. Math. Soc.*, 65 :1–13, 1949.

[39] Ioannis Karatzas and Steven E. Shreve. *Brownian motion and stochastic calculus*, volume 113 of *Graduate Texts in Mathematics*. Springer-Verlag, New York, second edition, 1991.

[40] Michael J. Kearney and Satya N. Majumdar. On the area under a continuous time Brownian motion till its first-passage time. *J. Phys. A*, 38(19) :4097–4104, 2005.

[41] F. B. Knight. Random walks and a sojourn density process of Brownian motion. *Trans. Amer. Math. Soc.*, 109 :56–86, 1963.

[42] Satya N. Majumdar. Random matrices, the ulam problem, directed polymers, growth models, and sequence matching. *ArXiv e-prints*, 2007.

[43] C. M. Newman and K. Ravishankar. Convergence of the Tóth lattice filling curve to the Tóth-Werner plane filling curve. *ALEA Lat. Am. J. Probab. Math. Stat.*, 1 :333–345, 2006.

[44] C. M. Newman, K. Ravishankar, and E. Schertzer. Marking (1, 2) points of the brownian web and applications. *Ann. Inst. H. Poincaré Probab. Statist.*, 46(2) :537–574, 2010.

[45] S. P. Obukhov and L. Peliti. Renormalisation of the "true" self-avoiding walk. *J. Phys. A*, 16(5) :L147–L151, 1983.

[46] L. Peliti and L. Pietronero. Random walks with memory. *Riv. Nuovo Cimento*, 10(6) :1–33, 1987.

[47] Harry Pollard. The completely monotonic character of the Mittag-Leffler function $E_a(-x)$. *Bull. Amer. Math. Soc.*, 54 :1115–1116, 1948.

[48] J. A. Ramírez, B. Rider, and B. Virág. Beta ensembles, stochastic Airy spectrum, and a diffusion. *J. Amer. Math. Soc.*, To appear. *arXiv :math/0607331v4*, 2006.

[49] Daniel Ray. Sojourn times of diffusion processes. *Illinois J. Math.*, 7 :615–630, 1963.

[50] W. H. Reid. Integral representations for products of Airy functions. *Z. Angew. Math. Phys.*, 46(2) :159–170, 1995.

[51] Daniel Revuz and Marc Yor. *Continuous martingales and Brownian motion*, volume 293 of *Grundlehren der Mathematischen Wissenschaften [Fundamental Principles of Mathematical Sciences]*. Springer-Verlag, Berlin, third edition, 1999.

[52] Barry Simon. *Functional integration and quantum physics*. AMS Chelsea Publishing, Providence, RI, second edition, 2005.

[53] Florin Soucaliuc, Bálint Tóth, and Wendelin Werner. Reflection and coalescence between independent one-dimensional Brownian paths. *Ann. Inst. H. Poincaré Probab. Statist.*, 36(4) :509–545, 2000.

[54] Rongfeng Sun and M. Swart, Jan. The brownian net. *Ann. Probab.*, 36(3) :1153–1208, 2008.

[55] Brian D. Sutton. *The stochastic operator approach to random matrix theory*. ProQuest LLC, Ann Arbor, MI, 2005. Thesis (Ph.D.)–Massachusetts Institute of Technology.

[56] Pierre Tarrès, Bálint Tóth, and Benedek Valkó. Diffusivity bounds for 1d brownian polymers. *Ann. Probab.*, 40(2) :695–713, 2012.

[57] Bálint Tóth. The "true" self-avoiding walk with bond repulsion on $\mathbf{Z}$: limit theorems. *Ann. Probab.*, 23(4) :1523–1556, 1995.

[58] Bálint Tóth and Bálint Vető. Continuous time 'true' self-avoiding random walk on $\mathbb{Z}$. *ALEA Lat. Am. J. Probab. Math. Stat.*, 8 :59–75, 2011.

[59] Bálint Tóth and Wendelin Werner. The true self-repelling motion. *Probab. Theory Related Fields*, 111(3) :375–452, 1998.

[60] C. A. Tracy and H. Widom. Asymptotics in ASEP with Step Initial Condition. *Communications in Mathematical Physics*, 290 :129–154, August 2009.

[61] Craig A. Tracy and Harold Widom. Level-spacing distributions and the Airy kernel. *Comm. Math. Phys.*, 159(1) :151–174, 1994.

[62] Craig A. Tracy and Harold Widom. On orthogonal and symplectic matrix ensembles. *Comm. Math. Phys.*, 177(3) :727–754, 1996.

[63] Boris Tsirelson. Scaling limit, noise, stability. In *Lectures on probability theory and statistics*, volume 1840 of *Lecture Notes in Math.*, pages 1–106. Springer, Berlin, 2004.

[64] Benedek Valkó and Bálint Virág. Large gaps between random eigenvalues. *Ann. Probab.*, 38(3) :1263–1279, 2010.

[65] J. Warren and M. Yor. The Brownian burglar : conditioning Brownian motion by its local time process. In *Séminaire de Probabilités, XXXII*, volume 1686 of *Lecture Notes in Math.*, pages 328–342. Springer, Berlin, 1998.

[66] Eugene P. Wigner. On the statistical distribution of the widths and spacings of nuclear resonance levels. *Mathematical Proceedings of the Cambridge Philosophical Society*, 47(04) :790–798, 1951.